SEP 7 1981

AEDC-TR-76-97

VARIABLE-AREA EJECTOR DEVELOPMENT

ENGINE TEST FACILITY
ARNOLD ENGINEERING DEVELOPMENT CENTER
AIR FORCE SYSTEMS COMMAND
ARNOLD AIR FORCE STATION, TENNESSEE 37389

August 1976

Final Report for Period June 1, 1974 – August 31, 1975

Approved for public release, distribution unlimited

Property of U. S. Air Force
AEDC LIBRARY
F40600-81-C-0004

Prepared for

DIRECTORATE OF TECHNOLOGY (DY)
ARNOLD ENGINEERING DEVELOPMENT CENTER
ARNOLD AIR FORCE STATION, TENNESSEE 37389

NOTICES

When U. S. Government drawings specifications, or other data are used for any purpose other than a definitely related Government procurement operation, the Government thereby incurs no responsibility nor any obligation whatsoever, and the fact that the Government may have formulated, furnished, or in any way supplied the said drawings, specifications, or other data, is not to be regarded by implication or otherwise, or in any manner licensing the holder or any other person or corporation, or conveying any rights or permission to manufacture, use, or sell any patented invention that may in any way be related thereto.

Qualified users may obtain copies of this report from the Defense Documentation Center.

References to named commercial products in this report are not to be considered in any sense as an endorsement of the product by the United States Air Force or the Government.

This report has been reviewed by the Information Office (OI) and is releasable to the National Technical Information Service (NTIS). At NTIS, it will be available to the general public, including foreign nations.

APPROVAL STATEMENT

This technical report has been reviewed and is approved for publication.

FOR THE COMMANDER

William E Cole

WILLIAM E. COLE
Captain, USAF
Requirements Planning Division
Directorate of Technology

Robert O Dietz

ROBERT O. DIETZ
Director of Technology

ERRATA

AEDC-TR-76-97, August 1976
(UNCLASSIFIED REPORT)

VARIABLE-AREA EJECTOR DEVELOPMENT

Delbert Taylor, David Duesterhaus,
Frank Lee, and Marvin Simmons - ARO, Inc.

Arnold Engineering Development Center
Air Force Systems Command
Arnold Air Force Station, Tennessee

Please make the following changes in your copy of the above report.

1. Page 13, Item 5, change valve to value.

2. Page 38, Fig. 12, the abscissa scale should read 1, 2, 4, 6, 8, 10.

3. Page 49, Fig. 16b, the value of $\dot{m}''/\dot{m}'$ should be 0.05 instead of 0.5.

4. Page 51, Fig. 17a, the abscissa scale should read 0.1, 0.2, 0.3, 0.4, 0.5, 0.6, 0.7, 0.8

5. Page 71, Fig. 24b, in the symbol block for data without nozzle plug installed, add (Ref. 1 Data).

REPORT DOCUMENTATION PAGE		READ INSTRUCTIONS BEFORE COMPLETING FORM
1 REPORT NUMBER AEDC-TR-76-97	2 GOVT ACCESSION NO	3 RECIPIENT'S CATALOG NUMBER
4 TITLE (and Subtitle) VARIABLE-AREA EJECTOR DEVELOPMENT		5 TYPE OF REPORT & PERIOD COVERED Final Report - June 1, 1974 - August 31, 1975 6 PERFORMING ORG REPORT NUMBER
7 AUTHOR(s) Delbert Taylor, David Duesterhaus, Frank Lee, and Marvin Simmons - ARO, Inc.		8 CONTRACT OR GRANT NUMBER(s)
9 PERFORMING ORGANIZATION NAME AND ADDRESS Arnold Engineering Development Center (DY) Air Force Systems Command Arnold Air Force Station, Tennessee 37389		10 PROGRAM ELEMENT, PROJECT, TASK AREA & WORK UNIT NUMBERS Program Element 65807F
11 CONTROLLING OFFICE NAME AND ADDRESS Arnold Engineering Development Center(DYFS) Arnold Air Force Station Tennessee 37389		12 REPORT DATE August 1976 13 NUMBER OF PAGES 88
14 MONITORING AGENCY NAME & ADDRESS(if different from Controlling Office)		15 SECURITY CLASS. (of this report) UNCLASSIFIED 15a DECLASSIFICATION DOWNGRADING SCHEDULE N/A

16 DISTRIBUTION STATEMENT (of this Report)

Approved for public release; distribution unlimited.

17 DISTRIBUTION STATEMENT (of the abstract entered in Block 20, if different from Report)

18 SUPPLEMENTARY NOTES

Available in DDC

19 KEY WORDS (Continue on reverse side if necessary and identify by block number)

ejectors
diffusers
test facilities
test equipment
exhaust diffusers
performance

20 ABSTRACT (Continue on reverse side if necessary and identify by block number)

An experimental investigation was conducted to determine the performance of a variable-area ejector. Test equipment consisted of various fixed-geometry primary driving nozzles and either a constant-area or a conical-converging mixing duct attached to a conical-diverging exit section, which was equipped with a conical centerbody. Axial movement of the conical centerbody varied the minimum area of the ejector. Five primary driving nozzle geometries

DD FORM 1 JAN 73 1473 EDITION OF 1 NOV 65 IS OBSOLETE

20. ABSTRACT (Continued)

were used. Both steady-state and transient performance characteristics of the ejector configurations are presented. A constant-area (no centerbody) ejector having a diameter equivalent to that of the variable-area ejector mixing duct was also evaluated. In general, the performance of the variable-area ejector configurations exceeded that of the constant-area ejector.

AFSC
Arnold AFS Tenn

PREFACE

The work reported herein was conducted by the Arnold Engineering Development Center (AEDC), Air Force Systems Command (AFSC), for the Director of Technology (AEDC) under Program Element 65807F. The results of the test were obtained by ARO, Inc. (a subsidiary of Sverdrup & Parcel and Associates, Inc.), contract operator of AEDC, AFSC, Arnold Air Force Station, Tennessee, under ARO Project Number R32P-68A. The authors of this report were Delbert Taylor, David Duesterhaus, Frank Lee, and Marvin Simmons, ARO, Inc. The data analysis was completed on September 15, 1975, and the manuscript (ARO Control No. ARO-ETF-TR-76-29) was submitted for publication on March 10, 1976.

CONTENTS

		Page
1.0	INTRODUCTION	7
2.0	APPARATUS	8
3.0	PROCEDURE	11
4.0	RESULTS AND DISCUSSION	14
5.0	APPLICATION AND PERFORMANCE COMPARISONS	21
6.0	SUMMARY OF RESULTS	24
	REFERENCES	25

ILLUSTRATIONS

Figure

1. Installation of Variable-Area Ejector . . . 27
2. Details of Primary Nozzles . . . 28
3 Details of Constant-Area Ejector . . . 29
4. Variable-Area Ejector with the Constant-Area Mixing Duct . . . 30
5. Variable-Area Ejector with the Converging Mixing Duct . . . 31
6. Variable-Area Ejector with the Extended Constant-Area Mixing Duct . . . 32
7. Details of Centerbody . . . 33
8. Minimum Second-Throat Area versus Centerbody Position . . . 34
9. Installation of the Primary Nozzle Plug System . . . 35
10. Details of the Primary Nozzle Plug
    a. 1.685-in.-diam Plug . . . 36
    b. 0.912-in.-diam Plug . . . 36
11. Inlet Total Pressure Rake Probe Locations . . . 37
12. Estimated Engine Characteristics . . . 38
13 Constant-Area Ejector Performance
    a $A_d/A^* = 8.767$ . . . 39
    b. $A_d/A^* = 17.285$ . . . 40
    c. $A_d/A^* = 28.351$ . . . 41
14. Performance of Variable-Area Ejector with a Constant-Area Mixing Duct
    a. $A_d/A^* = 8.767$ . . . 42
    b. $A_d/A^* = 17.285$ . . . 43
    c. $A_d/A^* = 28.351$ . . . 44

Figure | Page

15. Performance of Variable-Area Ejector with Converging Inlet Duct
a. $A_d/A^* = 8.767$ . . . 45
b. $A_d/A^* = 17.285$ . . . 46
c. $A_d/A^* = 28.351$ . . . 47
16. Performance Comparison of Ejector Configurations
a. $A_d/A^* = 8.767$ . . . 48
b. $A_d/A^* = 17.285$ . . . 49
c. $A_d/A^* = 28.351$ . . . 50
17. Variable-Area Ejector Performance Characteristics $A_d/A^* = 3.987$
a. $P_t' = 5$ psia . . . 51
b. $P_t' = 10$ psia . . . 52
c. $P_t' = 20$ psia . . . 53
18. Variable-Area Ejector Performance Characteristics, $A_d/A^* = 5.756$
a. $P_t' = 5$ psia . . . 54
b. $P_t' = 10$ psia . . . 55
c. $P_t' = 20$ psia . . . 56
19. Variable-Area Ejector Performance Characteristics, $A_d/A^* = 8.767$
a. $P_t' = 10$ psia . . . 57
b. $P_t' = 35$ psia . . . 58
20. Variable-Area Ejector Performance Characteristics, $A_d/A^* = 17.285$
a. $P_t' = 10$ psia . . . 59
b. $P_t' = 35$ psia . . . 60
21. Variable-Area Ejector Performance Characteristics, $A_d/A^* = 28.351$
a. $P_t' = 10$ psia . . . 61
b. $P_t' = 35$ psia . . . 62
22. Effect of Driving Gas Pressure on Performance of Variable-Area Ejector with Constant-Area Inlet
a. $A_d/A^* = 3.987$ . . . 63
b. $A_d/A^* = 5.756$ . . . 64
c. $A_d/A^* = 8.767$ . . . 65
d. $A_d/A^* = 17.285$ . . . 66
e. $A_d/A^* = 28.351$ . . . 67
23. Effect of Stagnation Pressure on Ejector Performance
a. Constant-Area Ejector (Cylindrical) . . . 68
b. Variable-Area Ejectors . . . 69

Figure | Page

24. Variable-Area Ejector Performance with Primary Nozzle Plug Retracted
a. $A_d/A^* = 3.987$ . . . 70
b. $A_d/A^* = 17.283$ . . . 71
25. Variable-Area Ejector Performance with Nozzle Plug Inserted into Primary Nozzle Throat
a. $A_d/A^* = 5.756$ ($A_d/A^* = 3.987$ with Plug Inserted) . . . 72
b. $A_d/A^* = 28.351$ ($A_d/A^* = 17.283$ with Plug Inserted) . . . 73
26. Effect of Centerbody Position on P_c/P_t' at Constant Values of P_{ex}, with Ejector with Constant-Area Inlet
a. $A_d/A^* = 3.987$ (Nozzle Plug Retracted) . . . 74
b. $A_d/A^* = 5.756$ (Nozzle Plug Inserted) . . . 75
c. $A_d/A^* = 17.283$ and 28.351 (Nozzle Plug Inserted) . . . 76
27. Response of Variable-Area Ejector Performance Parameters to a Ramp Change in P_t' . . . 77
28. Effect of Withdrawing the Primary Nozzle Plug on P_c (Variable-Area Ejector)
a. $A_d/A^* = 5.756$ (Nozzle Plug Withdrawn Rapidly) . . . 78
b. $A_d/A^* = 5.756$ (Nozzle Plug Withdrawn Slowly) . . . 79
c. $A_d/A^* = 28.351$ (Nozzle Plug Withdrawn Slowly) . . . 80
29. Response of Test Cell Pressure to Ramp Changes in P_t' and Primary Nozzle Plug Retraction . . . 81
30. Effect of $\dot{m}''/\dot{m}'$ on Transient Response of P_c to Ramp-Type Increase in P_t'
a. Run No 1 . . . 82
b. Run No. 2 . . . 83
31. Ejector Comparisons Showing Altitude Gains with Turbojet Engine (Design Mach Number 3.8) . . . 84
32. Ejector Comparisons Showing Altitude Gains with Turbofan Engine (Design Mach Number 2.5) . . . 85
33. Ejector Comparisons Showing Altitude Gains with Turbojet Engine (Design Mach Number 2.5) . . . 86

NOMENCLATURE . . . 87

1.0 INTRODUCTION

Aerospace propulsion systems are developed and/or evaluated in ground test facilities at operating conditions simulating free-flight. As the airflow requirements for the propulsion systems increase, facility requirements become more stringent. A continuing effort is made in the Engine Test Facility, Arnold Engineering Development Center to develop and employ methods to produce the maximum facility operating efficiency to meet the increasing test requirements in the most expeditious and economical manner. In line with this concept, the experiment reported herein was conducted to improve the pressure recovery of ejectors used in jet engine testing. These ejectors, operating in series with the plant exhauster equipment, utilize the directed kinetic energy in the propulsion system exhaust jet to entrain test cell cooling air and to increase the pressure at the ejector exit. This produces a decrease in the plant volume flow rate and, consequently, decreases the electrical power required to operate the exhauster equipment.

Turbojets are normally tested from idle to maximum power levels over the full flight range of Mach numbers and altitudes, causing the directed kinetic energy in the exhaust jet to vary over a large range. Therefore, the ejector mixing duct area must be varied to produce the maximum pressure recovery and maintain the desired simulated altitude environment. The ratio of test cell pressure (simulated pressure altitude) to engine exhaust nozzle stagnation pressure (P_c/P_t'), referred to as the nozzle pressure ratio, must be controlled over a large range to simulate the engine free-flight operation. Since commercially available jet pumps are each designed for use at a specific value of mass ratio and primary pressure, they are not suited to this application. The present studies show that a properly designed ejector with a variable-area second-throat may be used to produce the desired variation of the nozzle pressure ratio at pressure recoveries approaching those of conventional ejectors, which are designed to produce optimum performance at the design point operating condition.

The present work is an extension of the ejector development program (Ref. 1) initiated in FY73 which produced encouraging results; however, the influence of the magnitude of the primary driving nozzle pressure on ejector pressure recovery and the transient performance characteristics of the ejector were not defined. Presented herein are the results of an experimental evaluation of an ejector with a variable-area second-throat using five different driving nozzle configurations at secondary-to-primary mass flow ratios from zero to approximately 1.4. The theory of both the constant-area and converging mixing duct ejector designs is presented in Ref. 2.

2.0 APPARATUS

The installation was basically identical to the single-angle centerbody diffuser installation in Ref. 1, which will hereafter be referred to as the variable-area ejector. The basic installation of the variable-area ejector with the constant-area mixing duct is presented in Fig. 1. The test cell was fabricated from nominal 20-in.-diam pipe 20 in. in length with standard pipe flanges. The upstream end of the test cell was sealed by a standard pipe flange which supported the 10-in.-diam air supply duct. The seal at the downstream end of the test cell was provided by the ejector inlet mounting flange.

The downstream end of the ejector section was joined to a 20-in.-diam exhaust plenum which contained two 15- by 6-in. rectangular windows. Access to the centerbody gearbox and position indicator was obtained through these windows.

A remotely controlled valve was located downstream of the exhaust plenum and was used to vary the pressure in the exhaust plenum.

Two 2-in.-diam ducts were coupled with the test cell through which secondary flow was injected to simulate test cell cooling flow. One of the ducts connected to the air supply system contained a manually controlled valve and a 1.058-in.-diam throat venturi for flow-metering purposes. The other 2-in.-diam duct was open to atmosphere and contained a manually controlled valve and a 1.25-in.-diam venturi for flow metering.

2.1 PRIMARY DRIVING NOZZLES

The nozzle pressure ratio (P_c/P_t') is the primary engine parameter to be simulated. To attain the value of P_c/P_t', in a ground test facility, the inlet or mixing duct area (A_d) of the ejector must be of proper size to allow passage of the engine flow through the ejector at the required value of P_c and to obtain a maximum pressure rise across the ejector (P_{ex}/P_c). To do this most efficiently for a large variation in altitude and Mach number, a large variation in mixing duct area is required. To simulate these conditions in a model installation, it becomes impractical to vary the mixing duct diameter and maintain the same length-to-diameter ratio (L/D). Consequently, varying the primary driving nozzle throat area can effectively provide the variation in A_d/A^* at the same L/D. Five area ratios were chosen for simulation: 3.987, 5.756, 8.760, 17.285, 28.351. These correspond to the nozzles shown in Figs. 2a through e, respectively. The area ratios were chosen in an attempt to cover the thrust range of engines operating at intermediate and maximum power levels. The nozzle area ratios (A_{ne}/A^*) were designed to simulate as nearly as possible the nozzle expansion ratios of present and future engines. The nozzles shown in Figs 2a and b were designed for an exit Mach number of 1.95, and the nozzles shown in Figs. 2c, d, and e for an exit Mach number of 2.65.

2.2 CONSTANT-AREA EJECTOR

The constant-area ejector installation shown in Fig. 3 was identical to the installation used in Ref. 1. The length of the constant-area ejector was the same as that of the variable-area ejector. The primary nozzles were installed in the test cell connected to the 10-in.-diam air supply ducting concentric with the entire installation. The nozzle exit was located 2.06 in. inside the ejector mixing duct for all configurations and was maintained at that position. Calculations showed that this could cause choking of the secondary flow for the high secondary flow ratios ($\dot{m}''/\dot{m}'$) of approximately 0.9 for the $A_d/A^* = 8.76$ and 1.2 for $A_d/A^* = 17.285$. However, the effect on ejector performance was assumed to be minimal.

2.3 VARIABLE-AREA EJECTOR

Three similar, variable-area ejector installations were tested. The three configurations consisted of different mixing ducts: (1) constant area (Fig. 4), (2) converging (Fig. 5), and (3) extended constant area (Fig. 6).

The variable-area ejector with the constant-area mixing duct presented in Fig. 4 is identical to the single-angle centerbody diffuser configuration in Ref. 1. The ejector mixing duct was a 6.07-in.-diam constant-area section 10 in. long welded to an 8-deg half-angle divergent cone for a total length of 23 in. The 8-deg divergent cone was mounted inside a 10.2-in.-ID duct. The overall length of the ejector installation was 29.63 in., which results in an effective length-to-mixing duct diameter (from the nozzle exit) ratio of 4.54. The ejector with a convergent mixing duct is a modification of the previous installation (see Fig. 5). The constant-area mixing duct of the previous configuration was removed and replaced with a converging section with a 5-deg half-angle. The A_d used for the calculation of the A_d/A^* was the same for the converging mixing duct as for the other configurations ($A_d = 28.938$ in.^{2}). The variable-area ejector with the extended constant-area mixing duct is shown in Fig. 6 and was similar to the first configuration (see Fig. 4). The extension in length was necessitated by hardware requirements due to the modifications for the converging mixing duct.

The centerbody depicted in Fig. 7 and used in the three installations was 16.37 in. in total length which includes a 0.5-in.-radius blunt nose matched with a 12-deg half-angle cone to the 6-in. maximum diameter. A 4-in.-long cylinder was mounted on the maximum diameter of the centerbody for better subsonic diffusion. The centerbody position for the three installations was varied by a threaded positioning rod driven by a variable speed electric motor located in the exhaust plenum. The centerbody position was monitored using a linear potentiometer and a digital voltmeter. The centerbody position indicators were actuated by a rod attached directly to the centerbody. The primary nozzle axial

position remained stationary with respect to the diverging ejector section for all configurations.

The ejector configurations produced the same second-throat minimum area versus centerbody position relationship depicted in Fig. 8, which is identical to that of Ref. 1. The discontinuity in Fig. 8 at the centerbody position of 3.2 in. results when the point of minimum second-throat area transitions from the mixing duct to the maximum diameter of the centerbody.

2.4 PRIMARY NOZZLE PLUG SYSTEM

The primary nozzle plug system depicted in Fig. 9 was used to simulate the change in turbojet engine nozzle area variation for a transient from intermediate to maximum power. The nozzle plugs shown in Figs. 10a and b were used for the respective nozzles shown in Figs. 2a and d which have the A_d/A^* ratios of 3.987 and 17.285. The plugs were designed to provide A_d/A^* ratios of 5.756 and 28.351, respectively, when inserted in their respective nozzles. The actuating system employed an electrically operated servo-cylinder that was monitored using a multi-turn potentiometer and a digital voltmeter for a position indicator. The system was calibrated after each installation.

2.5 INSTRUMENTATION

Pressure and temperature values were measured with the aid of a digital data acquistion system capable of obtaining 25 channels of data with 12 pressures per channel. The data system automatically sequenced the ten scanner valves (one per channel) to measure the 120 pressures and record the information on magnetic tape from the 10 pressure transducers. Two channels of temperature data were also recorded employing iron-constantan-type thermocouples.

2.5.1 Instrumentation Calibration

The instrumentation system was calibrated before and after every test. The calibration consisted of impressing a known pressure on the transducers and recording the transducer outputs. Any discrepancies were resolved prior to the test.

2.5.2 Test Data Measurement Uncertainty

The uncertainty of the data measurement was calculated using information from the instruments in a set of equations from Ref. 3. With a confidence level of 95 percent, the uncertainty for all of the pressure parameters in the range of pressures greater than

1 psia was ±1.3 percent of the reading. For pressure data less than 1 psia, the uncertainty was ±0.01 psi. The uncertainty reflects the characteristics of the transducers, electrical systems, data recording systems, and data processing systems. Consideration was not given to the physical condition of the orifices or the flow conditions existing in the region of the orifices.

2.5.3 Instrument Sensing Locations

Two thermocouples were installed; one in the 10-in.-diam air supply ducting and the second in the exhaust plenum (see Fig. 1). The location of the inlet stagnation pressure rake in the ejector installation is depicted in Fig. 1, and the inlet total pressure probe arrangement is depicted in Fig. 11. The total pressure profile was so nearly a constant that the data are not presented herein.

Static pressures were measured at four equiangular positions at mid-length of the test cell. The pressures were averaged to give the value of cell pressure (P_c). The axial position of the exhaust static pressure orifice can be noted on Fig. 1

3.0 PROCEDURE

3.1 STEADY-STATE PERFORMANCE PROCEDURE

The secondary and primary fluids were air at approximately ambient temperature. The primary driving nozzle stagnation pressure was adjusted from 5 to 35 psia and the $\dot{m}''/\dot{m}'$ ratio was adjusted from 0 to 1.4. The exhaust pressure (P_{ex}) was adjusted for each test condition using the exhaust isolation valve or the exhaust plant. The centerbody position was optimized to achieve minimum cell pressure for each value of exhaust pressure for each configuration at a specific inlet stagnation pressure.

The normal test initiation sequence was as follows:

1. The test installation was evacuated by the exhaust plant to approximately 1.0 psia.

2. A test point was taken and all pressure lines were checked for any leaks or plugged lines in the installation.

3. The test was initiated by opening the primary air supply valve until flow was established at the desired primary total pressure.

A typical steady-state ejector performance characteristic was performed as follows:

1. After the test initiation sequence was completed and the primary flow stagnation pressure (P_t') established, the $\dot{m}''/\dot{m}'$ ratio was adjusted by varying the manual valve in one of the secondary flow ducts until the desired valve was obtained. These parameters were maintained constant for the entire characteristic.

2. The exhaust pressure (P_{ex}) was then adjusted to a value such that the cell pressure (P_c) was independent of P_{ex}. The P_c at this condition is the minimum P_c for this P_t' and $\dot{m}''/\dot{m}'$.

3. The data system was then activated to record the test information.

4. The exhaust pressure was then changed in small increments and step 3 was performed for each value of exhaust pressure until the ejector characteristic was established.

5. The $\dot{m}''/\dot{m}'$ ratio and/or P_t' was then changed, and steps 2, 3, and 4 were repeated.

This procedure was followed to attain the ejector performance characteristic for all the desired values of P_t' and $\dot{m}''/\dot{m}'$.

The procedure to obtain an ejector steady-state performance characteristic for the variable-area ejector was identical to the typical procedure presented above with the exception of the need to position the centerbody prior to step 3. The centerbody position was optimized in this step to attain the minimum value of test cell pressure for each value of P_{ex}. This procedure gave the maximum rise ratio (P_{ex}/P_c) for the specific primary and secondary flow parameters. The performance of the variable-area ejector was also attained for a fixed centerbody position.

3.2 TRANSIENT PROCEDURE

There are two fundamental types of transients to be simulated in ground environmental testing of turbojet engines. Mach number-altitude transients, and engine power transients. In order to cover the full range of these transients four independent methods were utilized. They are described below.

During altitude, Mach number, and altitude-Mach number transients, the engine exhaust nozzle pressure ratio (P_c/P_t'), varies according to a predetermined schedule derived from the engine and ejector performance characteristic. By translating the centerbody this variation can be controlled to produce the desired profile. Information from the centerbody transient lends some idea on how the centerbody could be used to help the exhaust plant simulate these various transients. The procedure for a simulation of a simple centerbody transient was as follows:

4. The centerbody was withdrawn to its maximum rearward position at predetermined values of P_t', $\dot{m}''/\dot{m}'$, and P_{ex} which were maintained constant for the entire transient.

2. The strip-chart recorders were started, and the transient was performed by moving the centerbody forward causing the variation in P_c until a desired value of P_c/P_t' was obtained or the limit of travel of the centerbody actuator was reached.

The procedure was repeated for various values of P_{ex} and for several of the primary nozzle configurations with and without the nozzle plug inserted.

The two methods derived for simulating engine power transients from intermediate to maximum power levels were (1) the primary nozzle driving pressure transients and (2) the nozzle plug transients. These methods simulate the engine nozzle area and thrust variation incurred when the turbojet engine is cycled from intermediate to maximum power.

The procedure for the primary nozzle driving pressure transient was as follows:

1. The desired conditions at the end of the transient were selected to be P_t' = 20 psia, $\dot{m}''/\dot{m}'$ = 0.05, with the resulting P_c/P_t' = 0.05 (P_c = 1.0 psia).

2. The centerbody was positioned for optimum performance at these operating conditions, which is the end point of the transient.

3. P_t' was adjusted from 20 to 10 psia since the desired excursion in P_t' was a delta of 10 psi.

4. P_{ex} was adjusted from 4.4 to 2.9 psia to re-establish P_c = 1.0 psia.

5. The strip-chart recorder was started, and the transient was performed by manually increasing the primary nozzle driving pressure to the original valve.

The procedure by which the nozzle plug transient was performed was slightly different than described above. The end point of the transient was once again used to set the initial conditions prior to the transient. The procedure was as follows.

1. P_t', $\dot{m}''/\dot{m}'$, P_c, and the preselected centerbody position were adjusted to the desired conditions with the nozzle plug withdrawn.

2. Insert the nozzle plug to the proper position relative to the nozzle and adjust P_{ex} until P_c maintains the same level as that in step 1.

3. The strip-chart recorders were started, and the transient was performed by retracting the nozzle plug out of the nozzle.

The final transient method, the constant altitude idle to maximum engine power transient, was basically a combination of the first two methods and consisted of performing the driving pressure transient just prior to the nozzle plug transient. This procedure was as follows:

1. The desired transient end point conditions were established, and P_c was noted.

2. The nozzle plug was inserted, and P_t' was adjusted to the level for the transient initiation point.

3. The P_{ex} was increased to attain the end point value of P_c.

4. Conditions were now set for performing the transient. The strip-chart recorder was started, and the transient was performed by manually increasing P_t', and after the maximum P_t' was attained, the nozzle plug was retracted out of the nozzle.

4.0 RESULTS AND DISCUSSION

4.1 GENERAL

The results of this experiment are presented and discussed as follows: (a) steady-state performance characteristics of the constant-area (cylindrical) and the variable-area second-throat ejectors (b) the effect of the stagnation pressure of the primary driving nozzles on the ejector performance; and (c) transient performance characteristics of the variable-area second-throat ejector.

4.2 STEADY-STATE PERFORMANCE

The steady-state performance characteristics are documented for thirteen ejector configurations at primary driving nozzle pressures, P'_t of 5, 10, 20, and 35 psia, and at secondary-to primary mass ratios ($\dot{m}''/\dot{m}'$) of from 0 to 0.1 and from 0.40 to 1.40, which are characteristic of turbine engine direct-connect and free-jet test techniques, respectively. The model tests reported herein were conducted with simulated engine nozzles using cold air. Therefore, these mass ratios should be corrected for actual engine-ejector application as follows (assuming Mach number 1 of the throat and equal total pressures and using the continuity equation and compressible flow relations):

$$\frac{\dot{m}''_{air}}{\dot{m}'_g} = \left(\frac{\dot{m}''_{air}}{\dot{m}'_{air}}\right)\left(\frac{\dot{m}'_{air}}{\dot{m}'_g}\right) = \left(\frac{\dot{m}''_{air}}{\dot{m}'_{air}}\right)\left[\frac{\left(\frac{\gamma_g+1}{2}\right)^{\frac{\gamma_g+1}{2(\gamma_g-1)}}}{\left(\frac{\gamma_{air}+1}{2}\right)^{\frac{\gamma_{air}+1}{2(\gamma_{air}-1)}}}\right]\sqrt{\frac{\gamma_{air}\,R_g\,T_{T_g}}{\gamma_g\,R_{air}\,T_{T_{air}}}}$$

An explanation of the method of operation of the constant-area and the variable-area second-throat ejectors in turbojet engine test application is presented in the following to aid in understanding the test results.

Turbojet engines operate over a very large range of thrust, Mach number, and altitude, and consequently, a considerable variation in exhaust nozzle pressure ratio $P_{amb}/P_{t_{ne}}$. The estimated variation in the exhaust nozzle pressure ratios ($P_{amb}/P_{t_{ne}}$) of a turbofan and a turbojet designed to operate at maximum flight Mach numbers of 2.5 and 3.8, respectively, versus flight Mach number is presented in Fig. 12. In the test installation, the exhaust jet is the primary driving medium for the ejector which is used in series with the exhaust equipment to extract the exhaust gases from the cell and maintain the required test cell pressure. The engine exhaust nozzle pressure ratio (P_c/P'_t), which is equivalent to $P_{amb}/P_{t_{ne}}$, is also an ejector performance parameter (see Fig. 13); therefore, it is used as the ordinate in the ejector characteristic graphs. The ratio of the exhaust plenum pressure (ejector exit) to primary driving nozzle stagnation pressure P_{ex}/P'_t (the ejector operating pressure ratio) is used as the abscissa of the characteristics graphs, with the pressure rise produced by the ejector (P_{ex}/P_c) shown as a parameter in the graphs. The constant-area ejector was sized to produce the minimum exhaust nozzle pressure ratio at maximum engine thrust, which corresponds to the maximum jet diameter. At flight Mach numbers and engine thrust levels less than maximum, energy is dissipated in expanding the jet sufficiently to fill the large duct. Consequently, the volume flow and power required of the exhaust equipment are larger than would be required if the ejector area could be

adjusted to produce the maximum pressure recovery (P_{ex}/P_c). The variable-area second-throat ejector provides for near optimum matching of the ejector and engine at all engine power levels.

4.2.1 Constant-Area Ejector

The ejector characteristics of the $A_d/A^* = 3.987$ and 5.756 configurations were presented in Ref. 1 and, therefore, will not be presented in this report. The characteristics of the remaining configurations are presented in Fig. 13. The ejector performance characteristics were for the most part determined at primary driving nozzle pressures of 20 and 35 psia. However for the $A_d/A^* = 8.767$ configuration, the secondary air supply system limit was exceeded for $\dot{m}''/\dot{m}'$ in excess of approximately 0.9 at primary driving nozzle pressures in excess of 14 psia, therefore, the performance of the $A_d/A^* = 8.767$ configuration at $\dot{m}''/\dot{m}' = 0.9$ was determined at $P_t' = 14$ psia.

4.2.2 Variable-Area Ejector

The performance characteristics of the variable-area ejector having constant-area and converging mixing ducts are presented in Figs. 14 and 15, respectively. These characteristics were determined at primary driving nozzle pressures (P_t') of 10 and 35 psia except for the $A_d/A^* = 8.767$ configuration. A comparison of configurations tested at $\dot{m}''/\dot{m}' = 0.05$ and maximum, which are typical of jet engine test operation in direct-connect and free-jet installations, respectively, are presented in Fig. 16. These data indicate that the minumum value of P_c/P_t' for all three geometries is essentially identical However, the values of P_{ex}/P_t' and thus P_{ex}/P_c, which are measures of the required exhaust system pressure produced by the variable-area ejector, exceeded those for the constant-area ejector by as much as 100 percent, as shown in Fig. 16. Note in Fig. 16a at $\dot{m}''/\dot{m}' = 0.05$ and $P_c/P_t' = 0.05$ that the values of P_{ex}/P_t' for the constant-area and the variable-area ejectors are 0.105 and 0.226, respectively, which corresponds to an improvement of 115 percent. The improvement decreases as A_d/A^* increases as is indicated in Figs 16a, b, and c in which the maximum improvement was 115, 104, and 76 percent for $A_d/A^* = 8.767$, 17.285, and 28.351, respectively. The results of these tests show that the use of the variable-area ejector can improve the pumping capability of the test plant exhauster system over that obtained with a constant-area (cylindrical) ejector.

4.3 EFFECT OF DRIVING GAS STAGNATION PRESSURE ON EJECTOR PERFORMANCE

The performance characteristics of the variable-area ejector with constant-area and converging mixing duct are presented in Figs. 17 through 21 at primary driving nozzle stagnation pressures (P_t') of 5, 10, 20, and 35 psia where possible and $\dot{m}''/\dot{m}'$ of 0, 0.05, and 0.10 to determine the effect of stagnation pressure variation on performance.

Performance graphs of individual configurations are presented in Figs. 17 through 21. The minimum value of P_c/P_t' and P_{ex}/P_t' was obtained for every configuration at all values of P_t' except for the $A_d/A^* = 5.756$ at $P_t' = 5$ psia (see Fig. 18a) for which the exhaust system pressure could not be decreased sufficiently to produce the minimum value of P_c/P_t'. The variation in the minimum value of P_c/P_t' for several values of P_t' at $\dot{m}''/\dot{m}'$ of 0.05 and 0.10 are presented in summary graphs in Fig. 22. These data show that the effect of the magnitude of P_t' on the minimum value of P_c/P_t' and P_{ex}/P_t' was for the most part small for $\dot{m}''/\dot{m}' = 0.05$ and 0.10 for all configurations tested. However, at $\dot{m}''/\dot{m}' = 0$, $(P_c/P_t')_{min}$ varied inversely with P_t', and the magnitude of the variation increased with increasing A_d/A^*, as shown in Figs. 23a and b. These characteristics are identical to those of Ref. 4 for secondary flow rate of zero.

4.4 TRANSIENT PERFORMANCE

Turbojet engines undergo power transients in flight as a result of throttle movement (rapid transients) and aircraft Mach number altitude changes (slow transients). The transients resulting from throttle movement usually occur at some fixed altitude and thus a constant value of ambient pressure while those resulting from Mach number-altitude transients may occur at a given altitude or during aircraft climbs or dives. The simulation of engine power transients in ground test facilities requires the control of the test cell (ambient) pressure. This is difficult to attain because of the interaction of the exhaust gas ejector and the plant exhaust systems. The performance characteristics of the variable-area ejector indicated that it might be used to control test cell pressure during these transients. Therefore, various methods were employed to simulate engine power transients and the control of test cell pressure during those transient operations

4.4.1 Effect of Nozzle Plugs on Ejector Characteristics

Nozzle plugs were used to produce a change in the primary driving nozzle throat areas to simulate engine power transients from intermediate to maximum and vice versa as discussed in Section 3.0. The steady-state performance characteristics of the ejectors with and without plugs are presented in Figs. 24 and 25 to show the degree of simulation achieved with the nozzle plugs. The performance of the $A_d/A^* = 3.987$ configuration at $P_t' = 20$ psia and $\dot{m}''/\dot{m}' = 0.05$ with and without the nozzle plug installed is presented in Fig. 24a. The performance indicates that the nozzle plug installation upstream of the primary driving nozzle had no adverse effect on the performance of the configuration. Figure 24b is a presentation of the same performance comparison for the $A_d/A^* = 17.285$ configuration. Again, the test results presented in Fig. 24b indicate that the nozzle plug installed in the retracted position produced no adverse effects on the performance of the ejector.

The plugs inserted into the primary driving nozzle throats of the $A_d/A^* = 3.987$ and 17.285 configurations were designed to produce area ratios equivalent to the $A_d/A^* = 5.756$ and 28.351 configurations, respectively. However, the nozzle area ratios (A_{ne}/A^*) of the primary driving nozzles with plugs inserted are considerably larger than the nozzles to be simulated. The primary driving nozzle in the $A_d/A^* = 3.987$ configuration with the plug inserted had an $A_{ne}/A^* = 2.363$ which corresponds to a one-dimensional Mach number, $M_{ne} = 2.38$; however, its counterpart, the $A_d/A^* = 5.756$ configuration nozzle, had an $A_{ne}/A^* = 1.660$ and a corresponding Mach number, $M_{ne} = 1.98$. The configuration having the larger value of nozzle exit Mach number should produce the best pumping performance. The experimental performance of these configurations is presented in Fig. 25a. The minimum value of P_c/P_t' for the configuration with the plug ($M_{ne} = 2.38$) was approximately 11 percent smaller than that of the $A_d/A^* = 5.756$ configuration ($M_{ne} = 1.98$). The same comparisons are presented in Fig. 25b for the $A_d/A^* = 28.351$ configuration and the $A_d/A^* = 17.285$ configuration with the plug inserted into the primary driving nozzle throat which produced an effective A_d/A^* of 28.351. The area ratios and Mach numbers of the primary nozzle with and without the plug inserted in the nozzle were $A_{ne}/A^* = 4.808$ ($M_{ne} = 3.13$) and $A_{ne}/A^* = 2.932$ ($M_{ne} = 2.61$), respectively. The minimum value of P_c/P_t' for the configuration with the plug ($M_{ne} = 3.13$) was approximately 20 percent larger than that of the $A_d/A^* = 28.351$ configuration ($M_{ne} = 2.61$). Although the exit Mach number was higher for the plug inserted case, the mass flow ratio was also higher by about 70 percent; therefore, no conclusion can be made regarding the effect of the exit Mach number on $(P_c/P_t')_{min}$.

4.4.2 Variable-Area Ejector Centerbody Transients

Variable-area ejector centerbody transients were conducted with the $A_d/A^* = 3.987$ and 17.285 configurations with and without nozzle plugs inserted into the nozzle throats to simulate jet engine operation at intermediate and maximum power, respectively. The results are presented in Figs. 26a, b, and c. The variation of P_c/P_t' for several values of P_{ex}/P_t' are presented as a function of the axial position of the variable-area ejector centerbody for the primary driving nozzle pressure of 20 psia and secondary mass flow ratio of 0.05 without and with primary driving nozzle plugs inserted. The $A_d/A^* = 3.987$ configuration with the nozzle plug inserted was evaluated at $\dot{m}''/\dot{m}' = 0.05$ and 0.072 to determine the influence of mass ratio on the response of P_c/P_t' to centerbody movement. The results, presented in Fig. 26b, indicate that the effect was a very small increase in the value of P_c/P_t' when $\dot{m}''/\dot{m}'$ increased from 0.05 to 0.072.

A step change in the minimum value of P_c/P_t' for the $A_d/A^* = 3.987$ occurred as the centerbody passed the position at which the minimum flow area of the ejector occurs simultaneously at the duct angle change and the maximum diameter of the centerbody

as shown in Fig. 26a (see Fig. 8). The useful range of centerbody movement for minimum values of P_c/P_t' was approximately 1.5 to 3 in. depending on the value of A_d/A^*, as indicated in Fig. 26. The useful range is that portion of the centerbody travel wherein P_c/P_t' is influenced, which for these tests was a movement of approximately one-half the ejector mixing duct diameter. The axial position at which the second-throat area began to affect P_c was a function of A_d/A^*, as can be seen by comparing the axial position (Y) at which P_c/P_t' began to increase in Figs. 26a, b, and c.

4.4.3 Primary Driving Nozzle Total Pressure Transients

Several exhaust nozzle-ejector transient methods were investigated to develop an operationally acceptable method for maintaining a constant value of P_c during engine power transient operation. The first method consisted of varying P_t' for a fixed value of A* which produces a thrust increase comparable to that produced in an engine transient. The pressure (P_t') was varied from 10.05 to 20 psia in the $A_d/A^* = 5.756$ configuration for the following initial values of the ejector inlet parameters: $\dot{m}'' = 0.116$ lbm/sec, $P_c = 1.0$ psia, $P_{ex} = 2.9$ psia, and the axial position of the centerbody fixed at Y = 2.3 in.

The results of the transient for the initial conditions stated above are presented in Fig. 27 and show that P_c decreased rapidly as P_t' was increased and returned to its original value of 1.0 psia as P_t' approached 20 psia. The decrease in P_c was the result of increasing the primary mass flow and hence decreasing the $\dot{m}''/\dot{m}'$ parameter as shown in Fig. 27. Thereafter, P_c increased with P_t' until P_t' reached 20 psia, the originally established transient end-point. The value of P_c decreased during the transient by 20 percent which corresponds to an altitude change from approximately 60,000 to 65,500 ft. The transient data presented in Fig. 27 can be correlated back to the performance data (Figs. 18b and c) by selecting a specific value for P_t' and determining from Fig. 27 the values of P_c/P_t', P_{ex}/P_t', and $\dot{m}''/\dot{m}'$ at the selected value of P_t'.

4.4.4 Nozzle Plug Transients

The second method of simulating engine power transients consisted of changing the primary nozzle throat area by moving a plug in and out of the nozzle throat, thus changing the primary mass flow at fixed values of nozzle stagnation pressure and secondary mass flow which more nearly simulates engine testing techniques. The primary nozzle pressure (P_t'), centerbody position (Y), ejector exit pressure (P_{ex}), and the secondary mass flow ($\dot{m}''$) were held constant while the nozzle plug was withdrawn from the $A_d/A^* = 3.987$ configuration nozzle ($A_d/A^* = 5.756$ at the initiation of transient) for each of the transients performed. The results of these tests are presented in Fig. 28. The transient points were established in the exact same manner as before, and the nozzle plug was very rapidly

withdrawn (Fig. 28a) and more slowly withdrawn (Figs. 28b and c) to simulate an engine power change from intermediate to maximum. The ability of the system to recover to the set value of P_c was determined by the precision employed in selecting the set conditions. The procedure employed (see Section 3.0) involved the use of the data in Figs. 26a and b. Cell pressure (P_c) varied from the initial set conditions approximately 8 to 14 percent for all transients presented in Fig. 28 with the exception of No. 3 in Fig. 28b which produced a variation of 22 percent. Therefore, the nozzle-plug system produced smaller variations in P_c during transient operation than did the P_t' transients presented earlier. The nozzle plug transients produced an increase in primary nozzle throat area and the associated primary mass flow which resulted in a decrease in A_{ne}/A^*, A_d/A^*, and $\dot{m}''/\dot{m}'$, while P_t' transients produced an increase in primary mass flow which resulted in a decrease in $\dot{m}''/\dot{m}'$ only.

4.4.5 Transients with Secondary Flow Variation

A review of the effect of $\dot{m}''/\dot{m}'$ on P_c/P_t' (see Fig. 14) indicates that the excursion in P_c during engine power transients using any of the methods outlined herein might be minimized or eliminated by the transient variation of secondary flow ($\dot{m}''$). Thus, the performance of the $A_d/A^* = 3.987$ configuration with the nozzle plug inserted was documented during a simulated engine power transient from idle to maximum to establish P_c response characteristics without transient variation of $\dot{m}''$. The initial conditions were: $P_t' = 5$ psia, $P_c = 2.4$ psia, $P_{ex} = 3.02$ psia, $\dot{m}'' = 0.168$ lbm/sec, and centerbody position $Y = 2.0$ in. The results are presented graphically in Fig. 29. Cell pressure (P_c) decreased from 2.4 to 1.0 psia (58-percent variation) during acceleration from idle to intermediate power ($P_t' = 5$ psia to $P_t' = 11$ psia) and recovered to 2.35 psia as the nozzle plug was withdrawn (maximum power). The intermediate power point was re-established by inserting the plug in the nozzle which caused P_c to decrease to the value of approximately 1.0 psia (see Fig. 29). Secondary mass flow ($\dot{m}''$) was then increased until P_c again reached 2.4 psia. The value of $\dot{m}''/\dot{m}'$ required to change P_c from 1.0 to 2.4 psia (the level of P_c at the beginning of the transient) was 0.16, which is equivalent to three times that required to cool the engine and test cell equipment during operation at maximum engine power. However, during engine testing, the increase in $\dot{m}''$ would occur at small values of thrust (mass and volume flow) and, therefore, would not tax the exhaust equipment which would be operating in the configuration required to pump the larger mass flow generated at the high power end of the transient.

4.4.6 Effect of $\dot{m}''$ Variation during a P_t' Transient

Pressure (P_t') transients, in which P_c was controlled by manually varying the secondary flow ($\dot{m}''$). were conducted for the $A_d/A^* = 8.767$ configuration. The results for two consecutive test points are presented in Figs. 30a and b. The initial conditions were: $P_t' = 5$ psia, $P_c = 0.58$ psia, $P_{ex} = 1.12$ psia, $\dot{m}''/\dot{m}' = 0.035$ for P_t' of 20 psia, and centerbody

position Y = 2.75 in. The manually controlled secondary airflow varied from 0.054 to 0.149 lbm/sec which corresponds to a range in $\dot{m}''/\dot{m}'$ of 0.035 to 0.097 for the A_d/A^* = 8.767 configuration operating at P_t' = 20 psia. The use of secondary flow variation for controlling P_c during engine power transients is thus shown to be practical and very effective when used in combination with a variable-area-type ejector. However, an automatic control system would be required to produce satisfactory results in turbine engine tests.

The following is a summary of the transient methods studied and reported herein. Altitude, Mach number, and the combination of altitude-Mach number transients were simulated by varying the ejector second throat (centerbody translation) at fixed values of P_{ex}. Since these transients are relatively slow (quasi steady-state), a relatively slow movement of the ejector centerbody meets the requirement. However, the centerbody is too heavy to move at the rate required to control P_c during engine power transients. Therefore, the engine power transients were simulated by prepositioning the ejector centerbody to establish the value of second-throat area required to make the desired value of P_c insensitive to P_{ex} at the high power end of the transient. Then, P_{ex} was preadjusted to effect the same value of P_c at the low power end of the transient The transient was then performed by either moving the nozzle plug into or out of the nozzle throat or by establishing a ramp change in P_t'. Test cell cooling airflow was varied during two engine power transients to minimize the variation in P_c. The combination of preadjusting the centerbody position and P_{ex} and varying cell cooling airflow during the transient operation resulted in satisfactory control of P_c during the simulated engine power transient operation without variation of the plant exhaust system pressure.

5.0 APPLICATION AND PERFORMANCE COMPARISONS

5.1 GENERAL

The application of the constant-area and the variable-area ejectors in aerospace propulsion system ground test facilities is presented to compare their performance. Performance comparisons of the ejectors were derived for tests of one low-bypass-ratio, mixed-flow turbofan with a design flight Mach number of 2.5 and the two turbojet engines with design flight Mach numbers of 2.5 and 3.8.

5.2 CONSTANT-AREA AND VARIABLE-AREA EJECTOR PERFORMANCE COMPARISON

Ejector design and performance analysis requires the knowledge of certain test engine geometrical and performance parameters which vary with engine type (mixed-flow turbofan, turbojet) and design Mach number. Exhaust nozzle pressure ratio versus flight Mach number for the typical engines under consideration is presented in Fig. 12. The remaining engine performance parameters of interest are functions of engine power settings and are presented in the following table:

Engine Power Setting	Mixed-Flow Turbofan		Turbojet	
	$\dot{m}''/\dot{m}'$	A^*_{max}/A^*_{int}	$\dot{m}''/\dot{m}'$	A^*_{max}/A^*_{int}
Intermediate	0.05	1	0.05	1
Maximum	0.10	1.8	0.10	1.44

Representative constant-area and variable-area ejector performance comparisons were calculated at the tropopause (36,089-ft altitude) using Ref. 5. It was assumed that the test facility exhaust system could maintain a test cell pressure corresponding to the ambient pressure at 36,089-ft altitude (3.29 psia). Therefore, the ejector exit pressure would be 3.29 psia, and the test cell pressure would decrease by the amount of the ejector pressure rise or $P_c = 3.29/(P_{ex}/P_c)$ psia.

The altitude gains versus flight Mach number which can reasonably be expected to result from the use of the variable-area ejector as compared to the cylindrical ejector are presented graphically in Figs. 31, 32, and 33. The zero altitude line in each figure corresponds to an altitude of 36,089 ft.

The method used to calculate the ejector comparison curves (Figs. 31, 32, and 33) is explained in the following example for the turbojet engine with a design Mach number of 3.8.

The minimum value of P_c/P'_t at the design Mach number of the engine (M_{design} = 3.8) was determined from Fig. 12 to be 0.0125. The ejector that will produce this value of P_c/P'_t at maximum power with a mass ratio ($\dot{m}''/\dot{m}'$) of 0.05 has an area ratio A_d/A^* = 17.285 (Fig. 13b for constant-area ejector and Fig. 15b for the variable-area ejector). The corresponding values of P_{ex}/P'_t from the figures are 0.063 for the constant-area ejector and 0.080 for the variable-area ejector. The ejector rise ratios

$$(P_{ex}/P_c) = (P_{ex}/P'_t)/(P_c/P'_t)$$

are 3.6 and 4.8, respectively. Therefore, the test cell pressure (ambient altitude pressure) produced by the ejectors

$$\left(P_c = \frac{P_{ex}}{(P_{ex}/P_c)} = \frac{3.29}{(P_{ex}/P_c)}\right)$$

are 0.654 and 0.507 psia, respectively. The corresponding ambient altitudes for the constant-area and the variable-area ejectors are 69,600 and 74,900 ft, respectively. Thus the altitude gain for the variable-area ejector exceeded that for the constant-area ejector by 5,300 ft for engine operation at the design Mach number and maximum power (Fig. 31). The procedure was repeated at various Mach numbers within the engine envelope to produce the characteristics at maximum power for the constant-area and the variable-area ejector configurations. Turbojet engine operation at maximum power results in an engine nozzle throat area of approximately 1.44 times that at intermediate power (see table above) and thus a corresponding decrease in A_d/A^*. Therefore, the ejector comparison at intermediate power requires an A_d/A^* of 17.28 x 1.44 = 24.89. The available configuration, however, is the A_d/A^* = 28.351, which was used for the comparisons. Corresponding altitude gains at intermediate power were 6,000 and -600 ft, M_∞ = 3.8 and 1.0, respectively. However, the maximum gains at both power settings occurred in the middle range of M_∞. The maximum gain at maximum power was 14,000 ft at M_∞ = 3.0 and at intermediate power was 10,000 ft at M_∞ = 2.5 to 3.0. In this application, the altitude gain increased from a minimun at M_∞ = 1.0 to a maximum at M_∞ = 2.5 to 3.0, at which point it begins a continual decrease to the M_∞ = 3.8 design point. The results of the comparison study show the performance advantage of the variable-area ejector, particulary at intermediate power operation. An altitude gain of 14,000 ft (36,000 to 50,000 ft) corresponds to an ejector rise ratio improvement of 1.96 or

$$(P_{ex}/P_c)_{var} = (P_{ex}/P_c)_{CYL} \times 1.96$$

The ejector configurations used in the comparisons for the other engines were: A_d/A^* = 5.756 and 8.767 for the design Mach number 2.5 turbojet and A_d/A^* = 3.987 and 8.767 for the design Mach number 2.5 mixed-flow turbofan.

In the mixed-flow turbofan test application (Fig. 32) the variable-area ejector altitude gains exceeded those of the cylindrical ejector by 8,000 ft at the design point (M_∞ = 2.5, maximum power) and by 2,600 ft at M_∞ = 1.0, maximum power. However, at intermediate power, the altitude gains of the variable-area ejector were 9,500 and 6,200 ft at M_∞ = 2.5 and 1.0, respectively.

In the M_∞ = 2.5 turbojet test application (Fig. 33), the variable-area ejector altitude gains exceeded those of the cylindrical ejector by 6,000 ft at the design point (M_∞ = 2.5, maximum power) and by 6,300 ft at M_∞ = 1.0, maximum power. However, at

intermediate power, the corresponding altitude gains were 13,000 and 6,200 ft, respectively. These gains exceed the corresponding gains in the mixed-flow turbofan application because the turbojet performance characteristic (P_c/P_t' versus M_∞ (Fig. 12)) is smaller and the turbojet exhaust nozzle throat undergoes a smaller increase in flow area during power change from intermediate to maximum than does that of the turbofan.

6.0 SUMMARY OF RESULTS

The results of the experimental study to determine the effect of primary driving nozzle pressure, mixing duct geometry, ratio of mixing duct area-to-nozzle throat area, and ratio of secondary-to-primary mass flow on the steady-state and transient performance characteristics of the centerbody-type variable-area second-throat ejector are summarized as follows:

1. The ejector driving nozzle pressure ratio ($(P_c/P_t')_{minimum}$) varied inversely with the nozzle stagnation pressure (P_t') at a mass ratio of zero for all configurations tested. The magnitude of the variation increased directly as the ratio of ejector mixing duct to driving nozzle area ratio (A_d/A^*) was increased. At ejector mass ratios from 0.05 to 1.4, the variation in P_t' had an insignificant effect on ejector performance parameters.

2. The difference in the performance characteristics of the variable-area ejector equipped with a constant area and a converging mixing duct was insignificant.

3. The control of test cell pressures (P_c) during simulated engine power transients was accomplished by prepositioning the variable-area ejector centerbody and/or by controlling secondary flow. The control of P_c during altitude, Mach number, and a combinations of altitude-Mach number transient simulations was accomplished by varying the centerbody position.

4. The altitude gains resulting from the use of the variable-area rather than the constant-area (cylindrical) ejector in testing a design Mach number 2.5 turbofan, 2.5 turbojet, and 3.8 turbojet were a maximum of 9,500, 23,000, and 14,000 ft at off-design conditions and 8,000, 6,000, and 5,300 ft at design conditions, respectively.

   The altitude increase of 14,000 ft corresponds to an altitude ambient pressure ratio of 1.96 which corresponds to an improvement of as much as 96 percent in the pumping capability of a plant exhauster system resulting from the use of a variable-area rather than a constant-area exhaust gas ejector.

5. The performance characteristics of all configurations tested were continuous except for that resulting from the ejector centerbody translation in the A_d/A^* = 3.987 configuration with and without the nozzle plug inserted in the nozzle throat.

REFERENCES

1. Taylor, Delbert, Duesterhaus, David A., and Simmons, Marvin. "Diffuser Studies." AEDC-TR-73-198 (AD774019). February 1974.

2. Lewis, W.G.E. and Drabble, J.S. "Ejector Experiments." National Gas Turbine Establishment, Pyestock, Haunts Report No. 151, February 1954.

3. Abernethy, R.B., Pratt & Whitney Aircraft, and Thompson, J. W., Jr., ARO, Inc. "Handbook Uncertainty in Gas Turbine Measurements." AEDC-TR-73-5 (AD755356), February 1973.

4. Bauer, R.C. and German, R.C. "Some Reynolds Number Effects on the Performance of Ejectors without Induced Flow." AEDC-TN-61-87 (AD262734), August 1961.

5. National Aeronautics and Space Administration, United States Weather Bureau. U.S. Standard Atmosphere. U.S. Government Printing Office, December 1962.

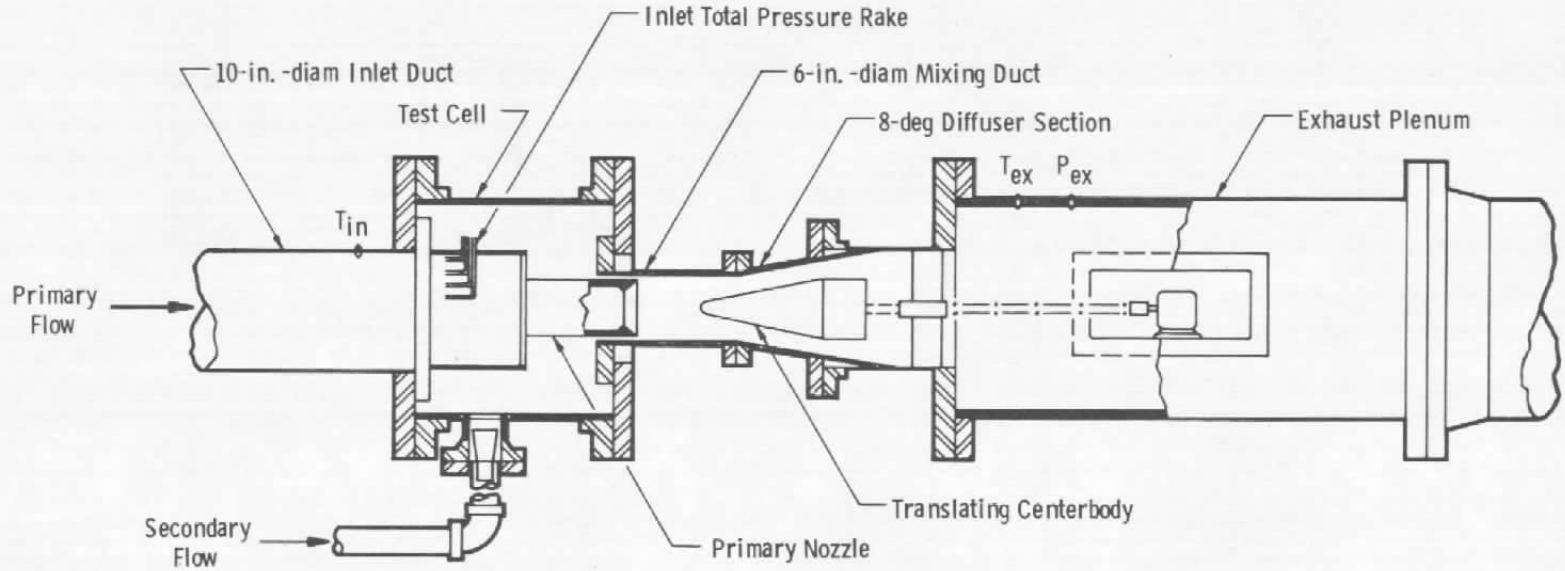

Figure 1. Installation of variable-area ejector.

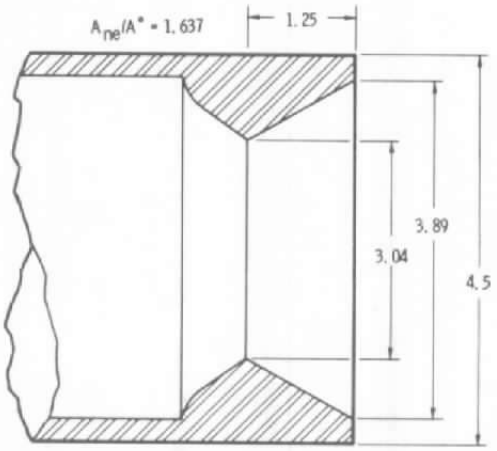

a. Details of the 3.04-in.-diam throat nozzle (A_d/A^* = 3.987)

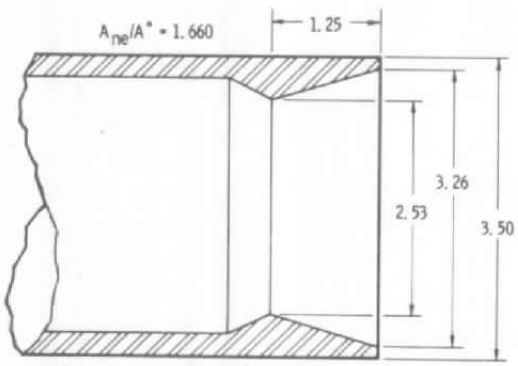

b. Details of the 2.53-in.-diam throat nozzle (A_d/A^* = 5.756)

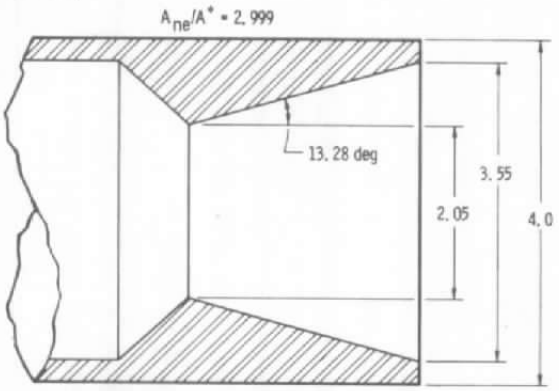

c. Details of the 2.05-in.-diam throat nozzle (A_d/A^* = 8.760)

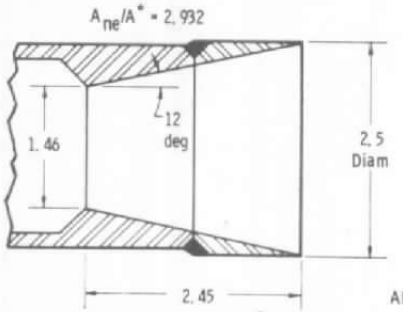

All Dimensions in Inches

d. Details of the 1.46-in.-diam throat nozzle (A_d/A^* = 17.285)

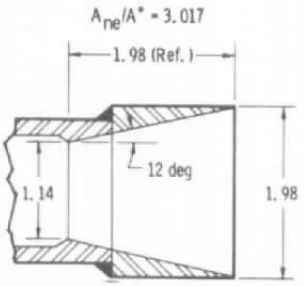

e. Details of the 1.14-in.-diam throat nozzle (A_d/A^* = 28.351)

Figure 2. Details of primary nozzles.

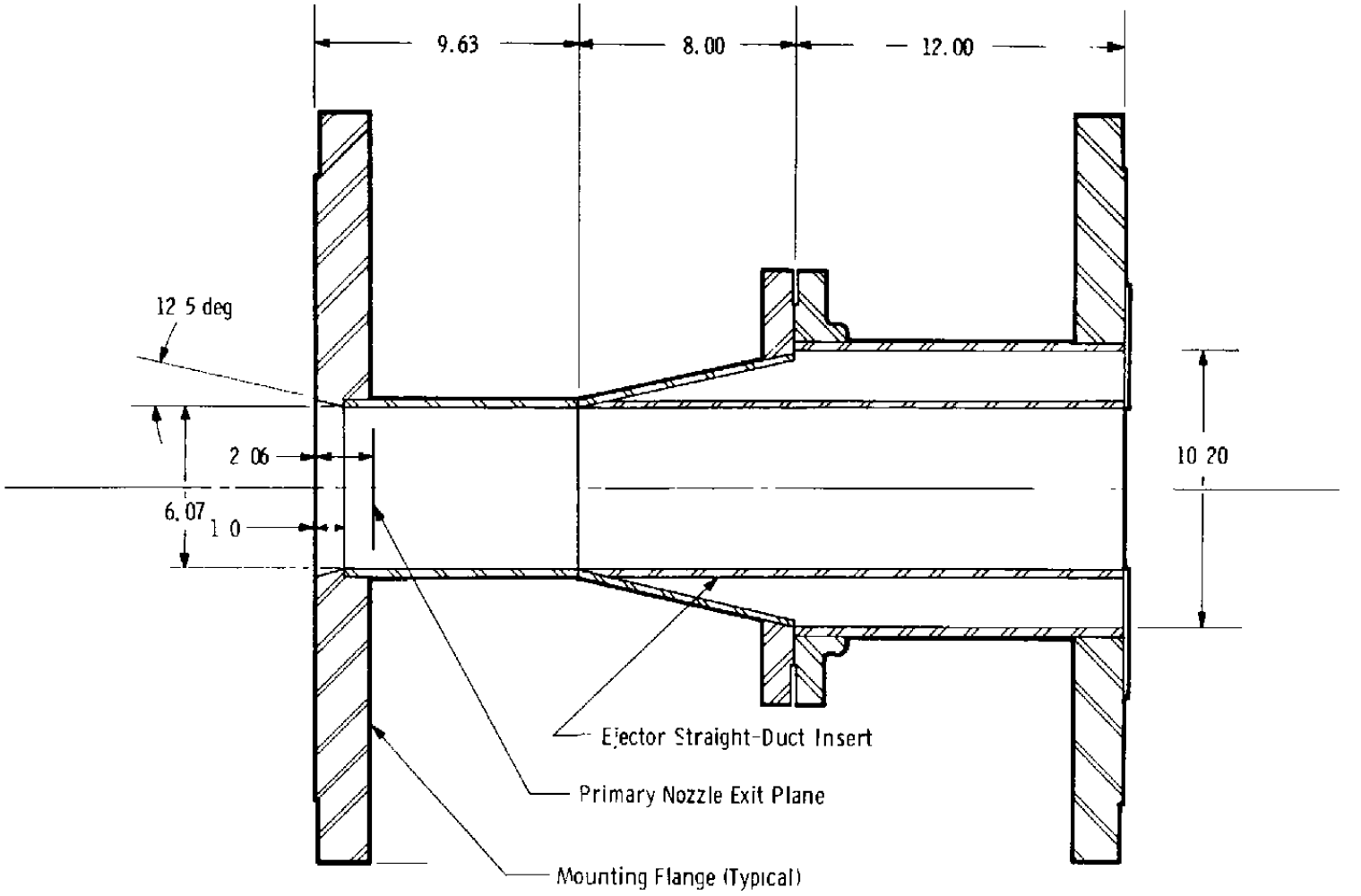

All Dimensions in Inches

Figure 3. Details of constant-area ejector.

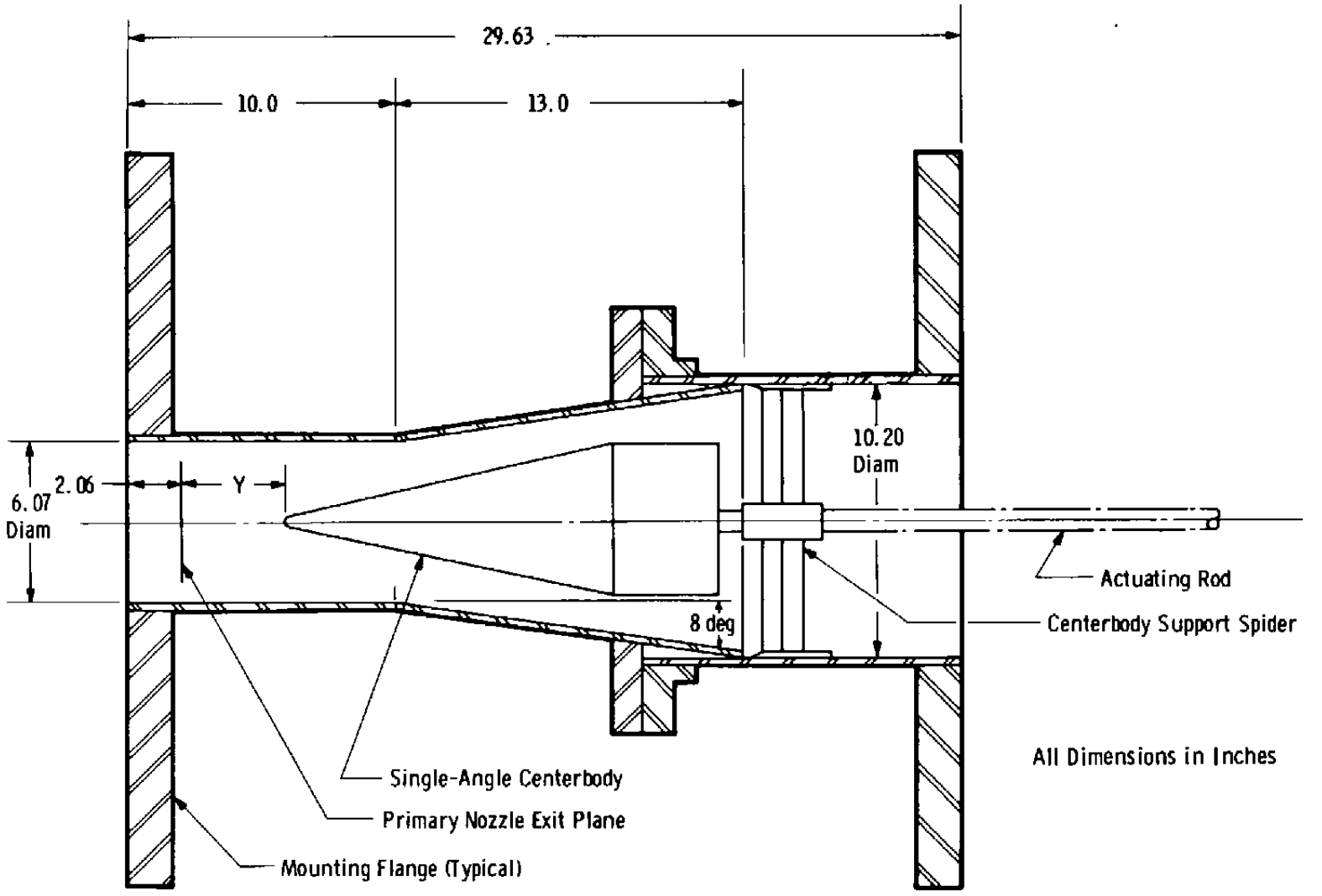

Figure 4. Variable-area ejector with the constant-area mixing duct.

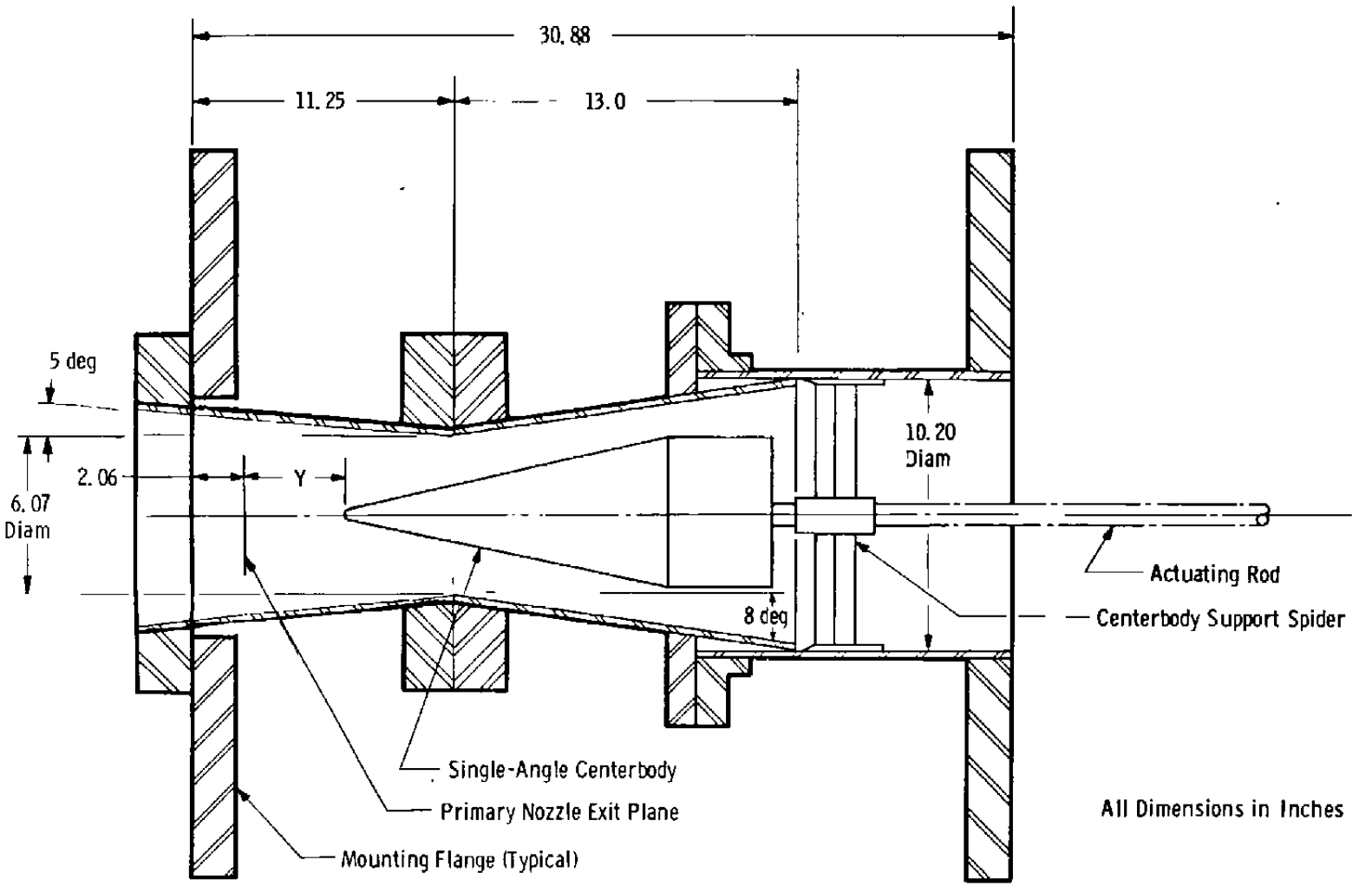

Figure 5. Variable-area ejector with the converging mixing duct.

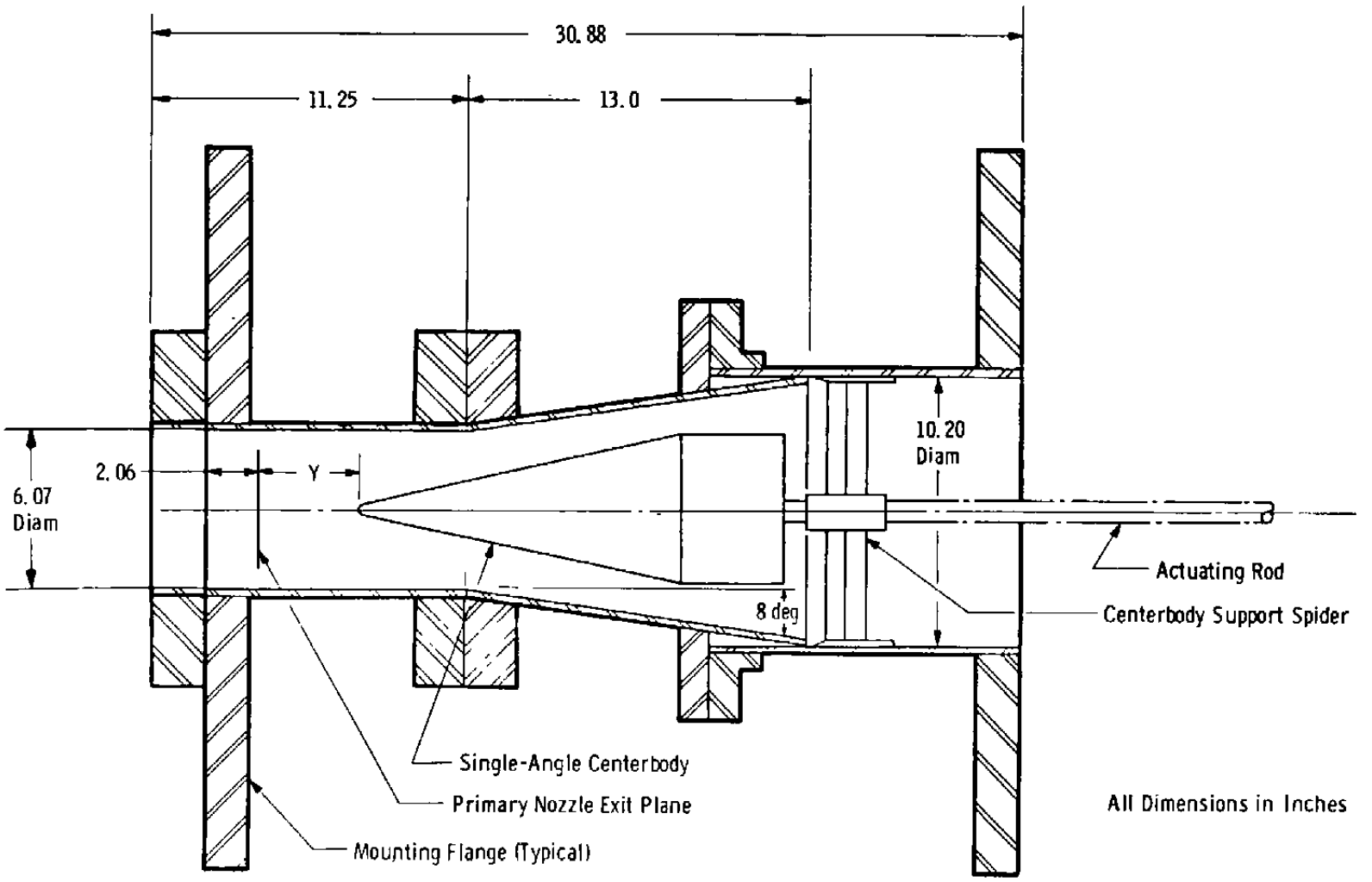

Figure 6. Variable-area ejector with the extended constant-area mixing duct.

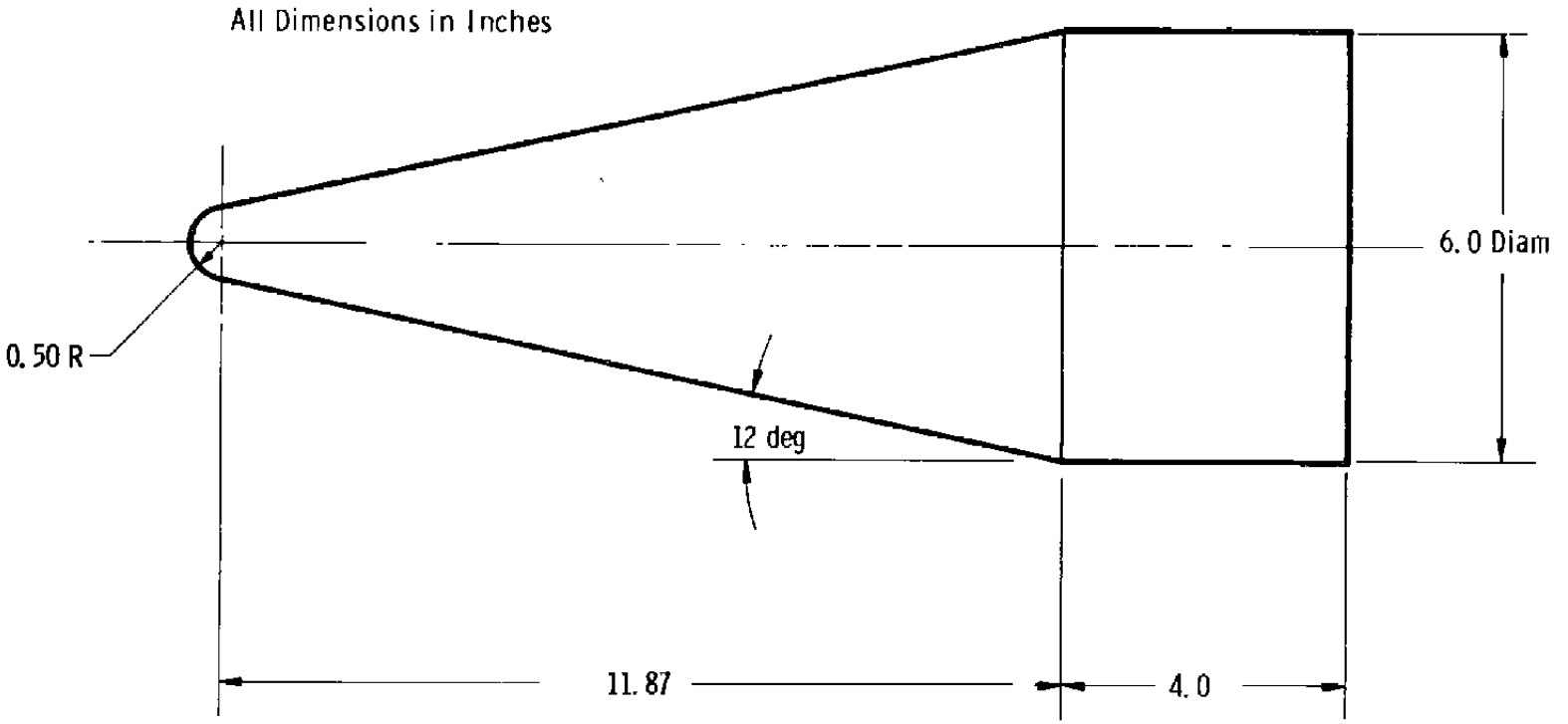

Figure 7. Details of centerbody.

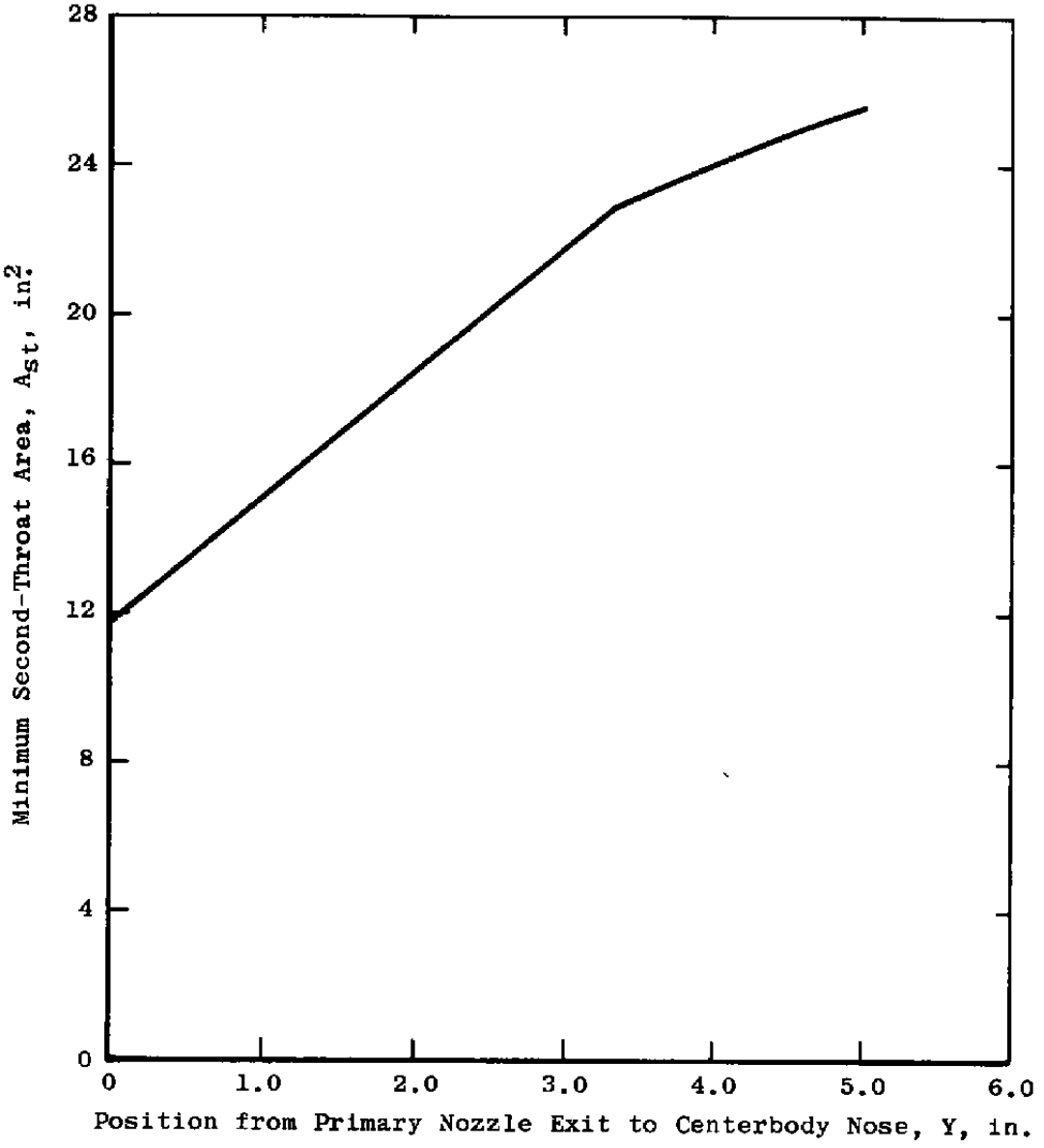

Figure 8. Minimum second-throat area versus centerbody position.

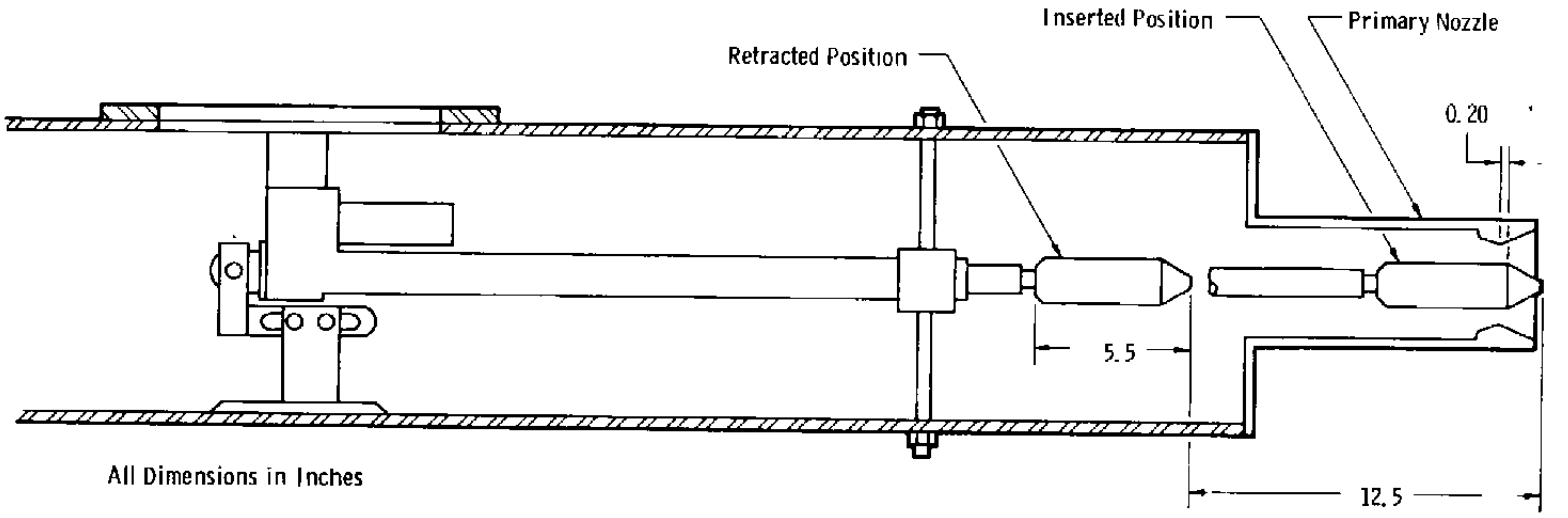

Figure 9. Installation of the primary nozzle plug system.

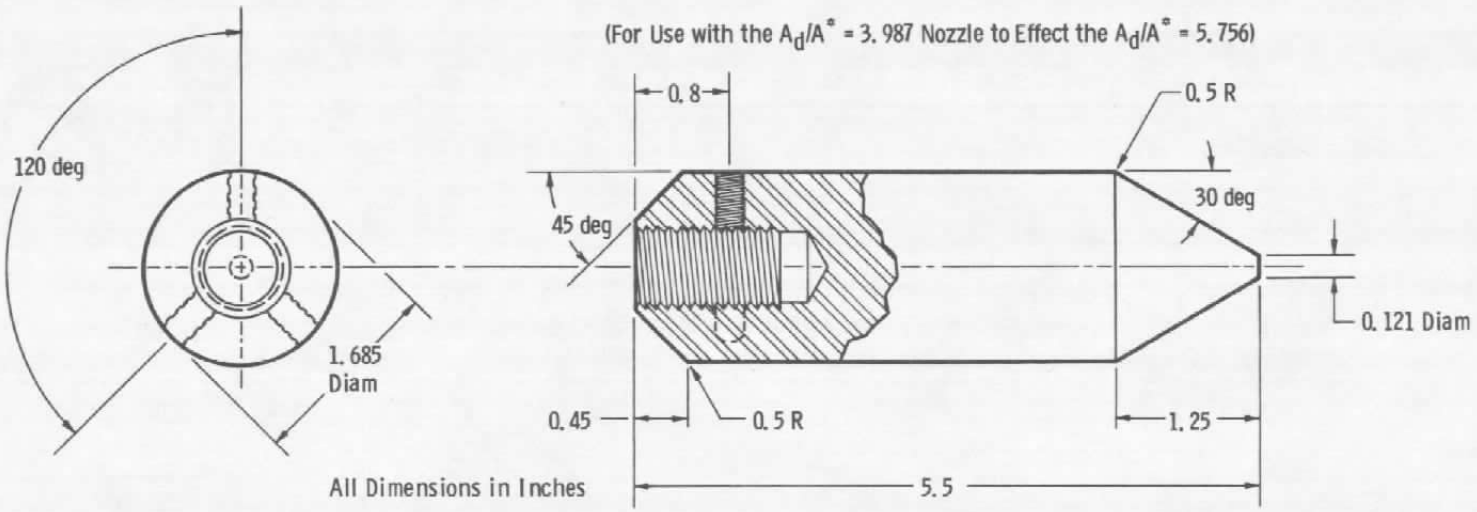

a. 1.685-in.-diam plug

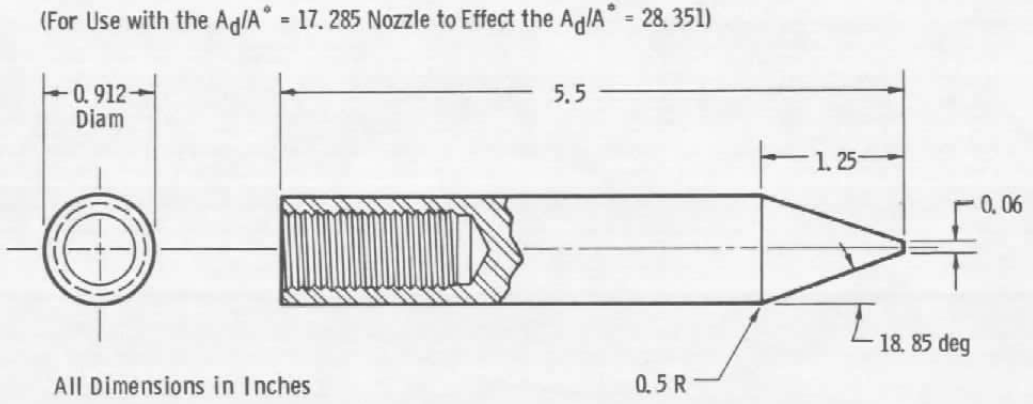

b. 0.912-in.-diam plug

Figure 10. Details of the primary nozzle plug.

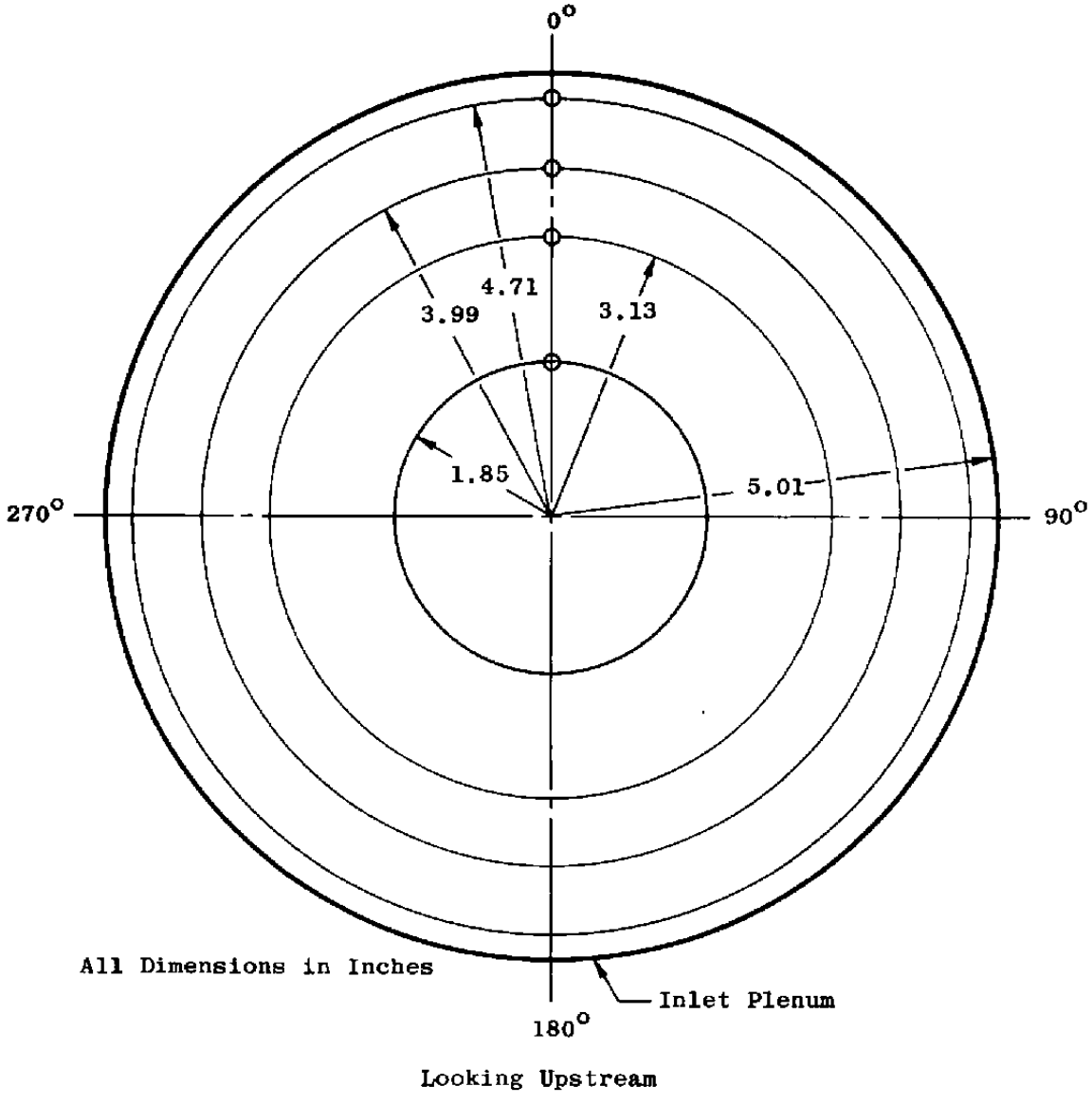

Figure 11. Inlet total pressure rake probe locations.

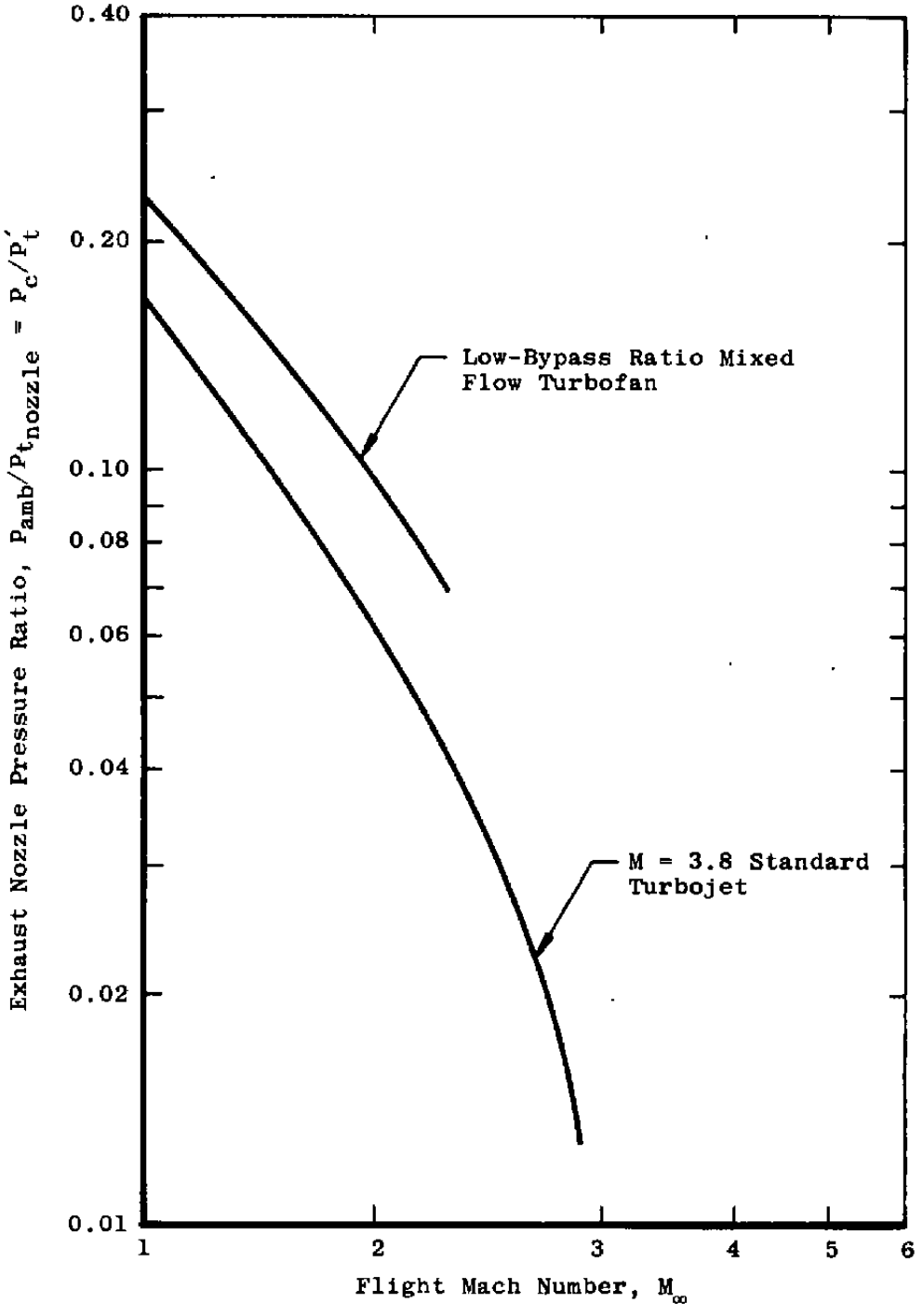

Figure 12. Estimated engine characteristics.

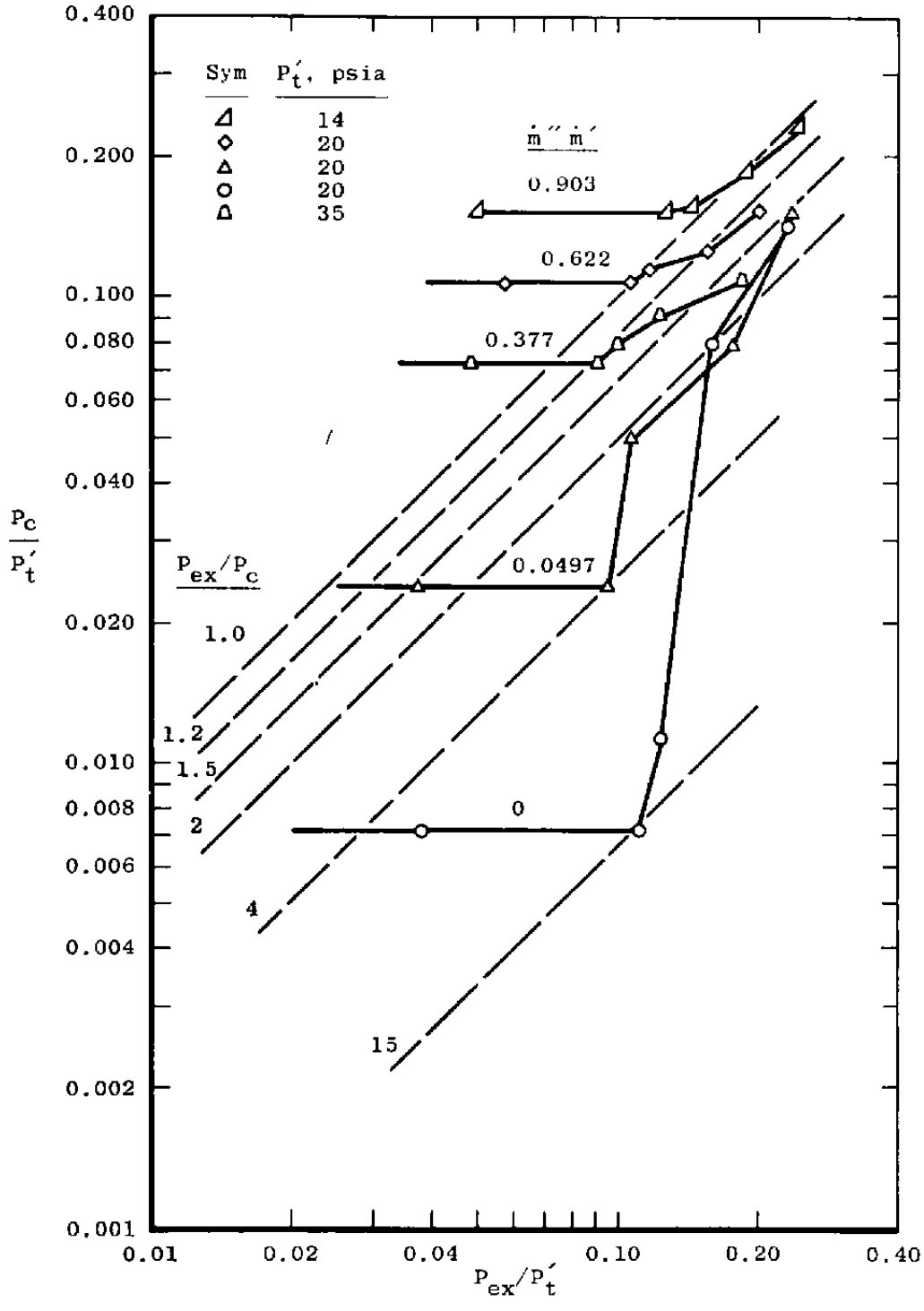

a. $A_d/A^* = 8.767$

Figure 13. Constant-area ejector performance.

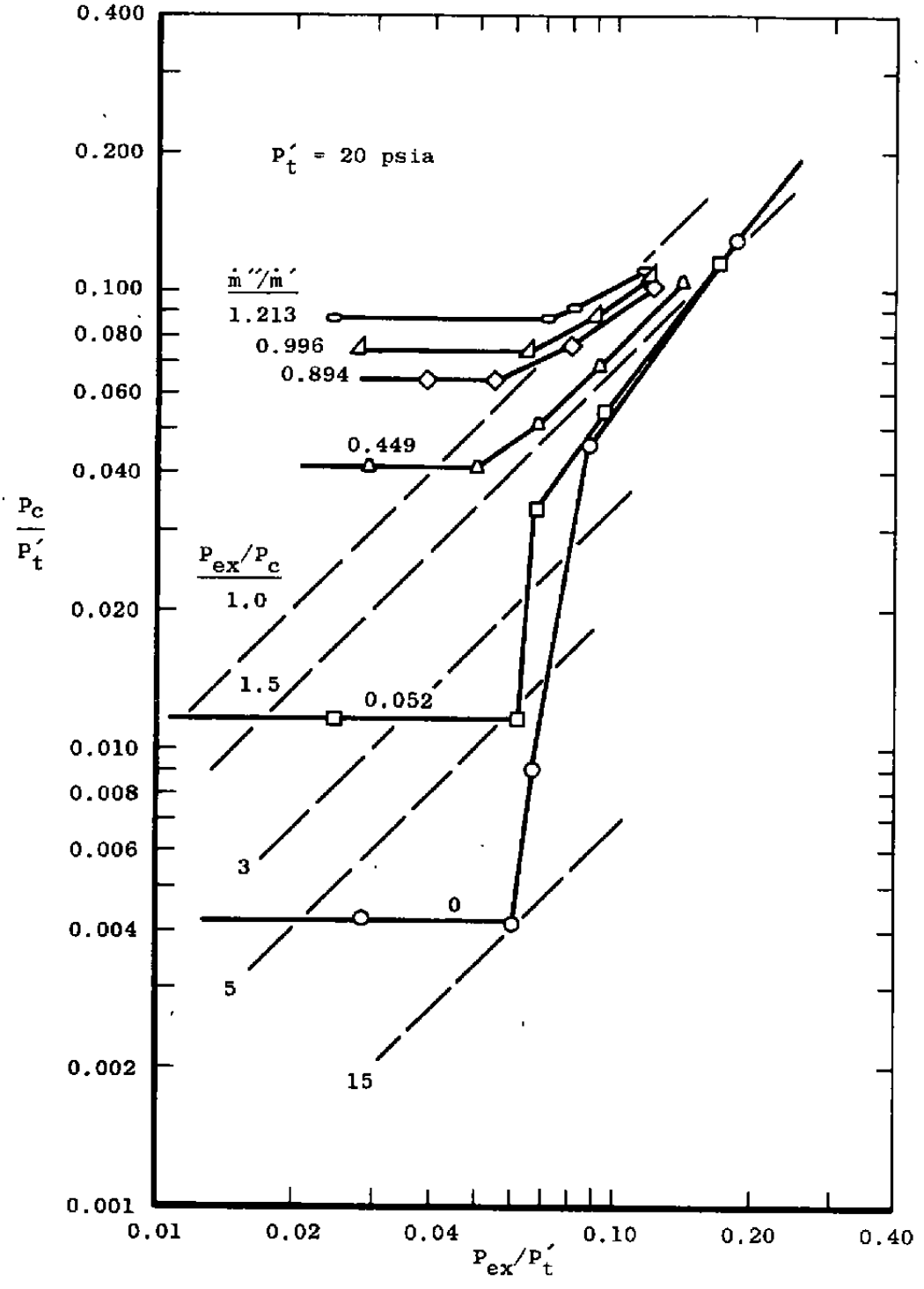

b. $A_d/A^* = 17.285$

Figure 13. Continued.

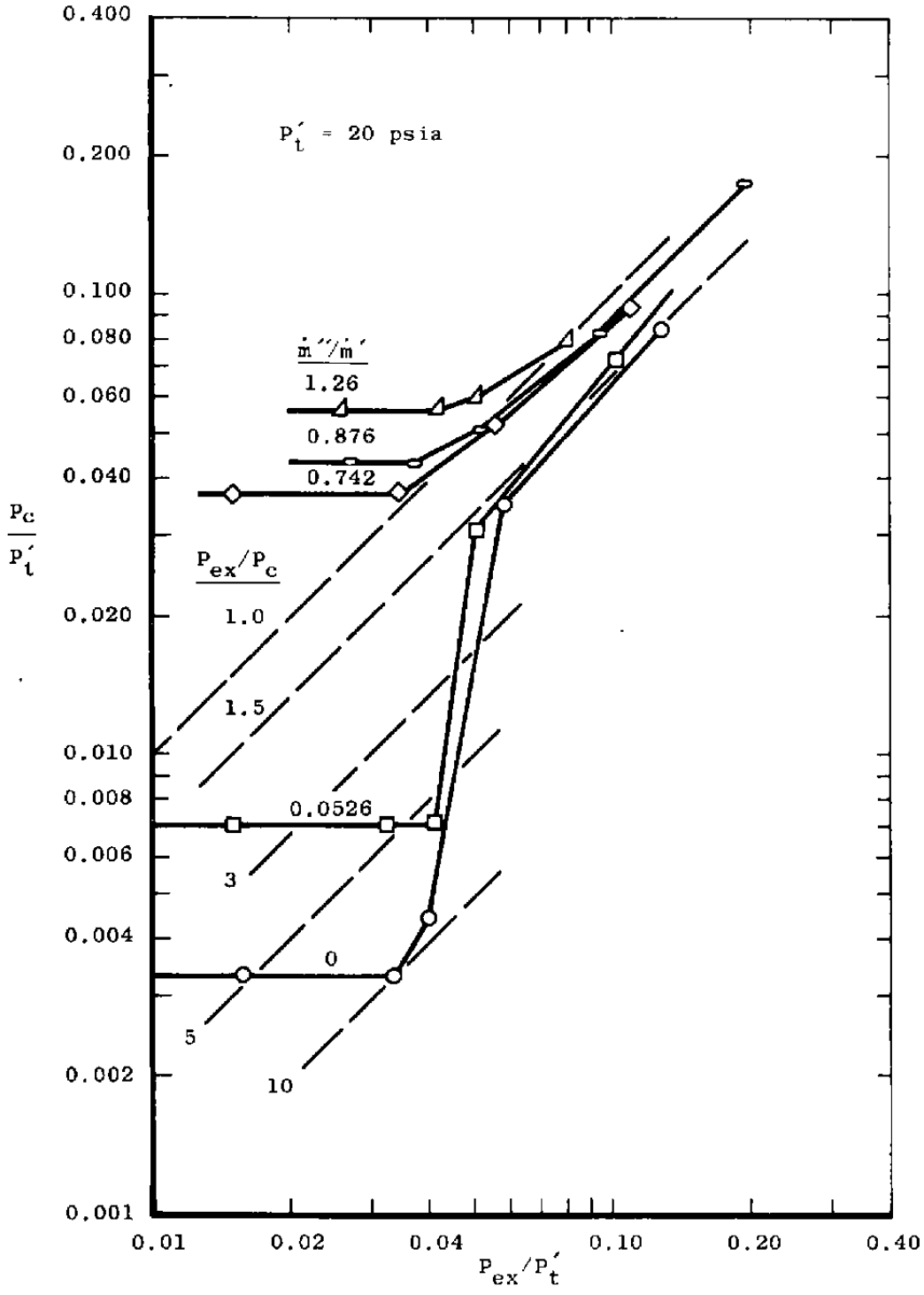

c. $A_d/A^* = 28.351$

Figure 13. Concluded.

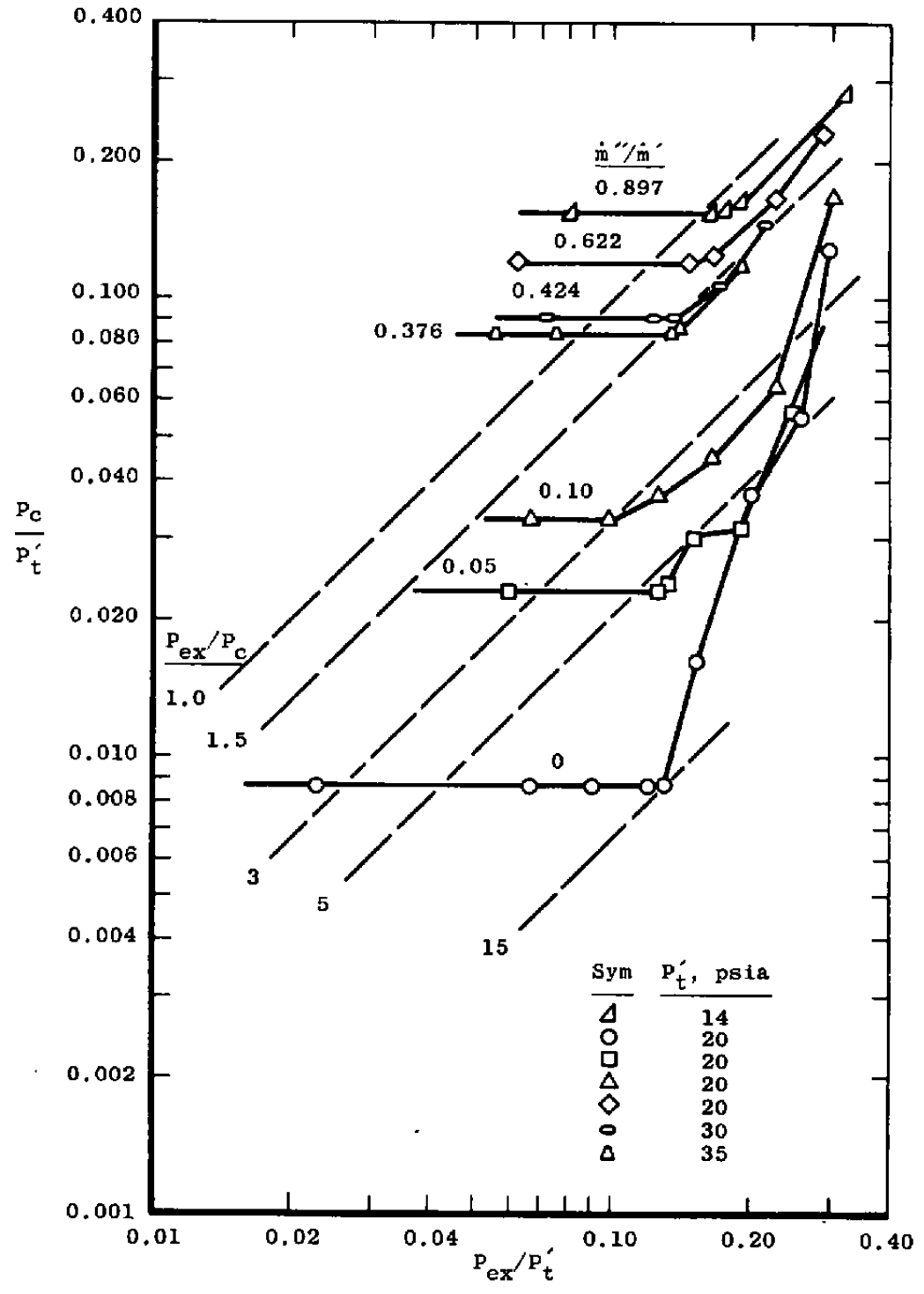

a. $A_d/A^* = 8.767$

Figure 14. Performance of variable-area ejector with a constant-area mixing duct.

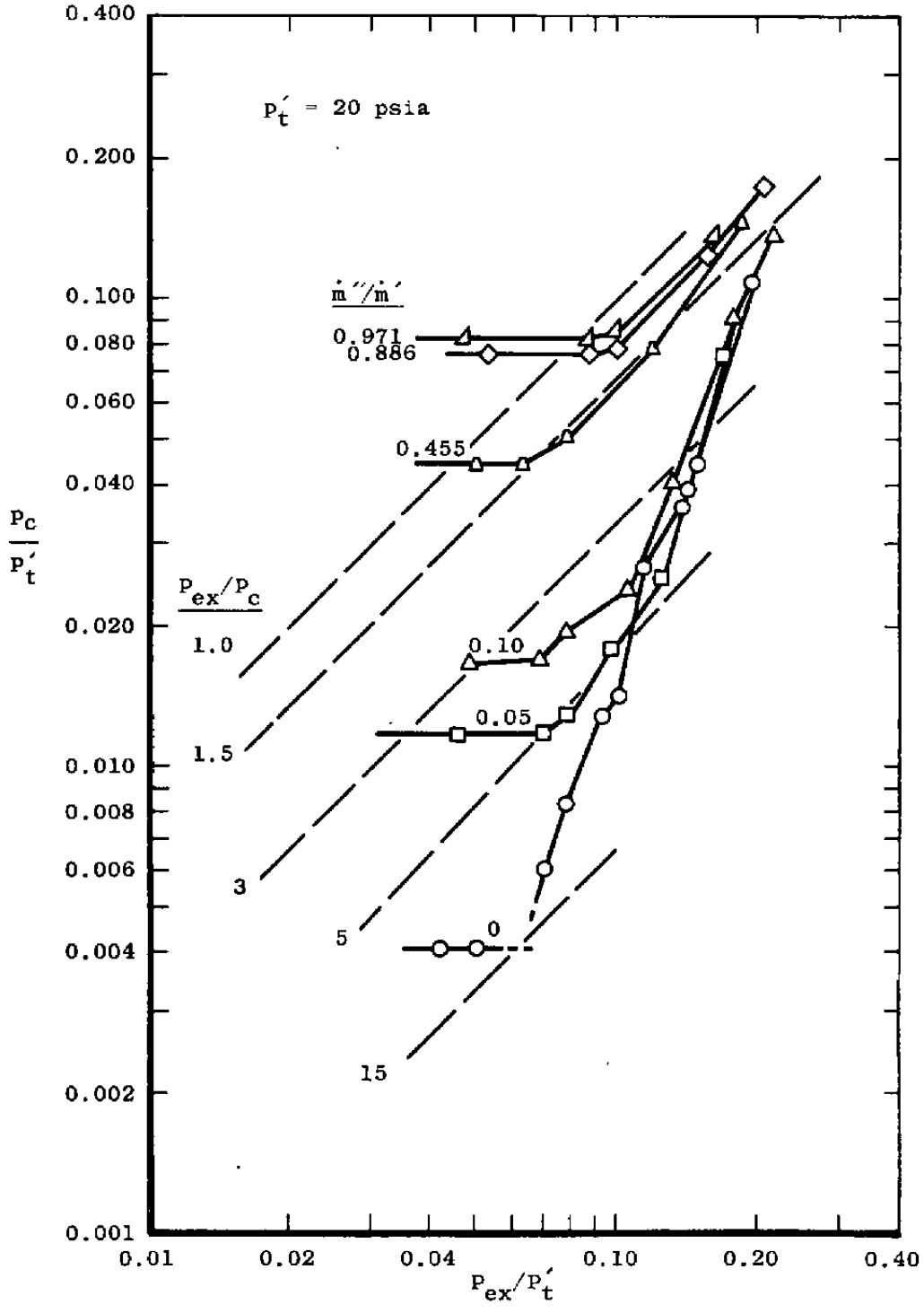

b. $A_d/A^* = 17.285$

Figure 14. Continued.

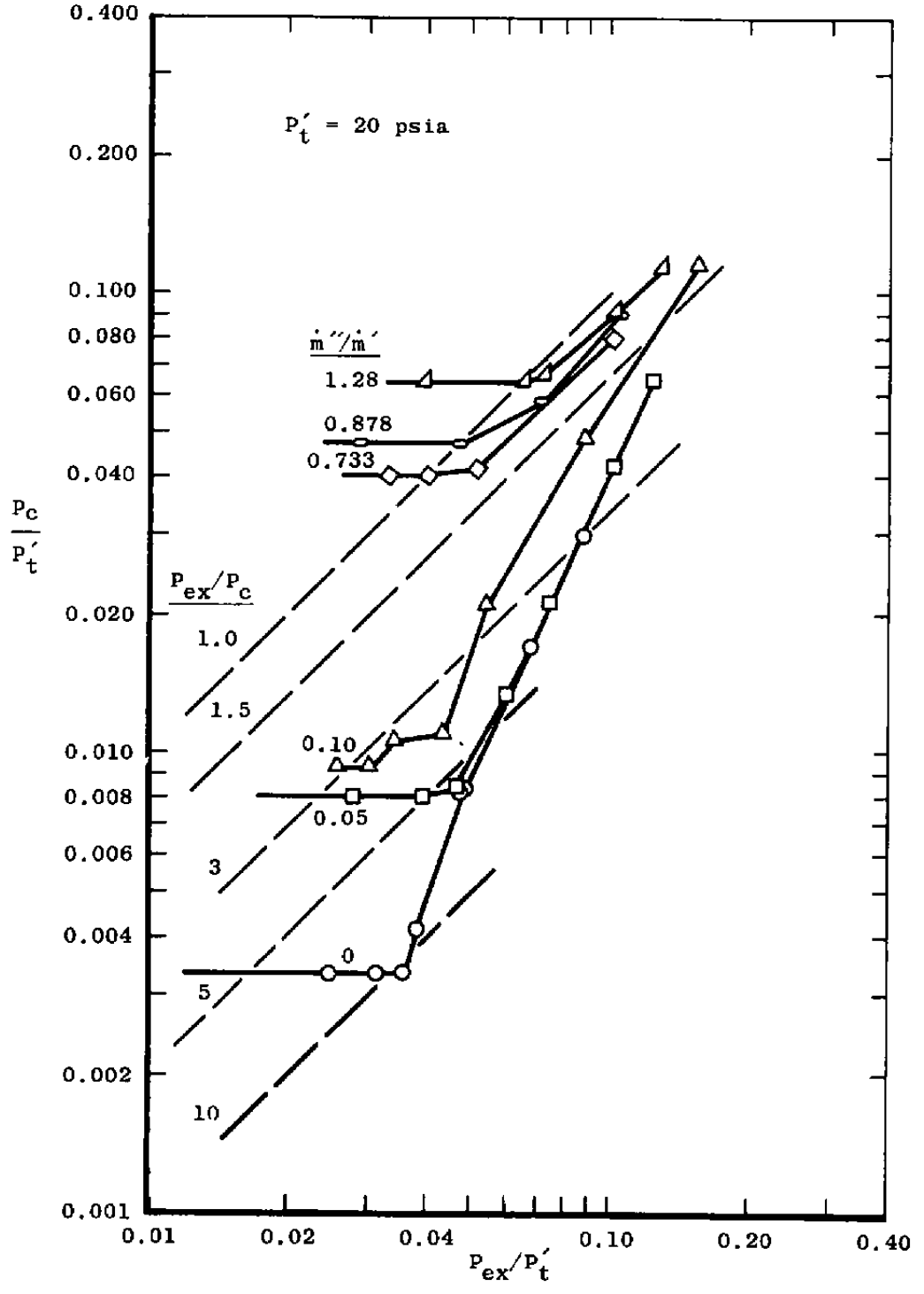

c. $A_d/A^* = 28.351$

Figure 14. Concluded.

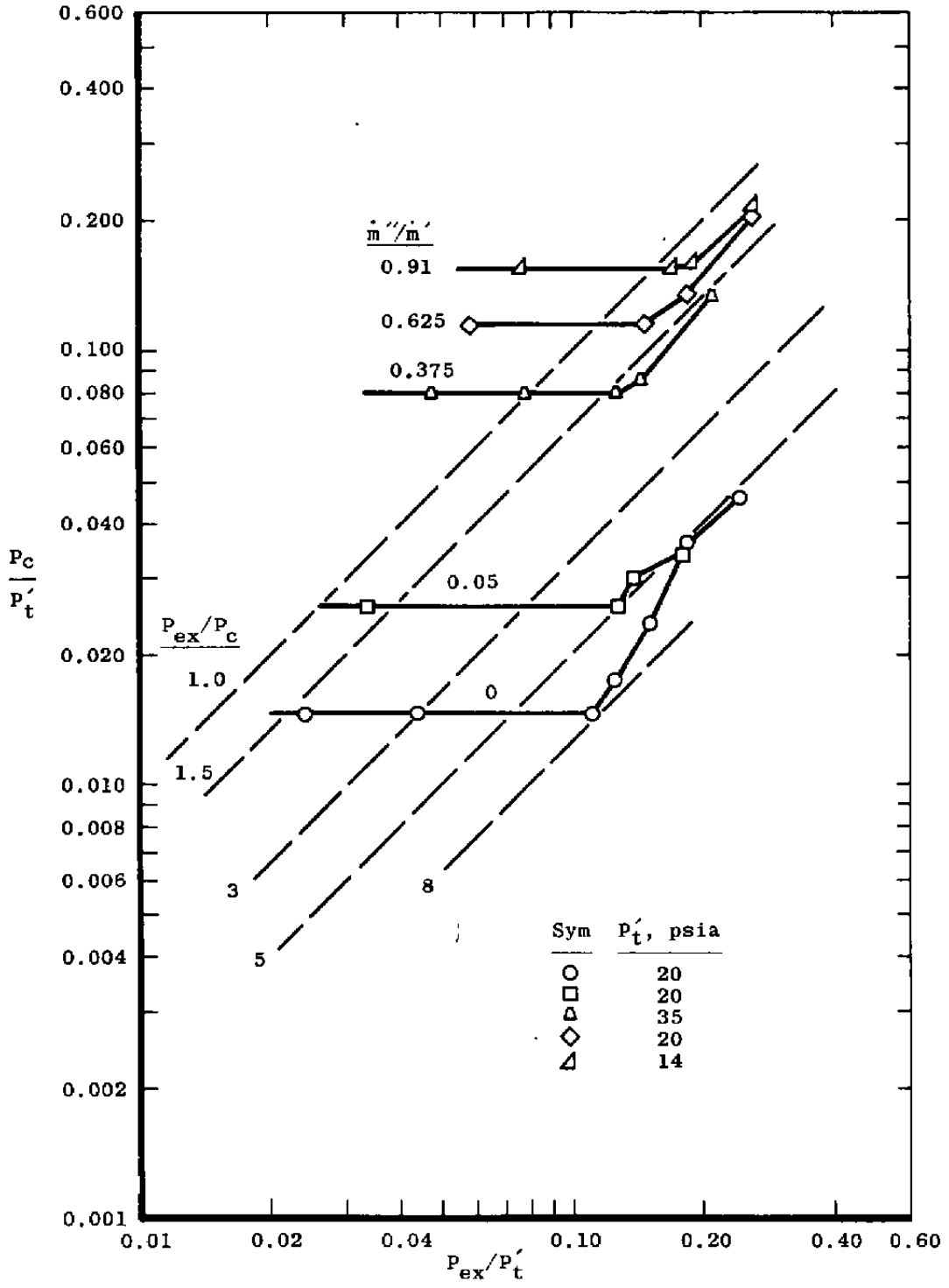

a. $A_d/A^* = 8.767$

Figure 15. Performance of variable-area ejector with converging inlet duct.

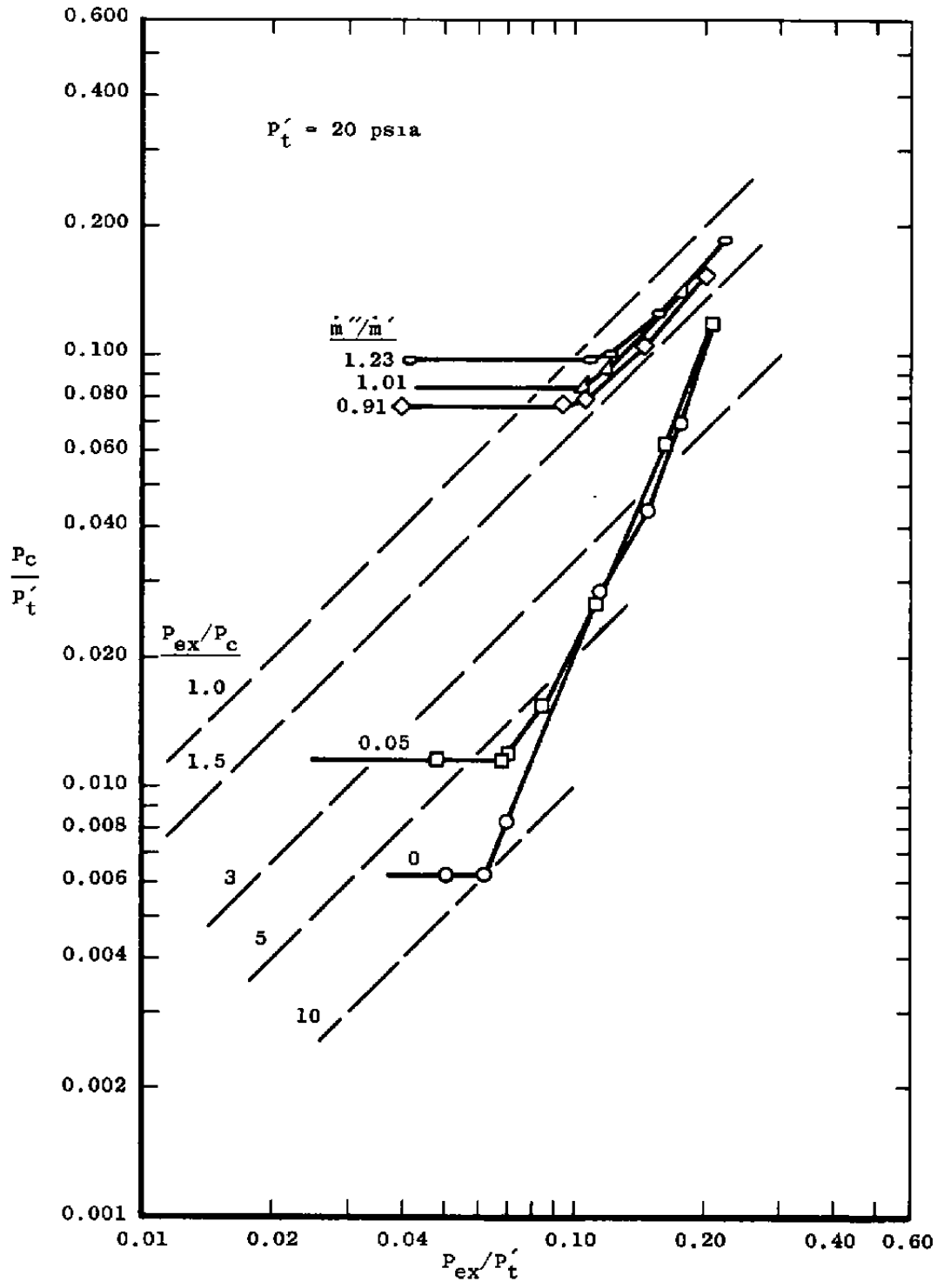

b. $A_d/A^* = 17.285$

Figure 15. Continued.

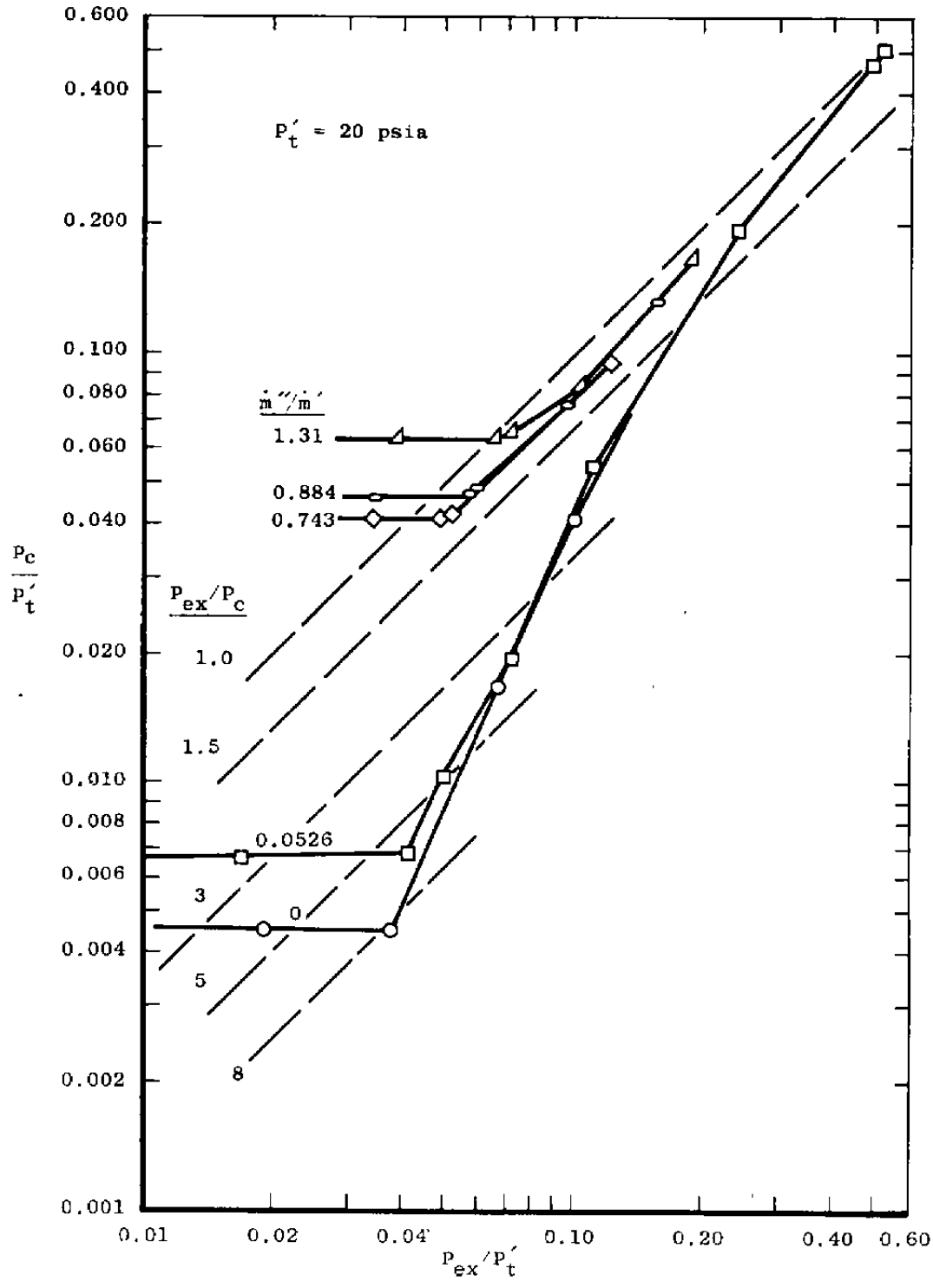

c. A_d/A^* = 28.351

Figure 15. Concluded.

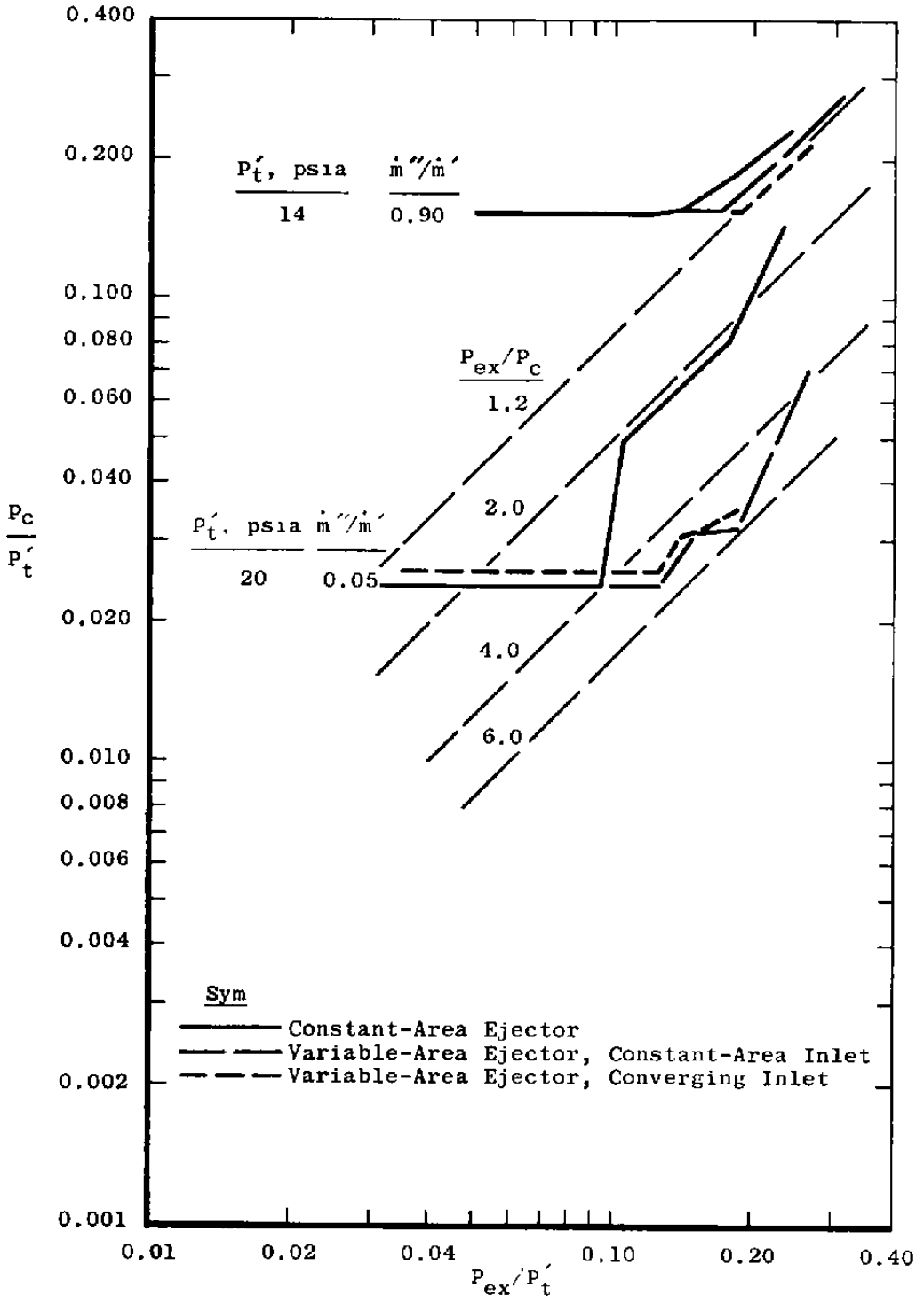

a. $A_d/A^* = 8.767$

Figure 16. Performance comparison of ejector configurations.

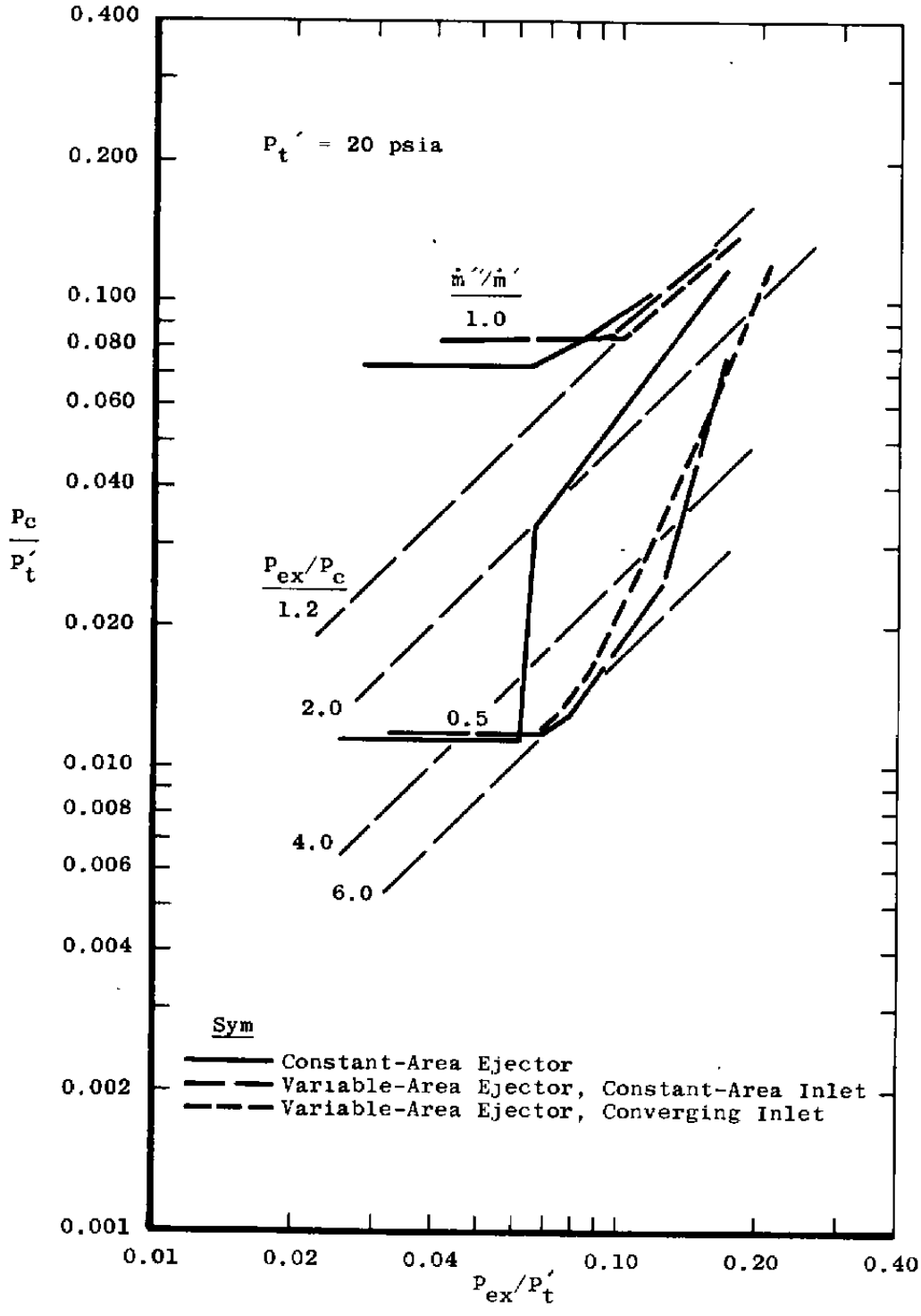

b. $A_d/A^* = 17.285$

Figure 16. Continued.

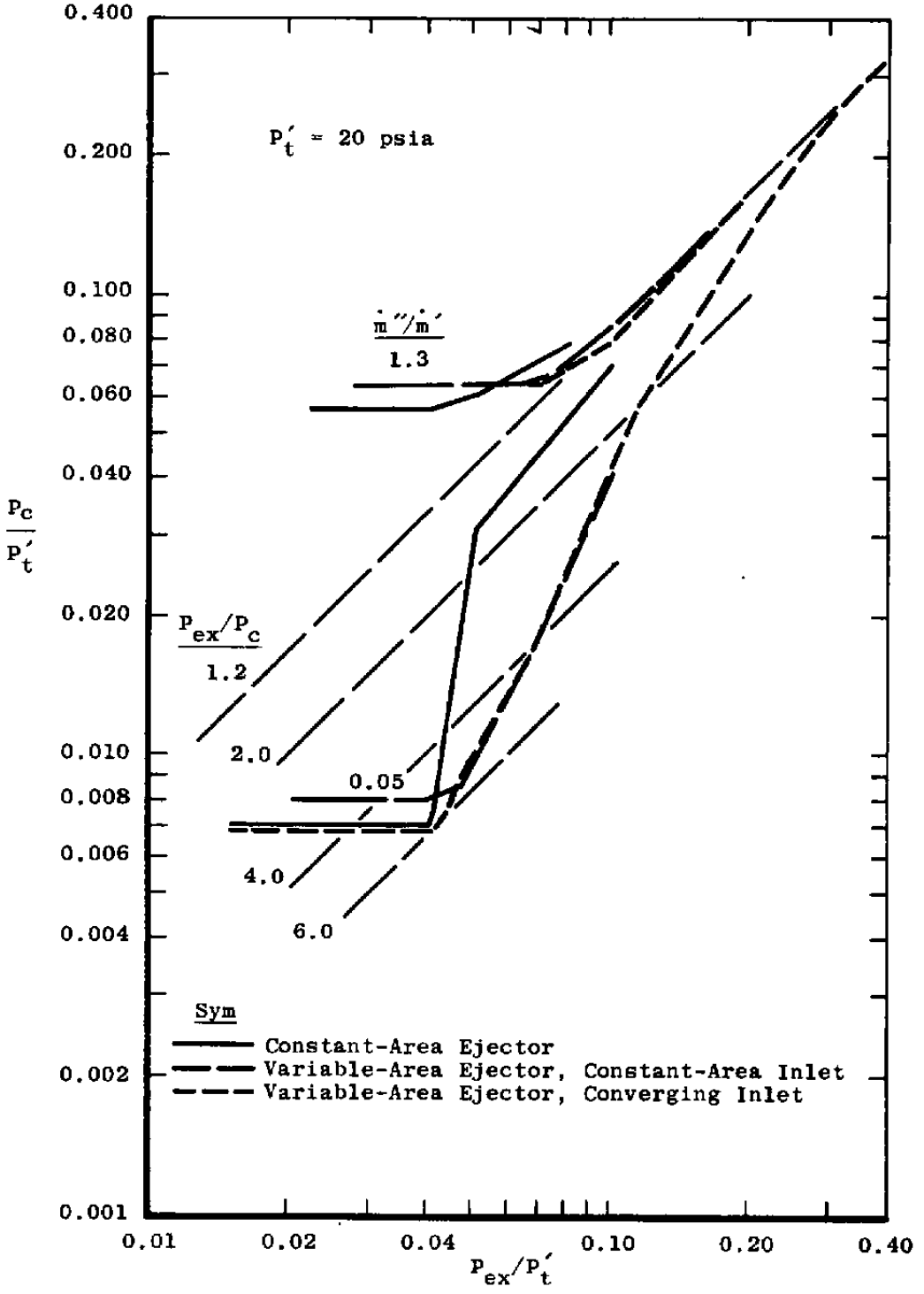

c. $A_d/A^* = 28.351$

Figure 16. Concluded.

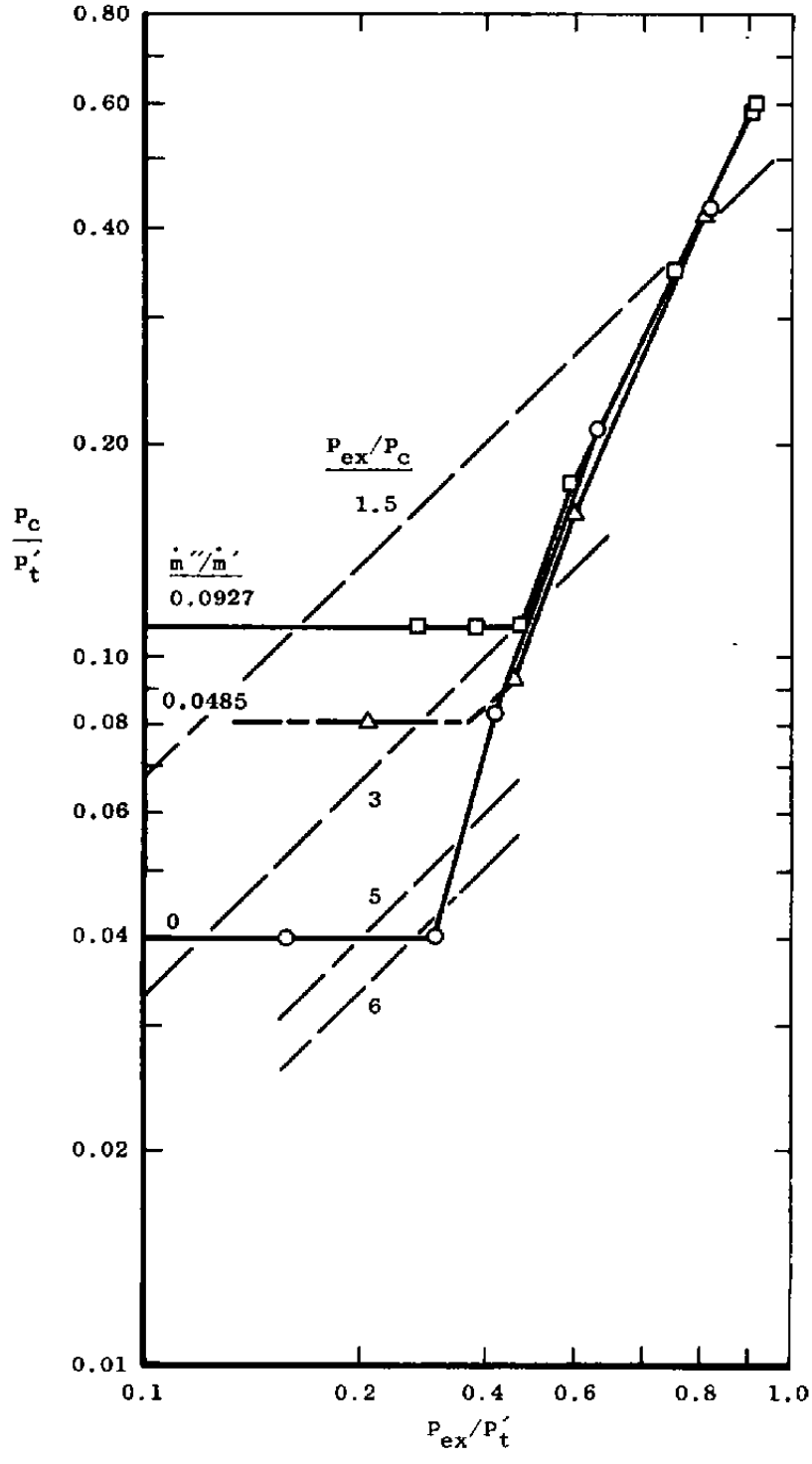

a. P_t' = 5 psia

Figure 17. Variable-area ejector performance characteristics A_d/A^* = 3.987.

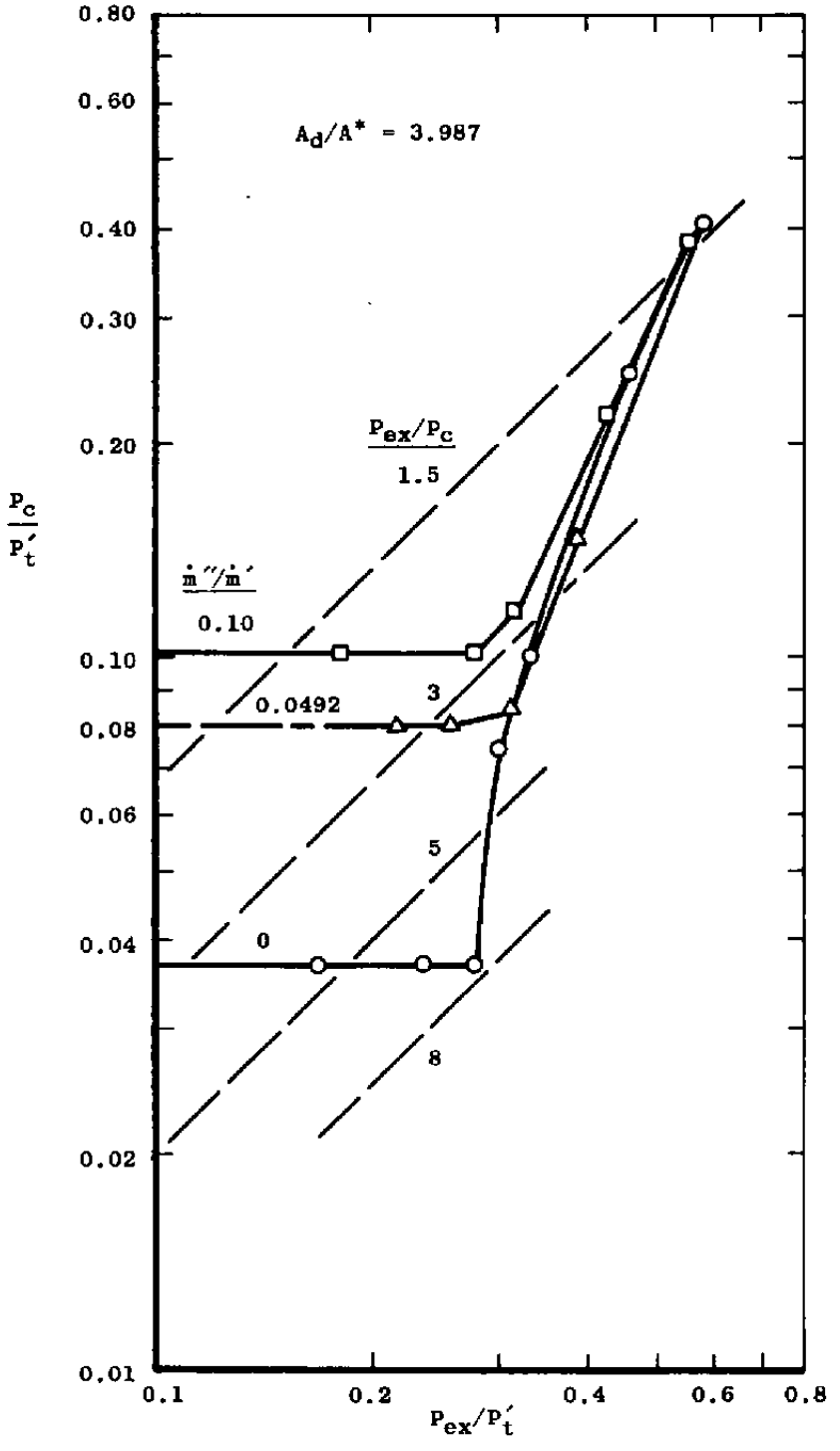

b. P_t' = 10 psia

Figure 17. Continued.

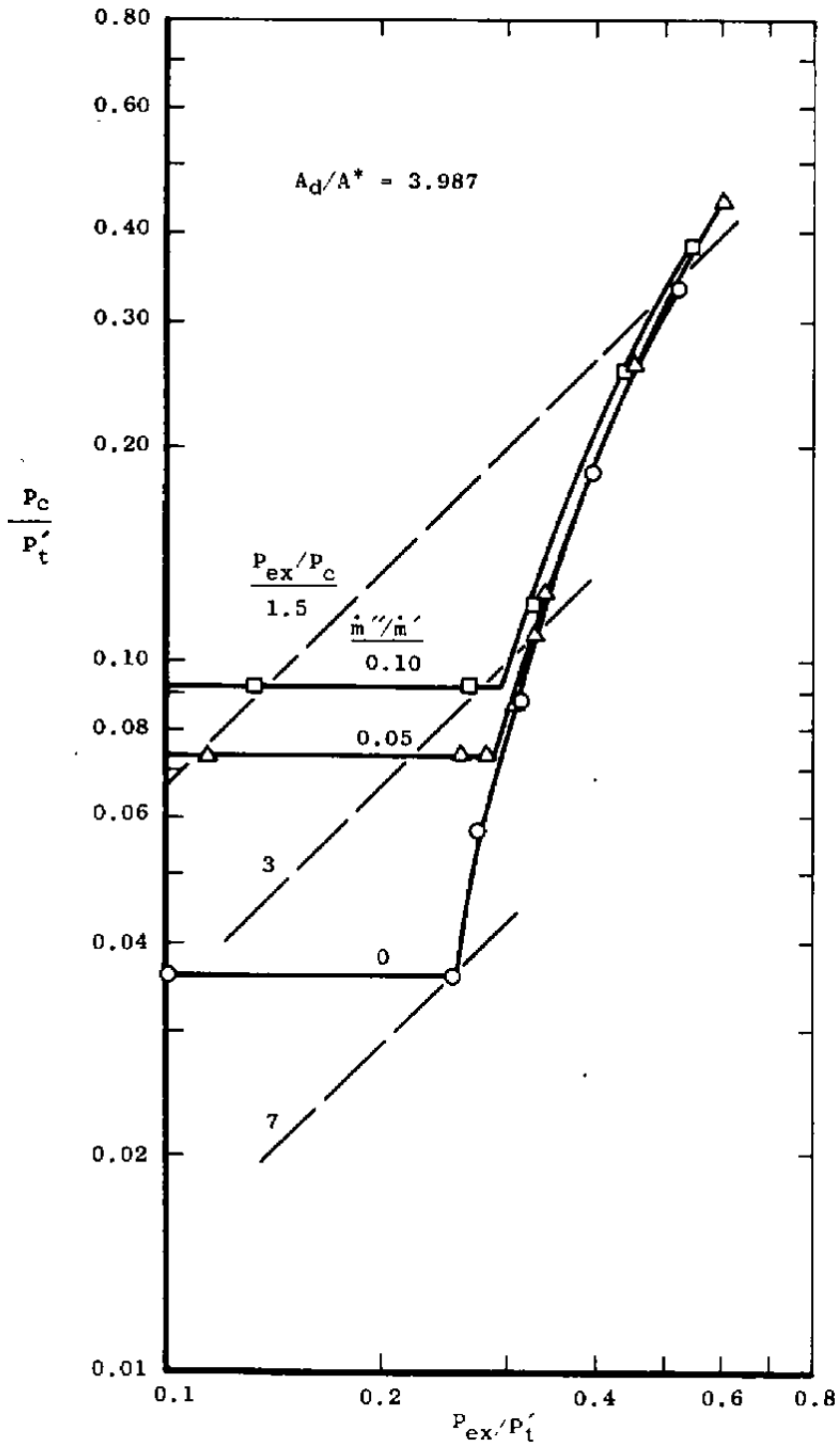

c. P_t' = 20 psia

Figure 17. Concluded.

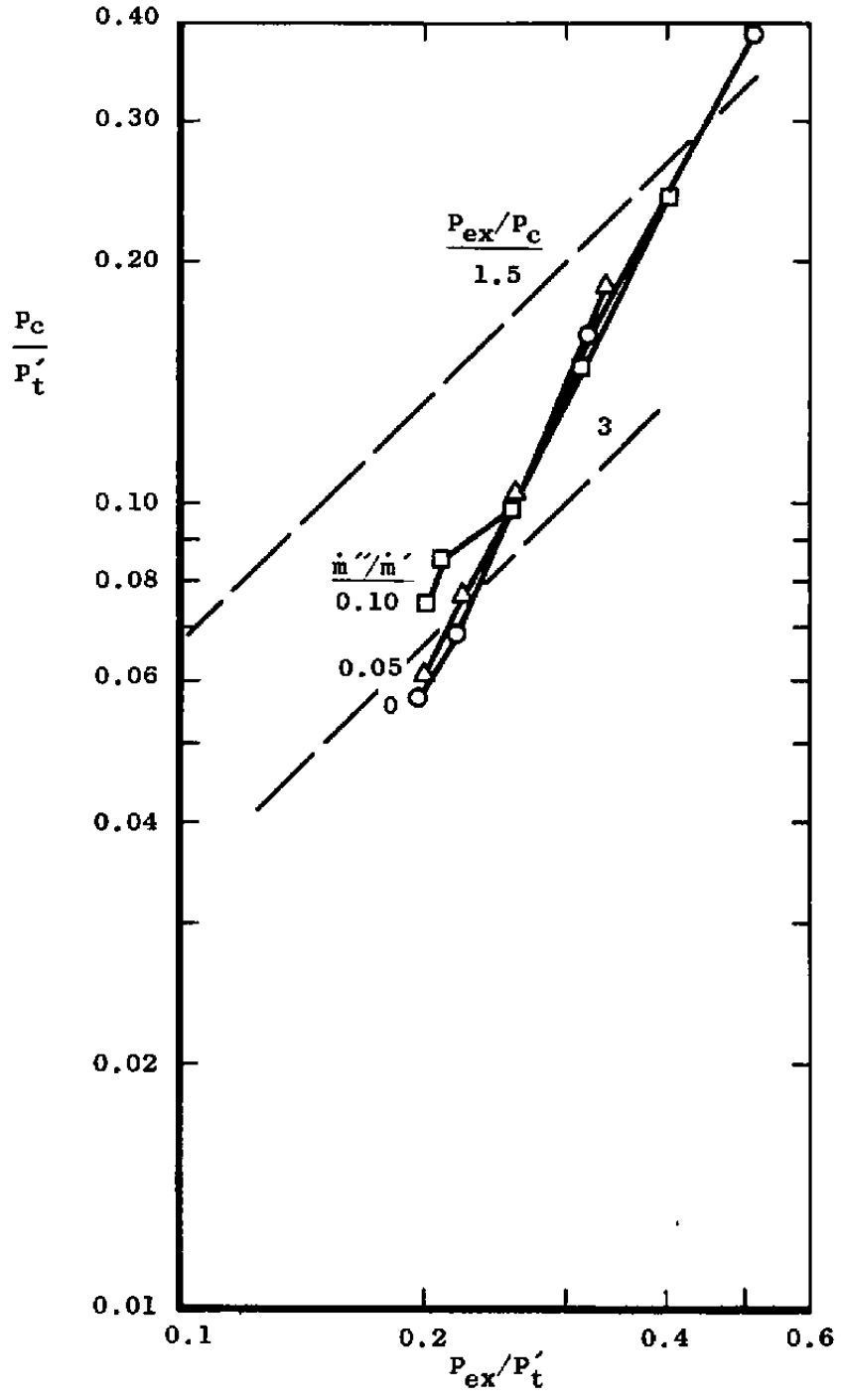

a. P_t' = 5 psia

Figure 18. Variable-area ejector performance characteristics, A_d/A^* = 5.756.

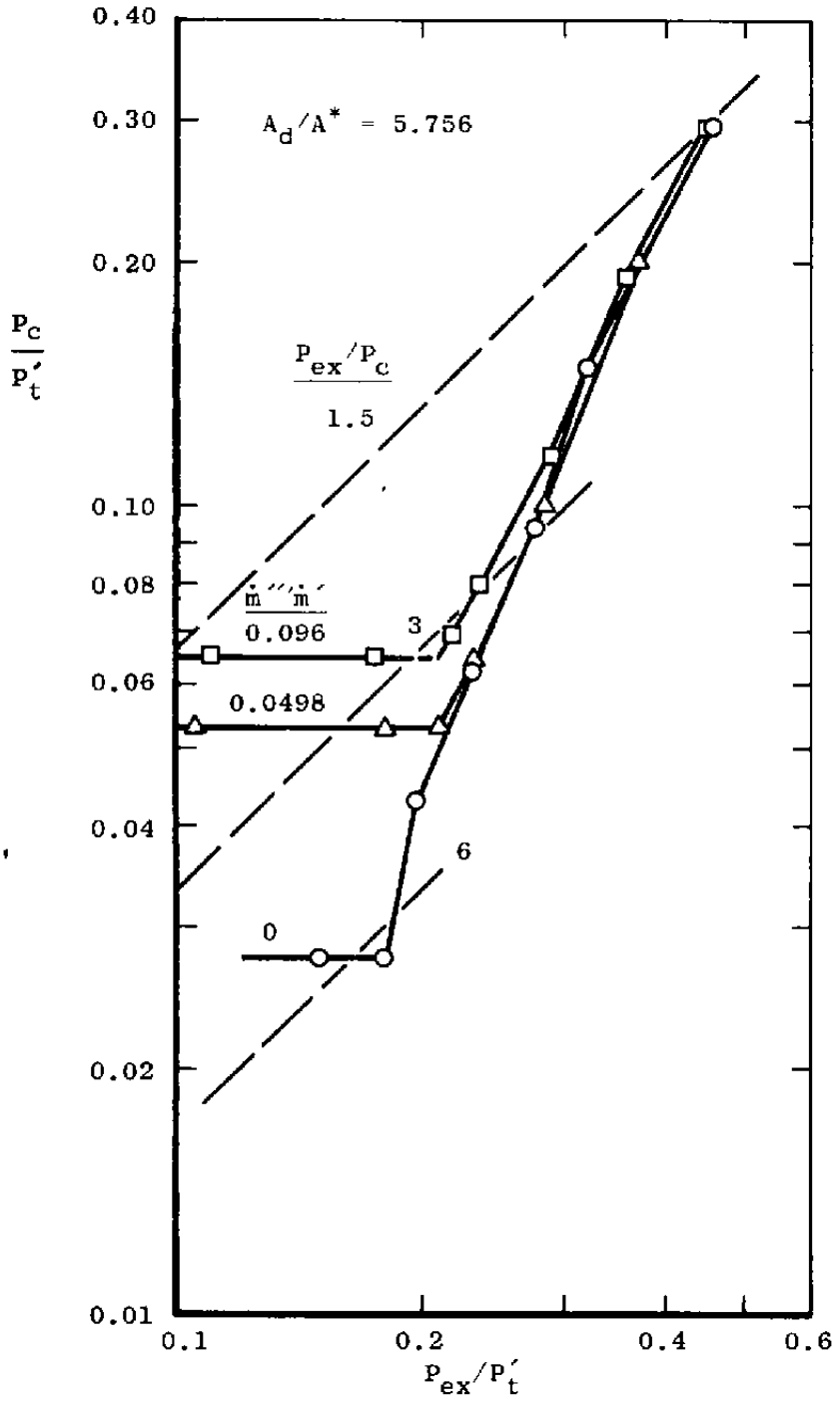

b. P_t' = 10 psia
Figure 18. Continued.

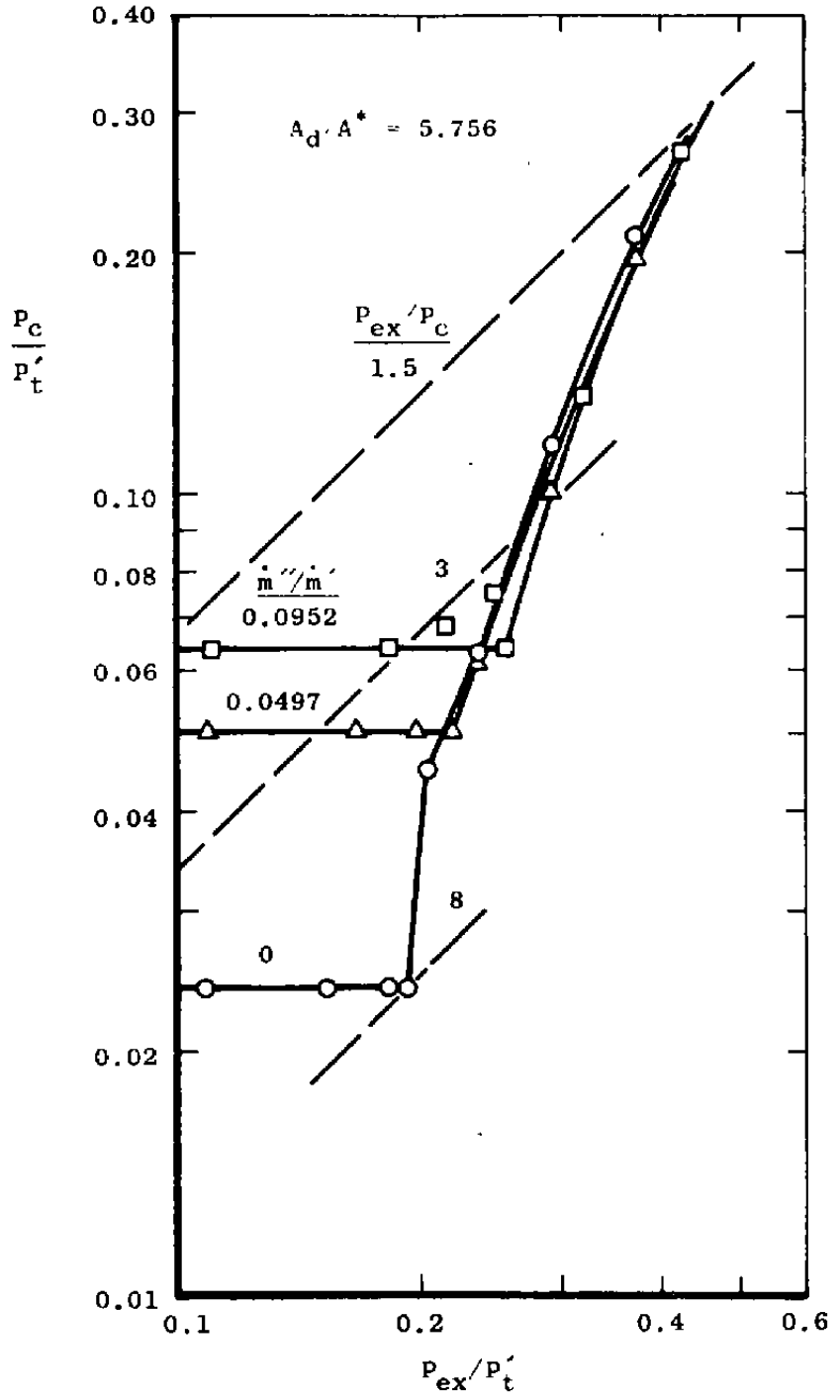

c. P_t' = 20 psia

Figure 18. Concluded.

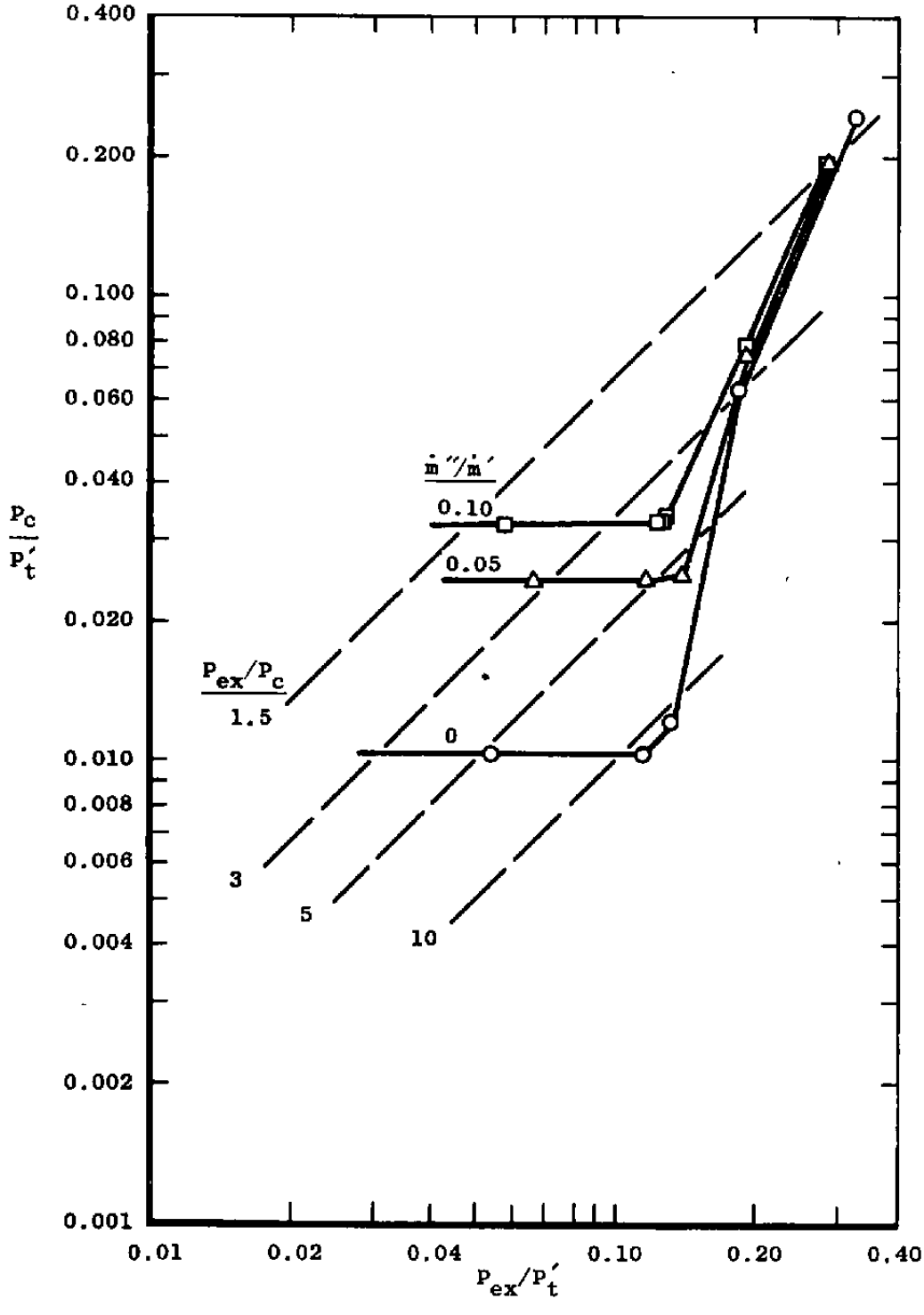

a. P_t' = 10 psia

Figure 19. Variable-area ejector performance characteristics, A_d/A^* = 8.767.

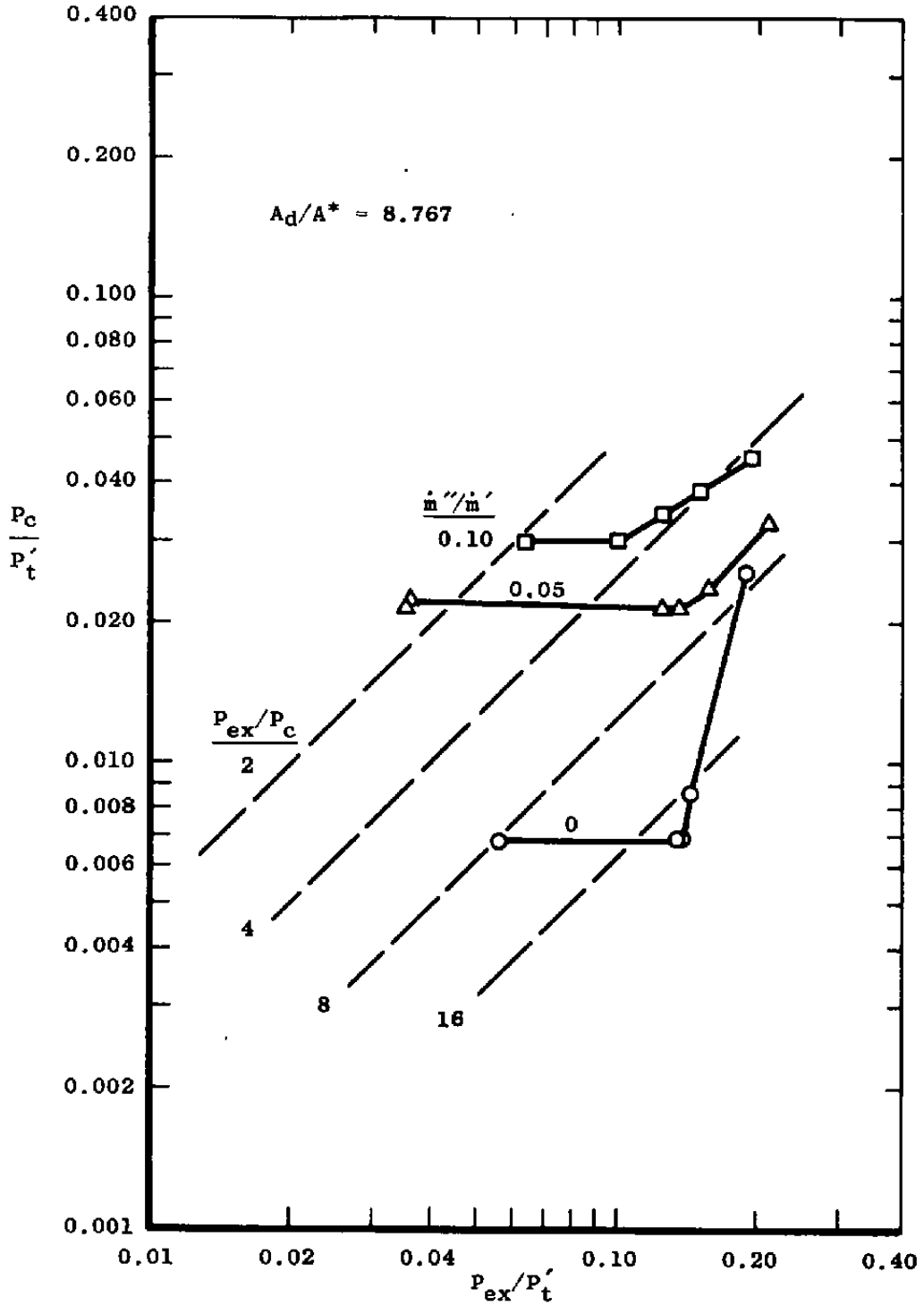

b. P_t' = 35 psia

Figure 19. Concluded.

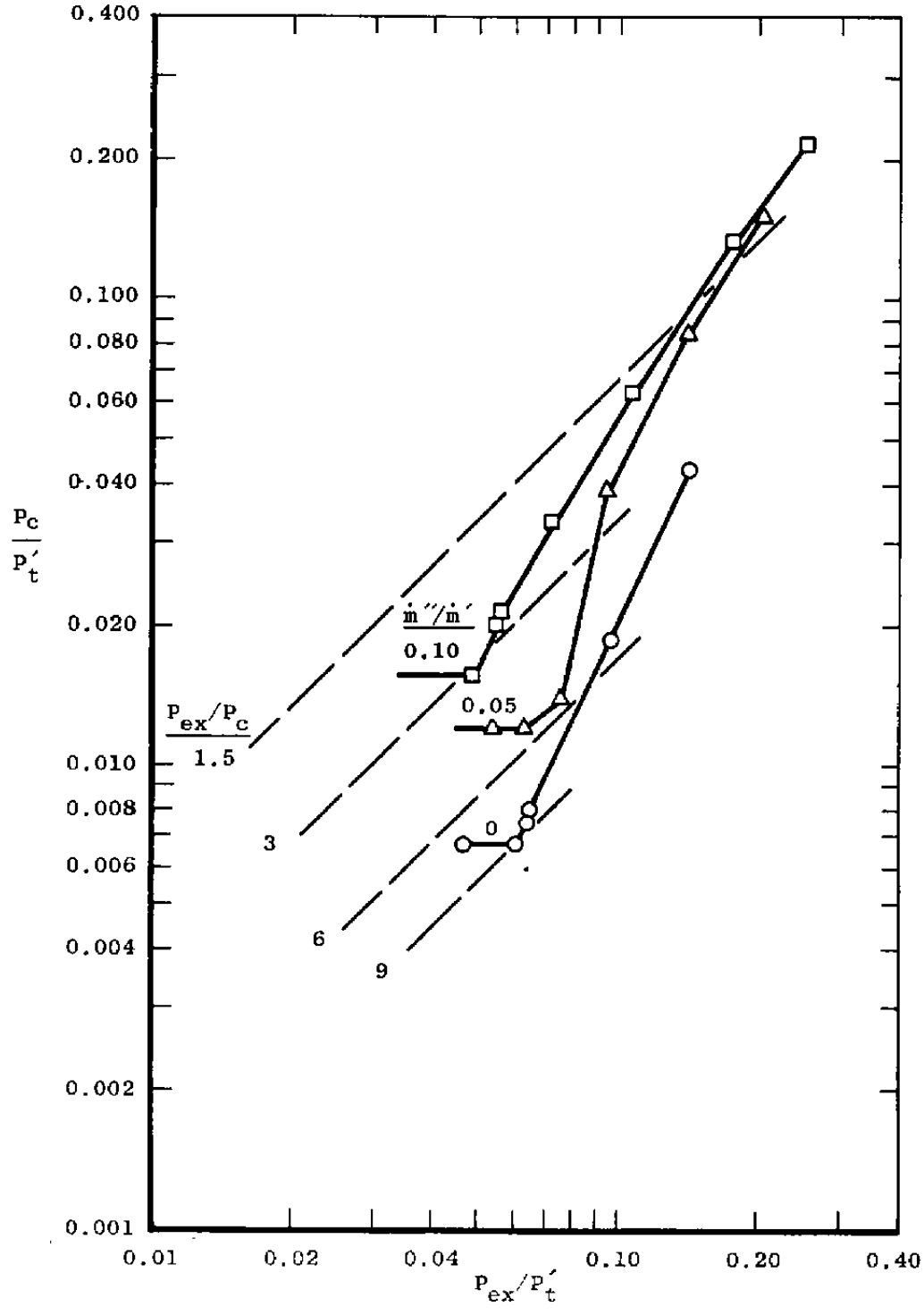

a. P_t' = 10 psia

Figure 20. Variable-area ejector performance characteristics, A_d/A^* = 17.285.

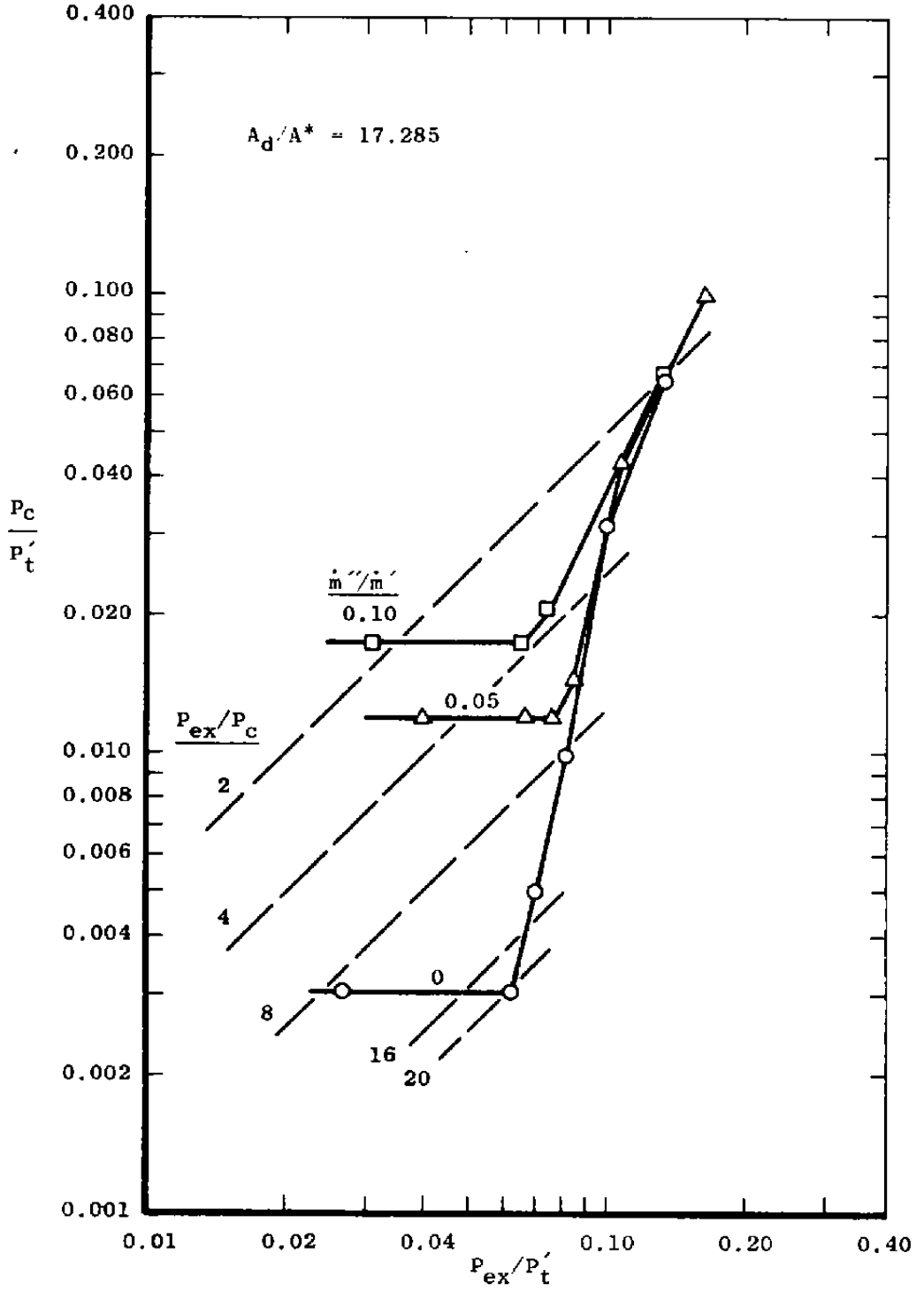

b. P_t' = 35 psia

Figure 20. Concluded.

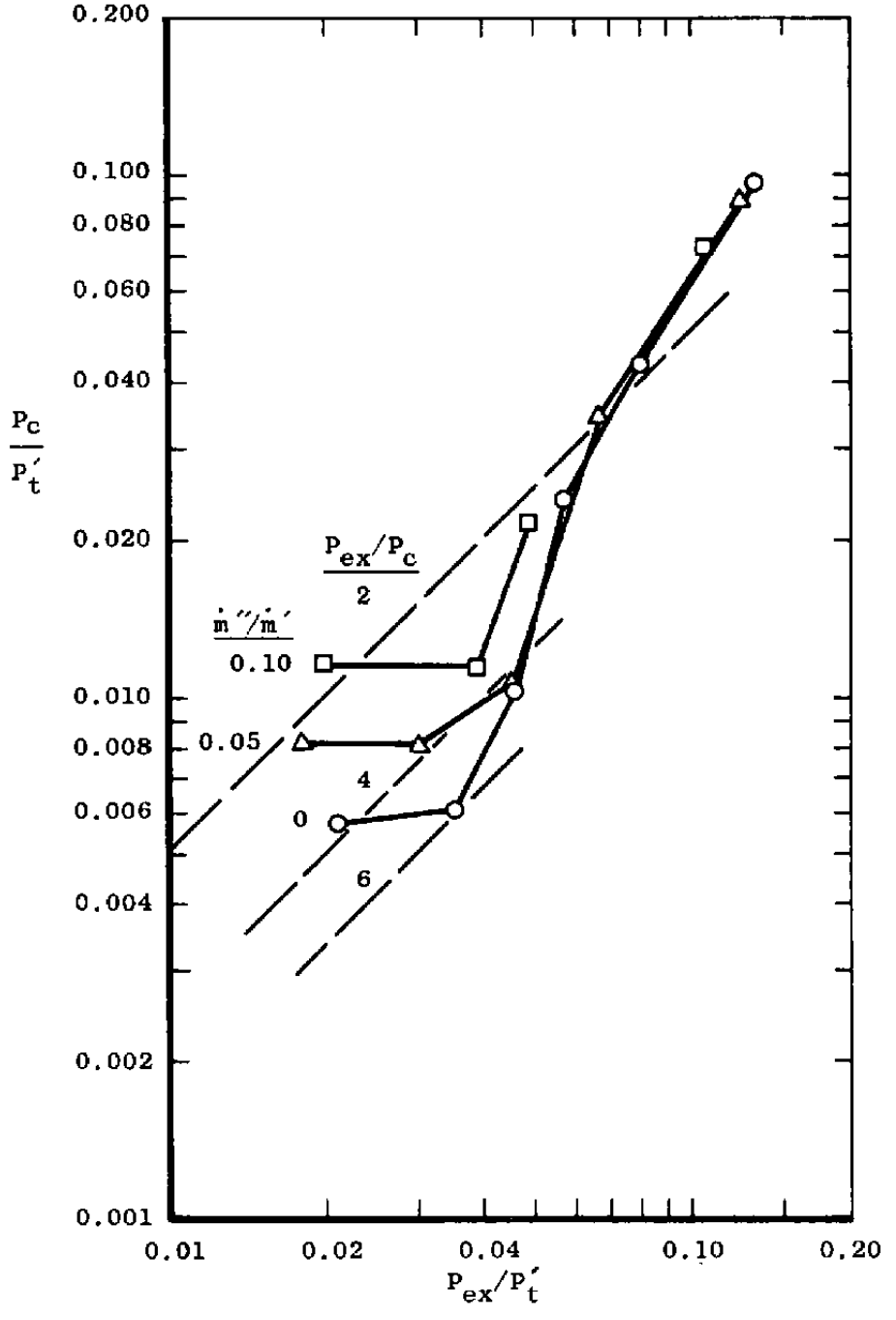

a. P_t' = 10 psia

Figure 21. Variable-area ejector performance characteristics, A_d/A^* = 28.351.

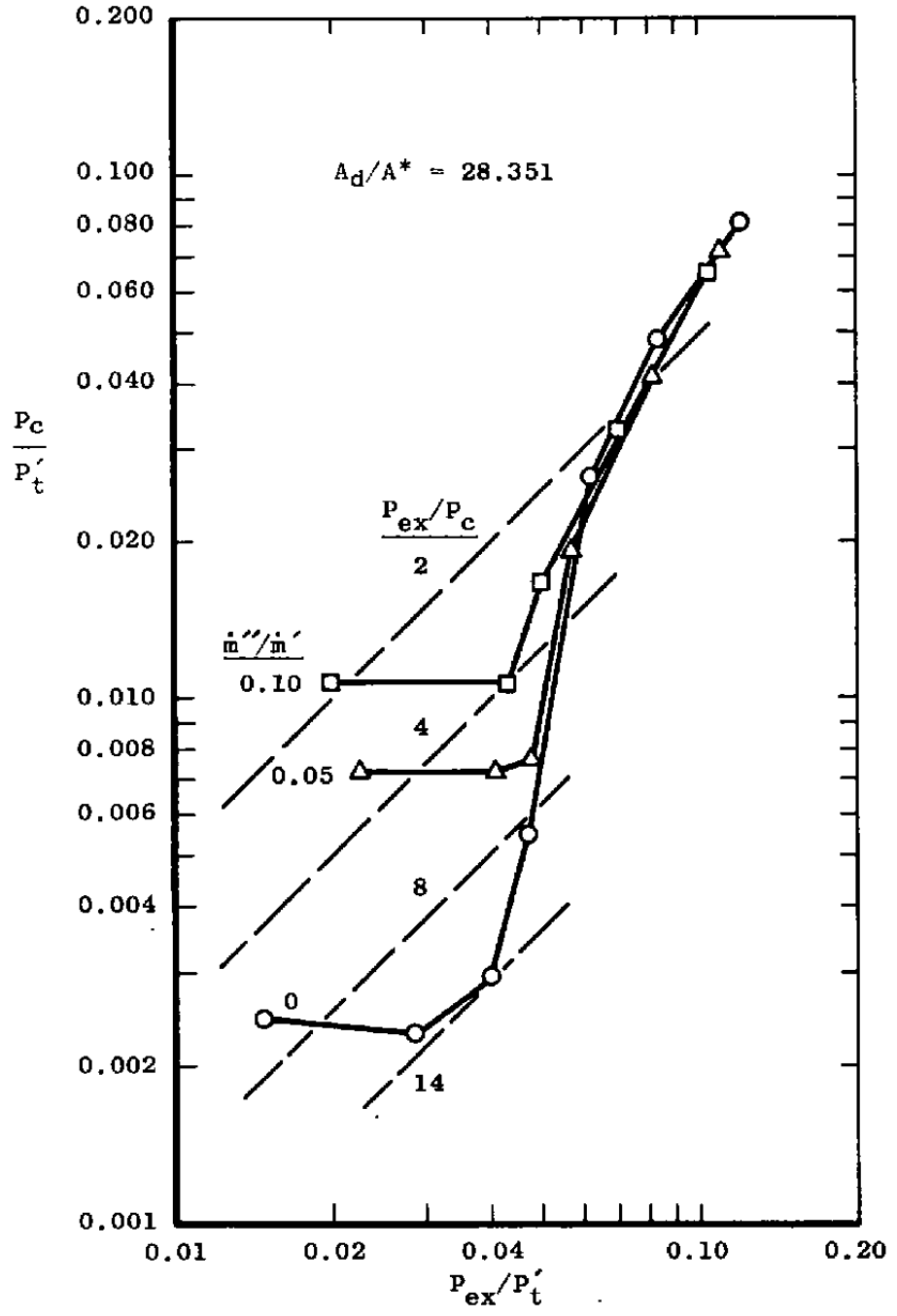

b. P_t' = 35 psia

Figure 21. Concluded.

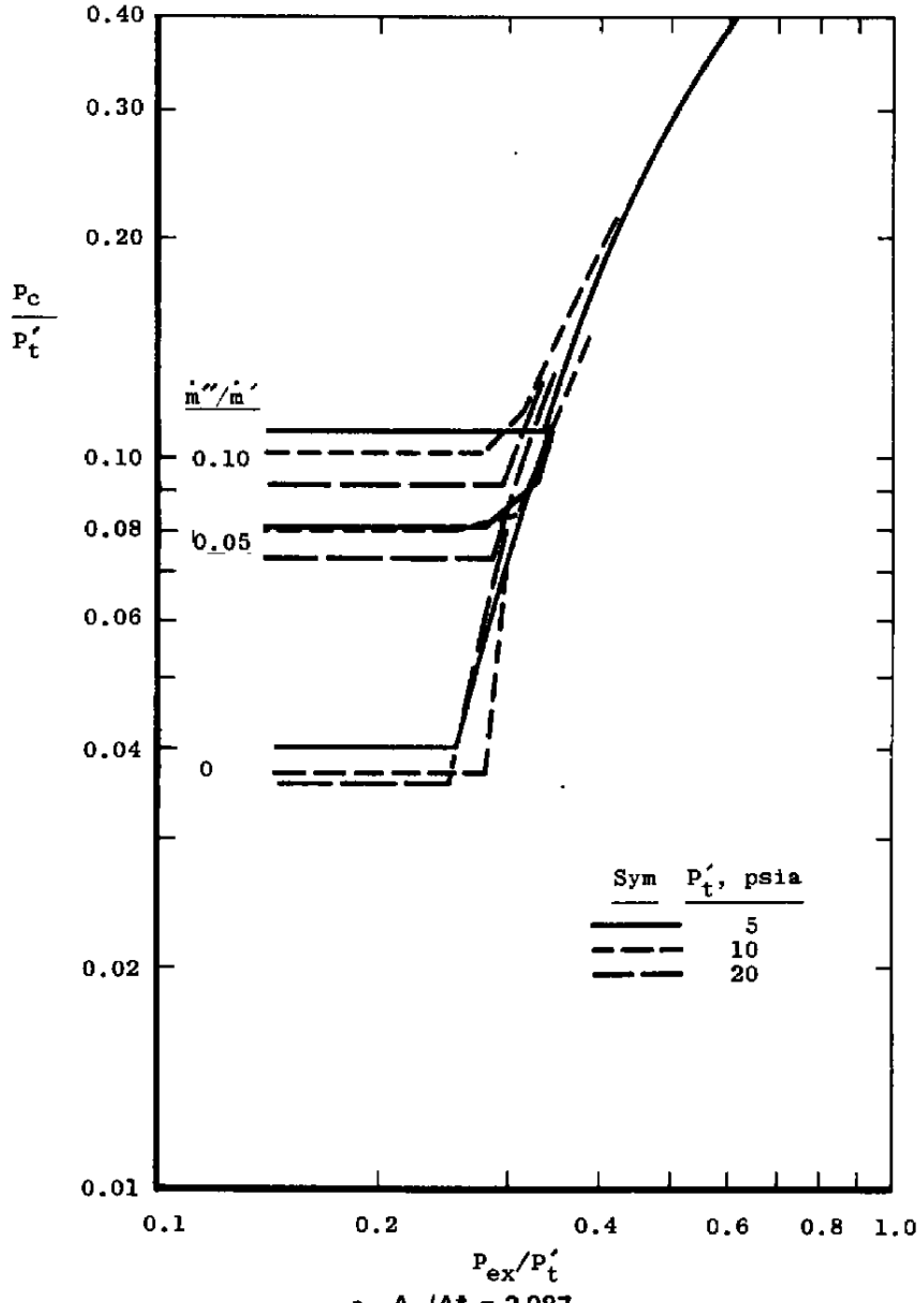

a. $A_d/A^* = 3.987$

Figure 22. Effect of driving gas pressure on performance of variable-area ejector with constant-area inlet.

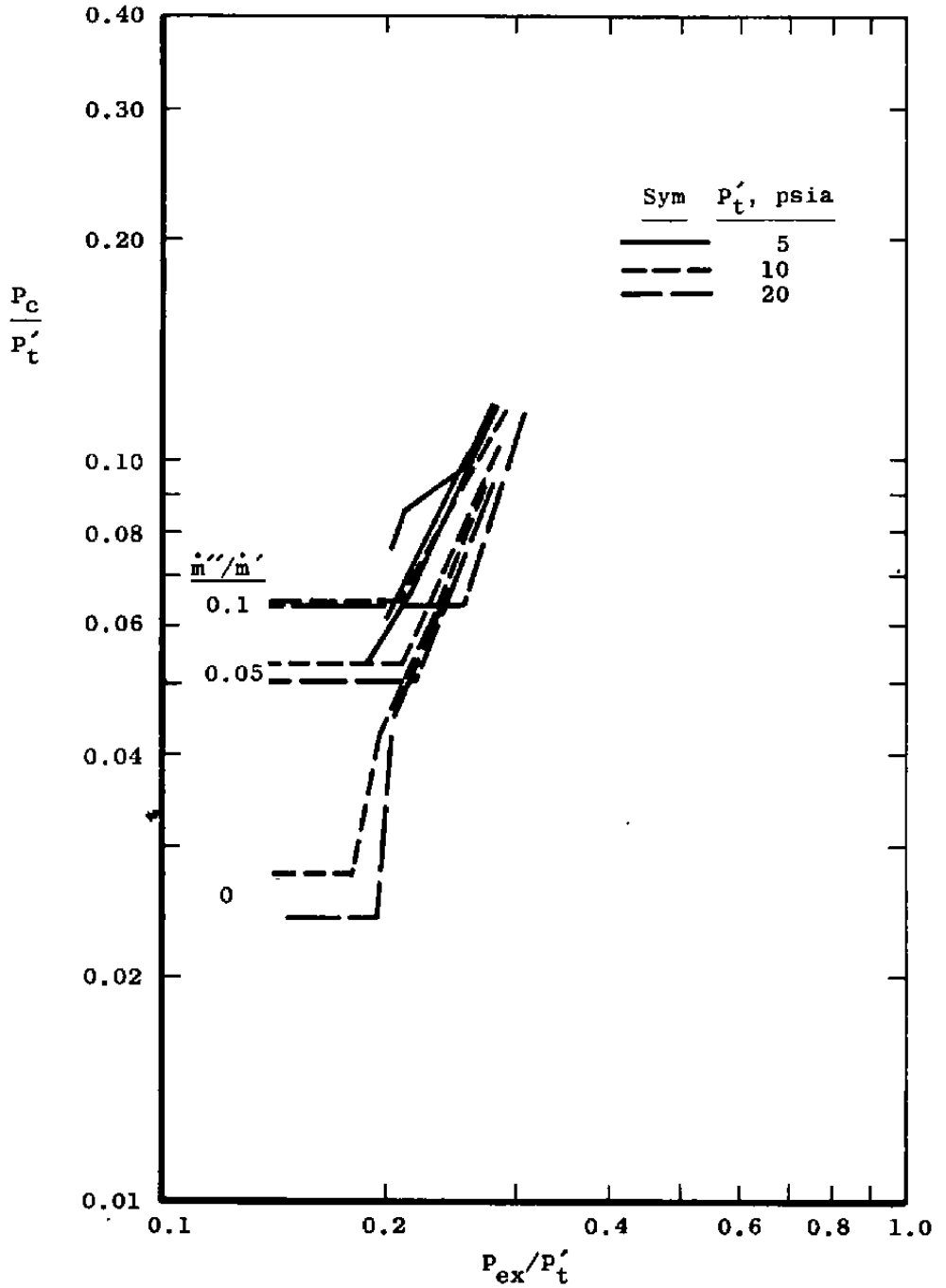

b. $A_d/A^* = 5.756$

Figure 22. Continued.

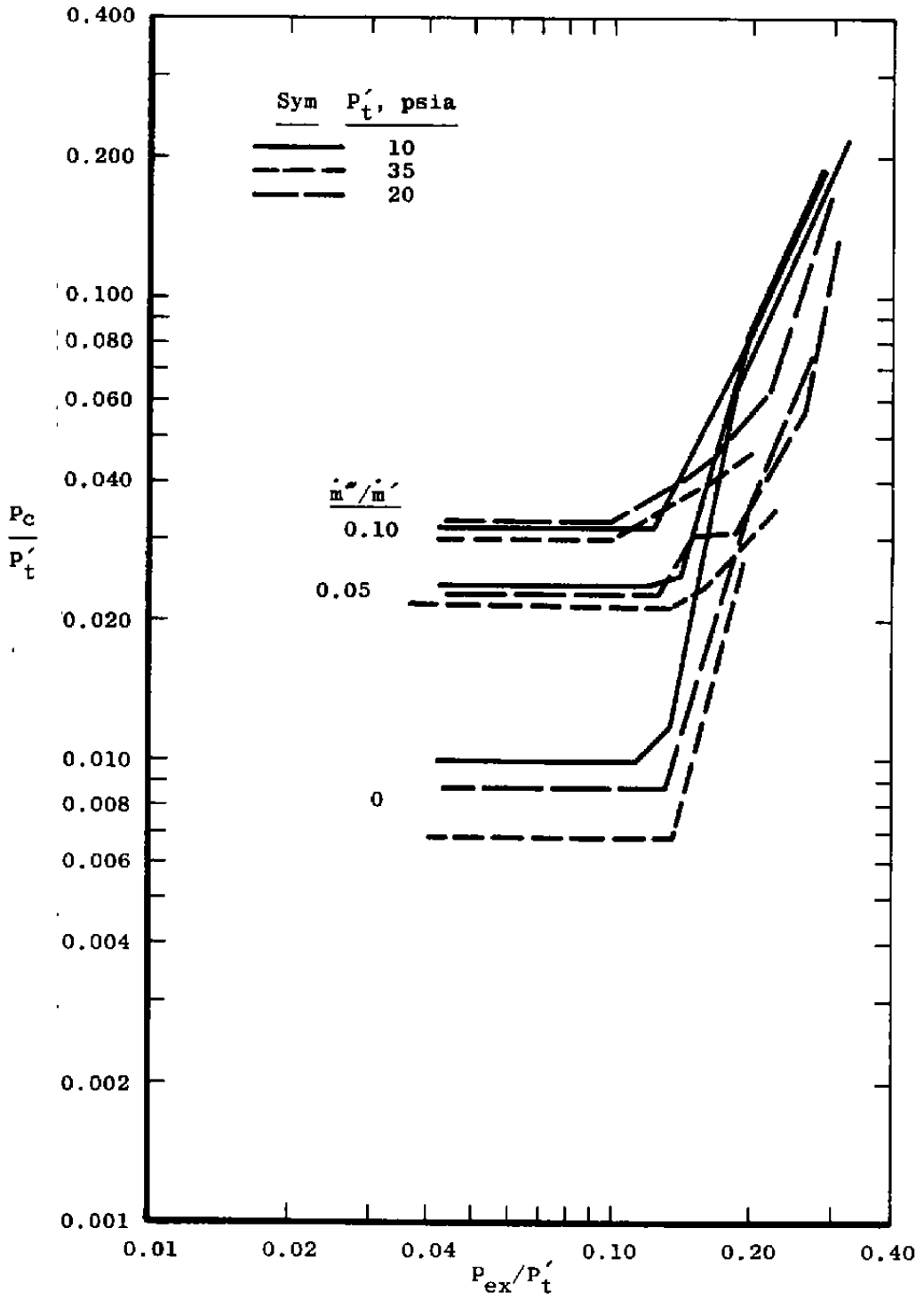

c. $A_d/A^* = 8.767$

Figure 22. Continued.

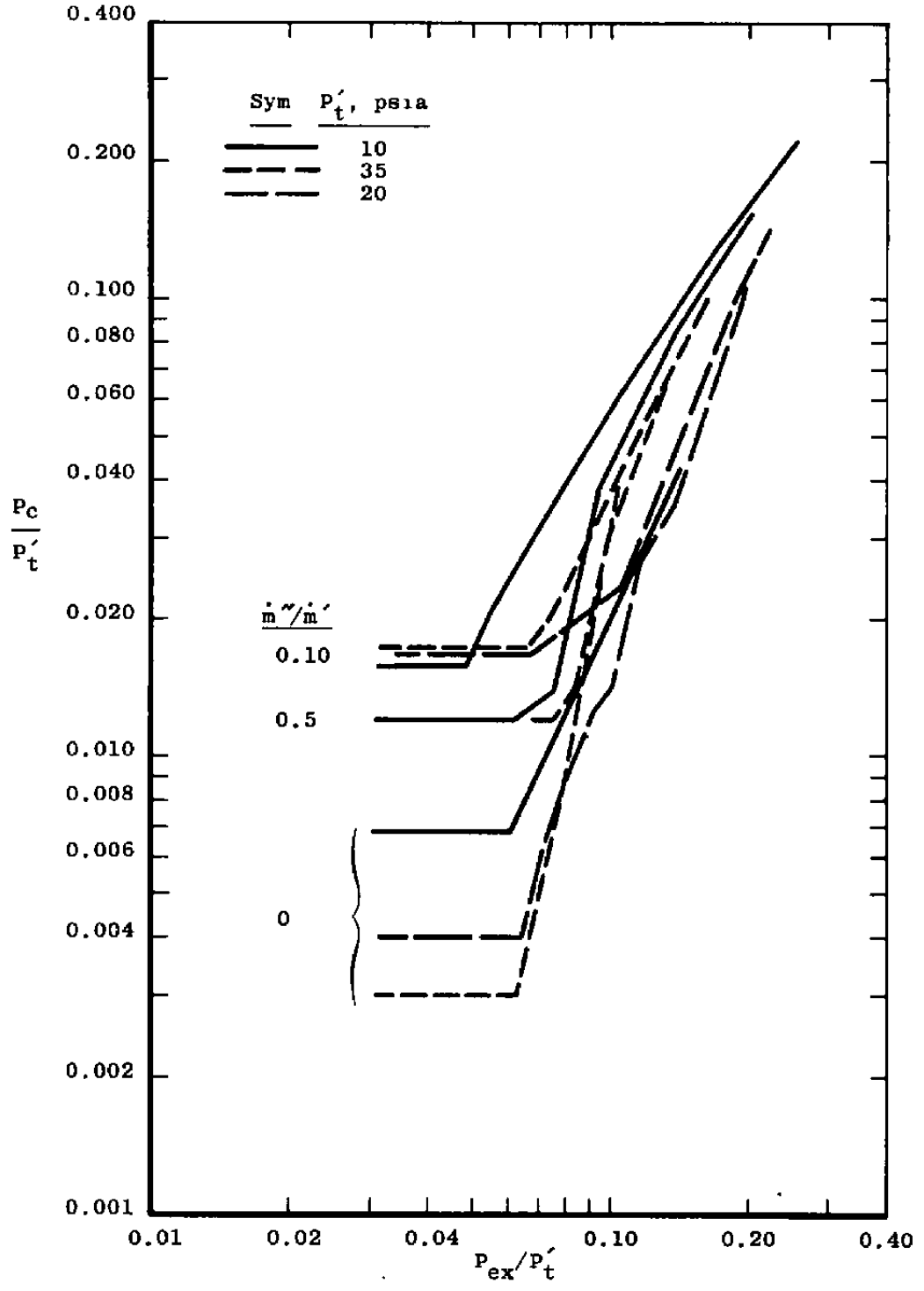

d. $A_d/A^* = 17.285$

Figure 22. Continued.

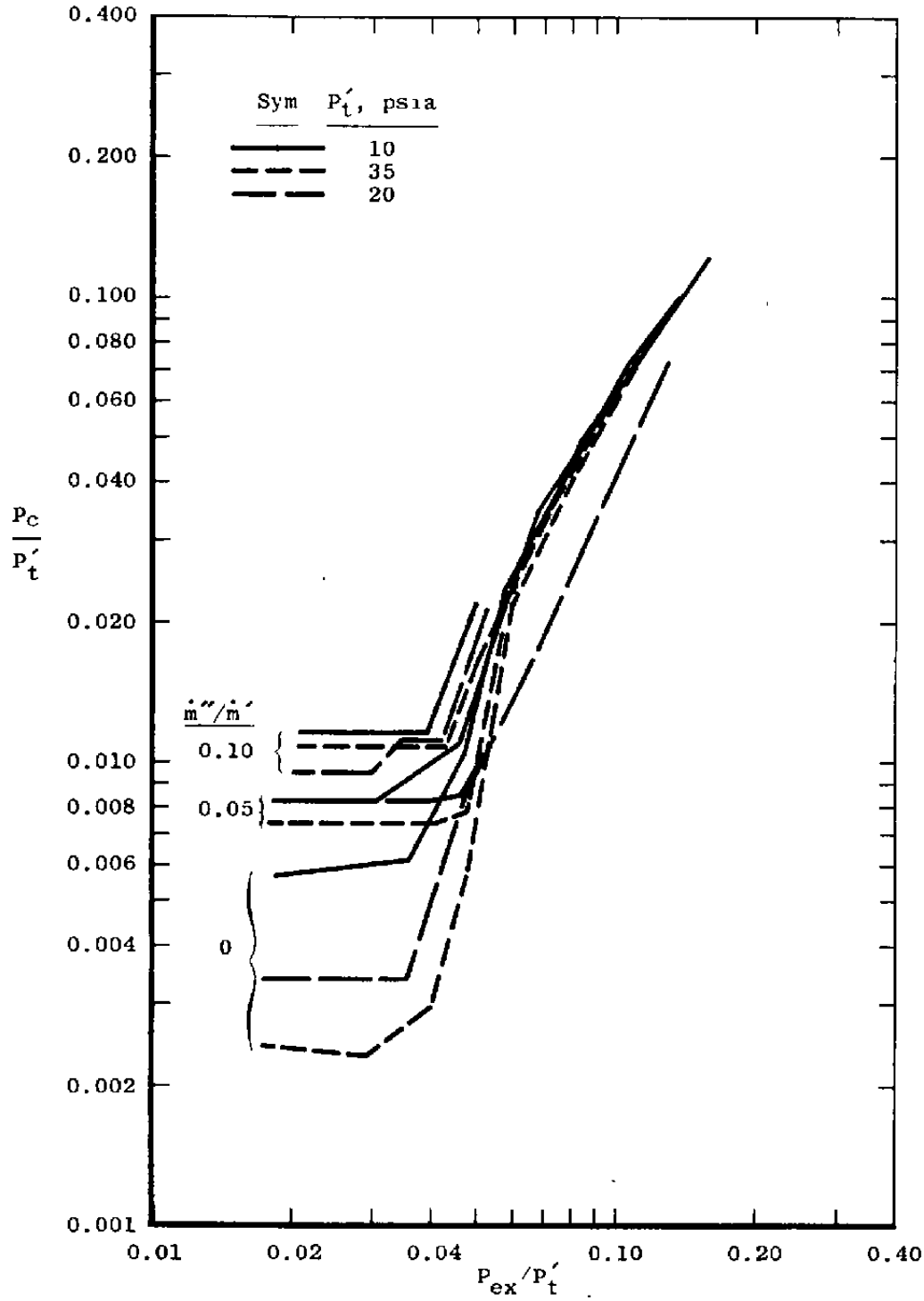

e. $A_d/A^* = 28.351$

Figure 22. Concluded.

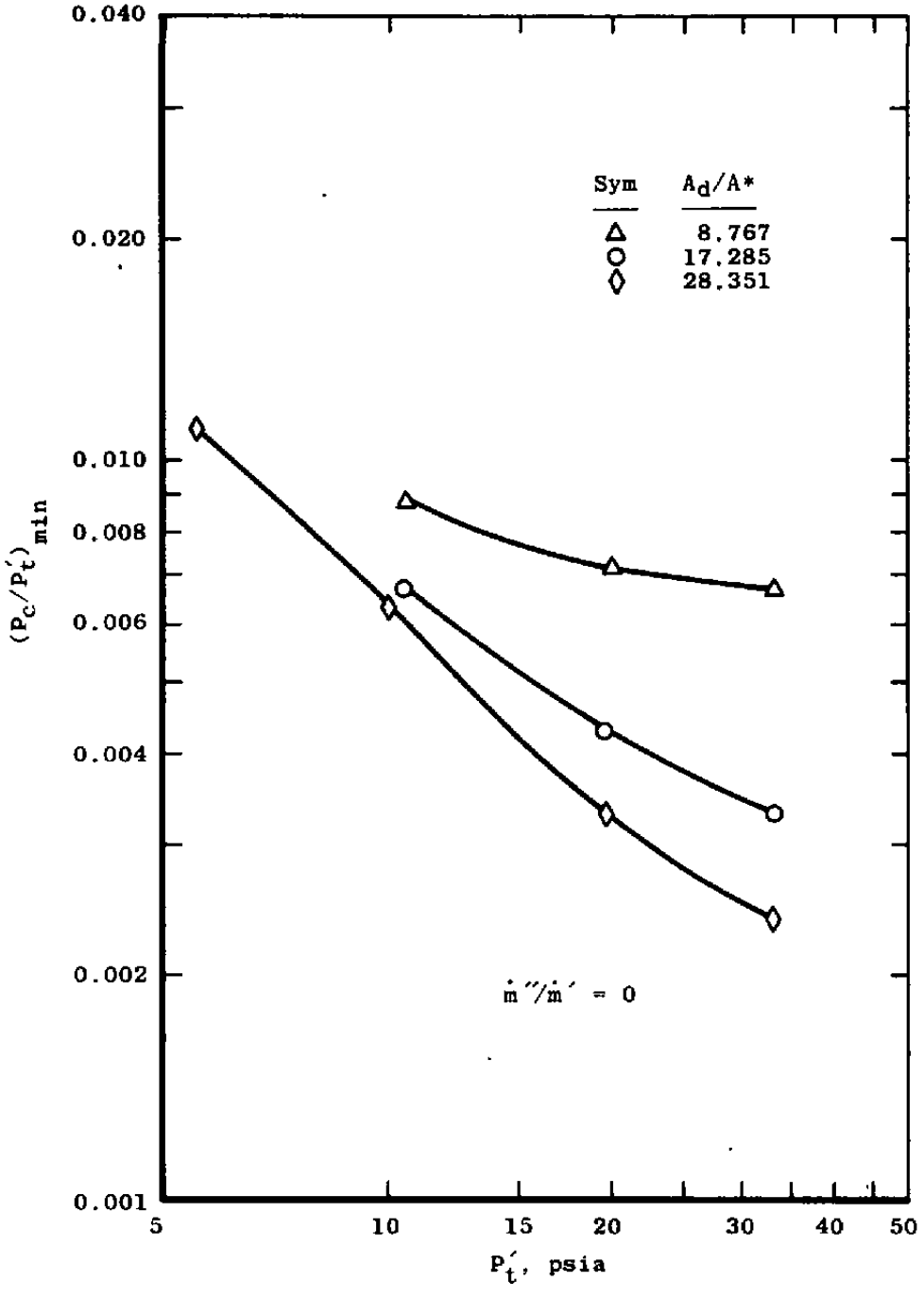

a. Constant-area ejector (cylindrical)

Figure 23. Effect of stagnation pressure on ejector performance.

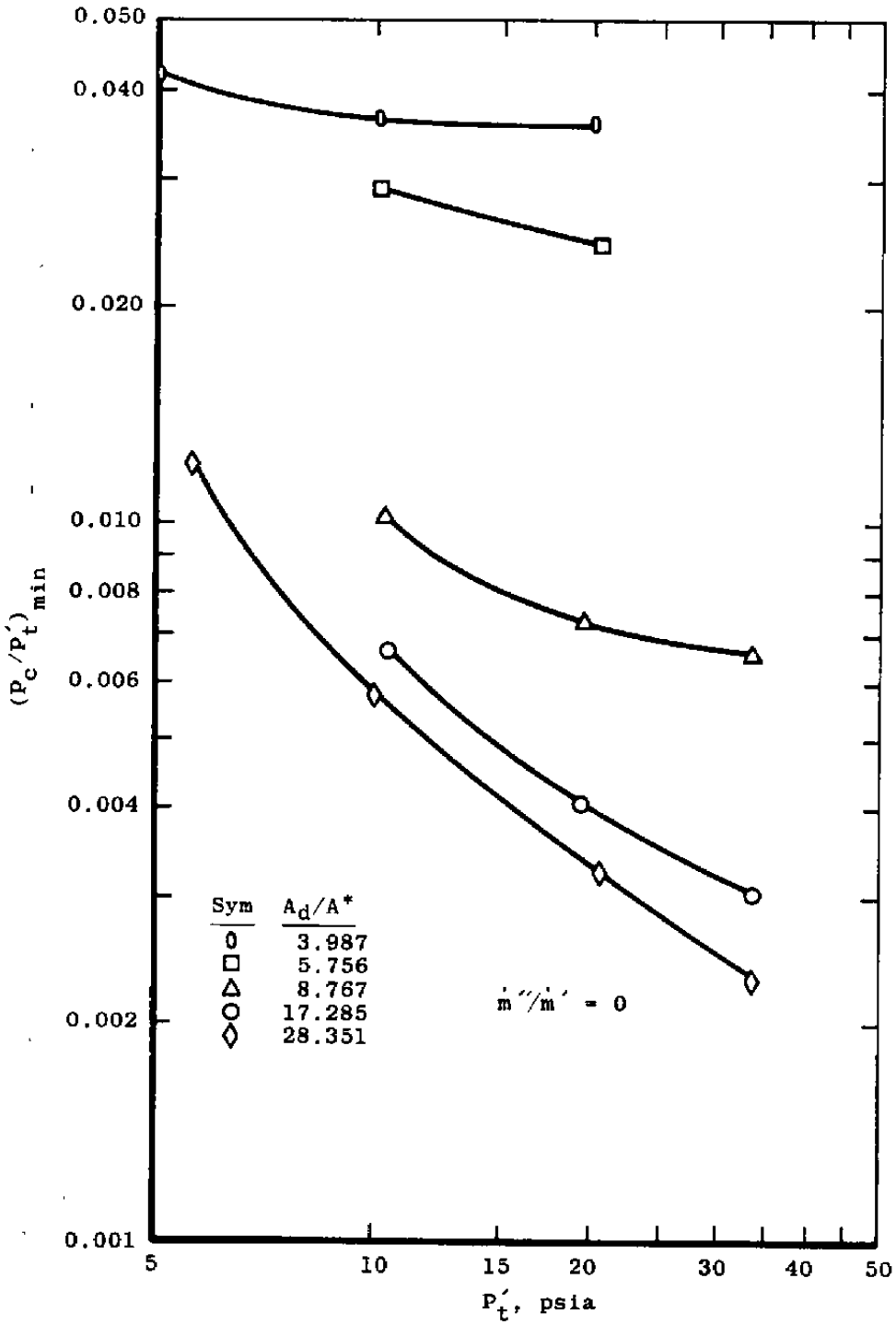

b. Variable-area ejectors

Figure 23. Concluded.

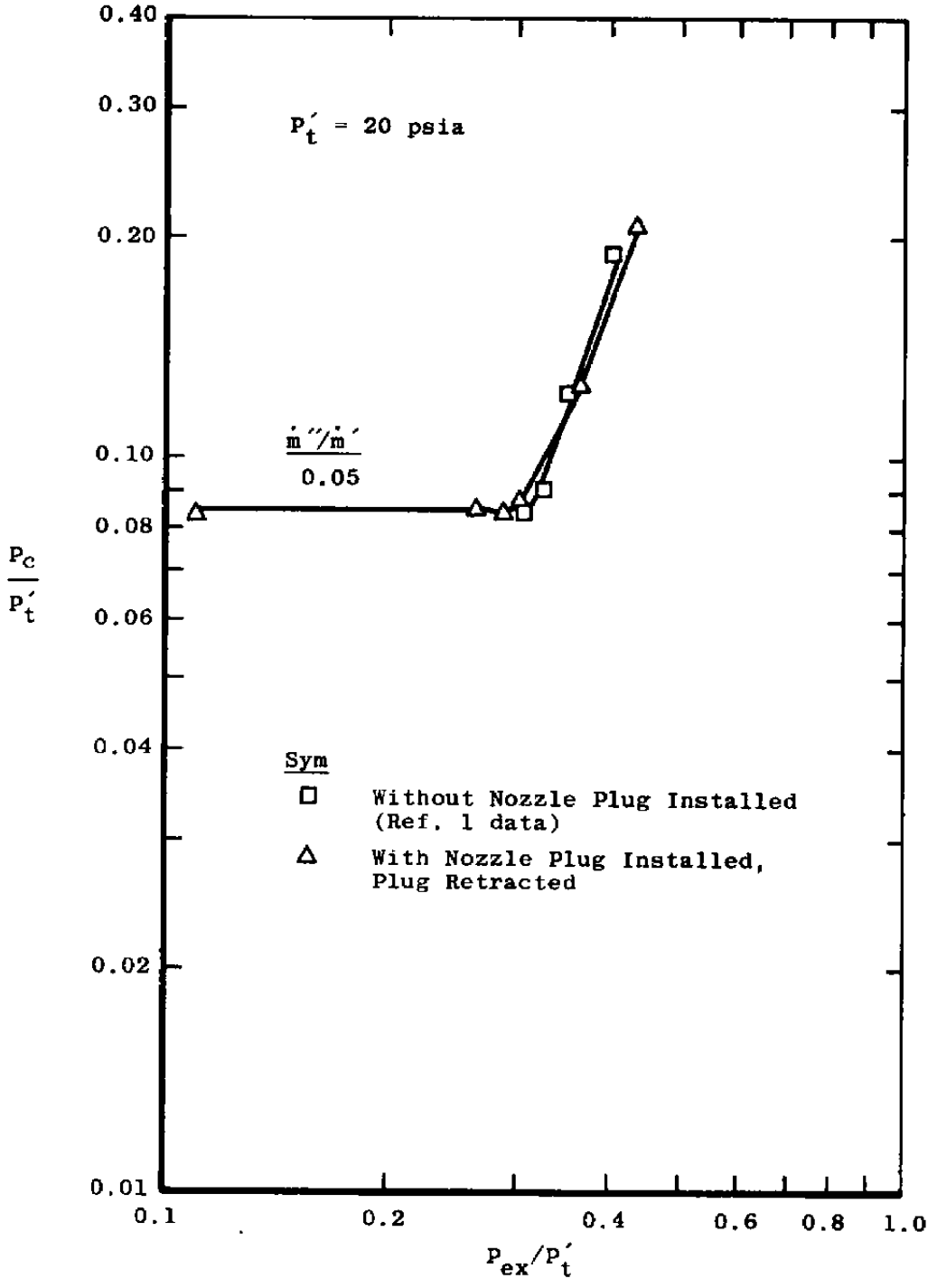

a. $A_d/A^* = 3.987$

Figure 24. Variable-area ejector performance with primary nozzle plug retracted.

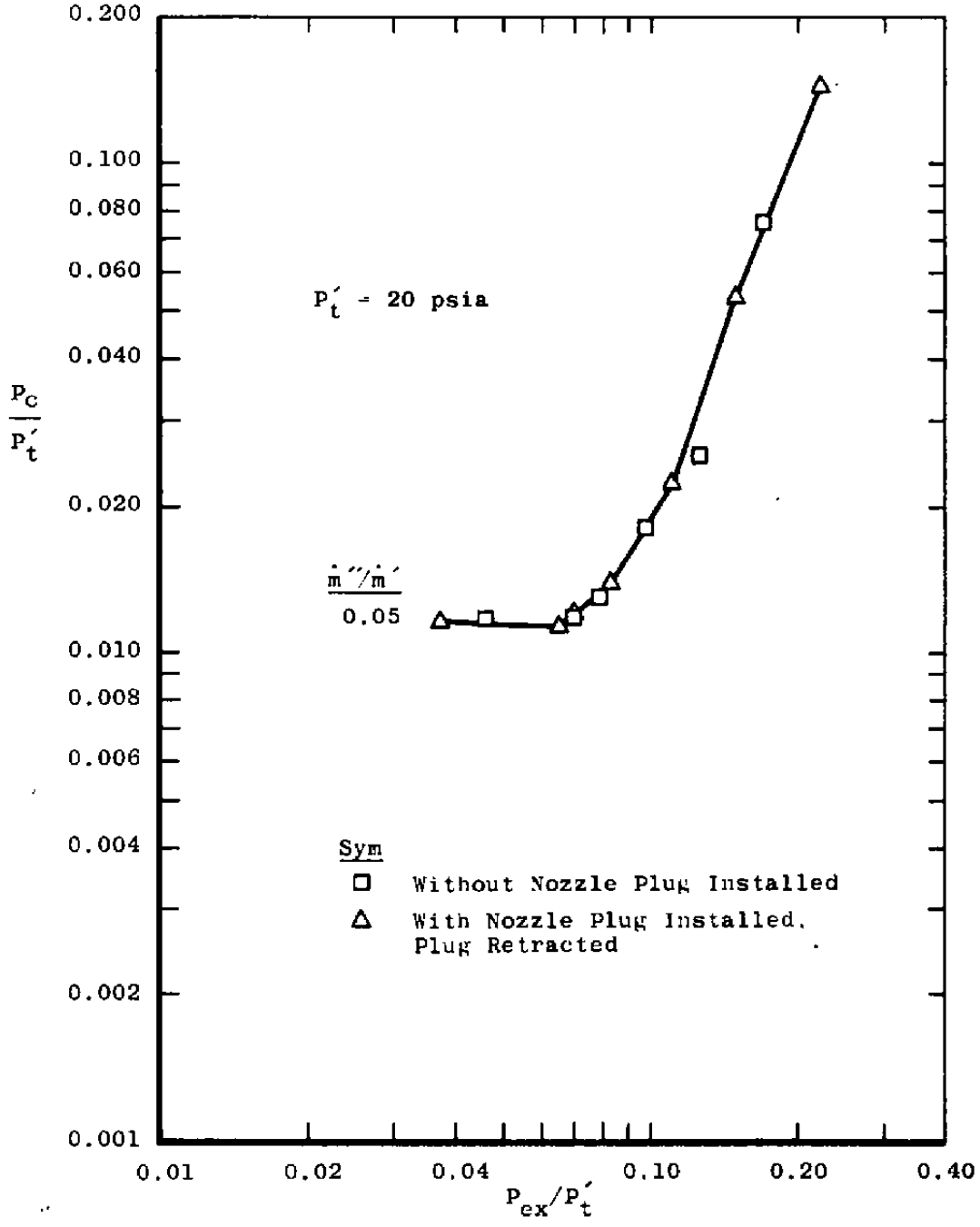

b. $A_d/A^* = 17.283$

Figure 24. Concluded.

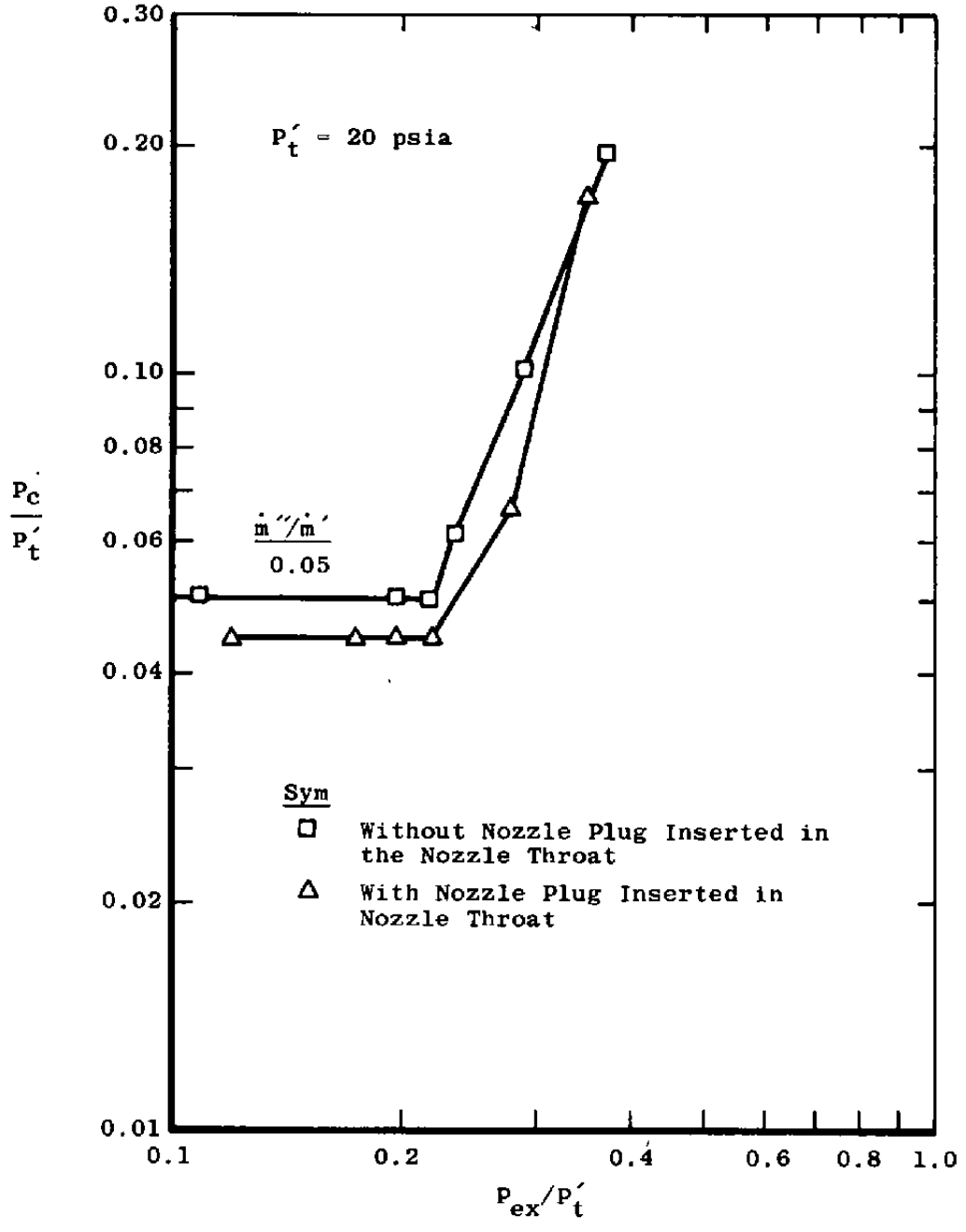

a. $A_d/A^* = 5.756$ ($A_d/A^* = 3.987$ with plug inserted)

Figure 25. Variable-area ejector performance with nozzle plug inserted into primary nozzle throat.

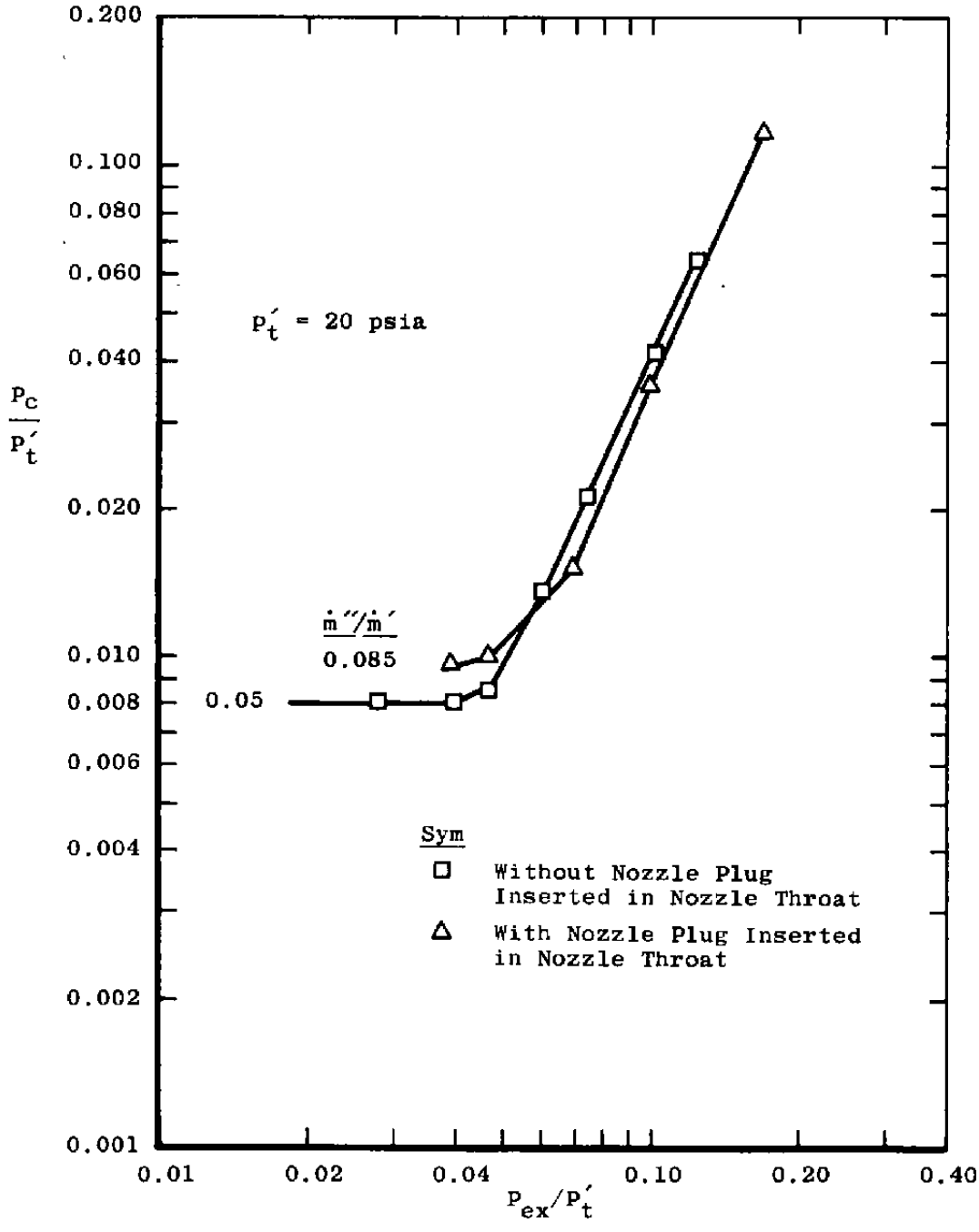

b. $A_d/A^* = 28.351$ ($A_d/A^* = 17.283$ with plug inserted)

Figure 25. Concluded.

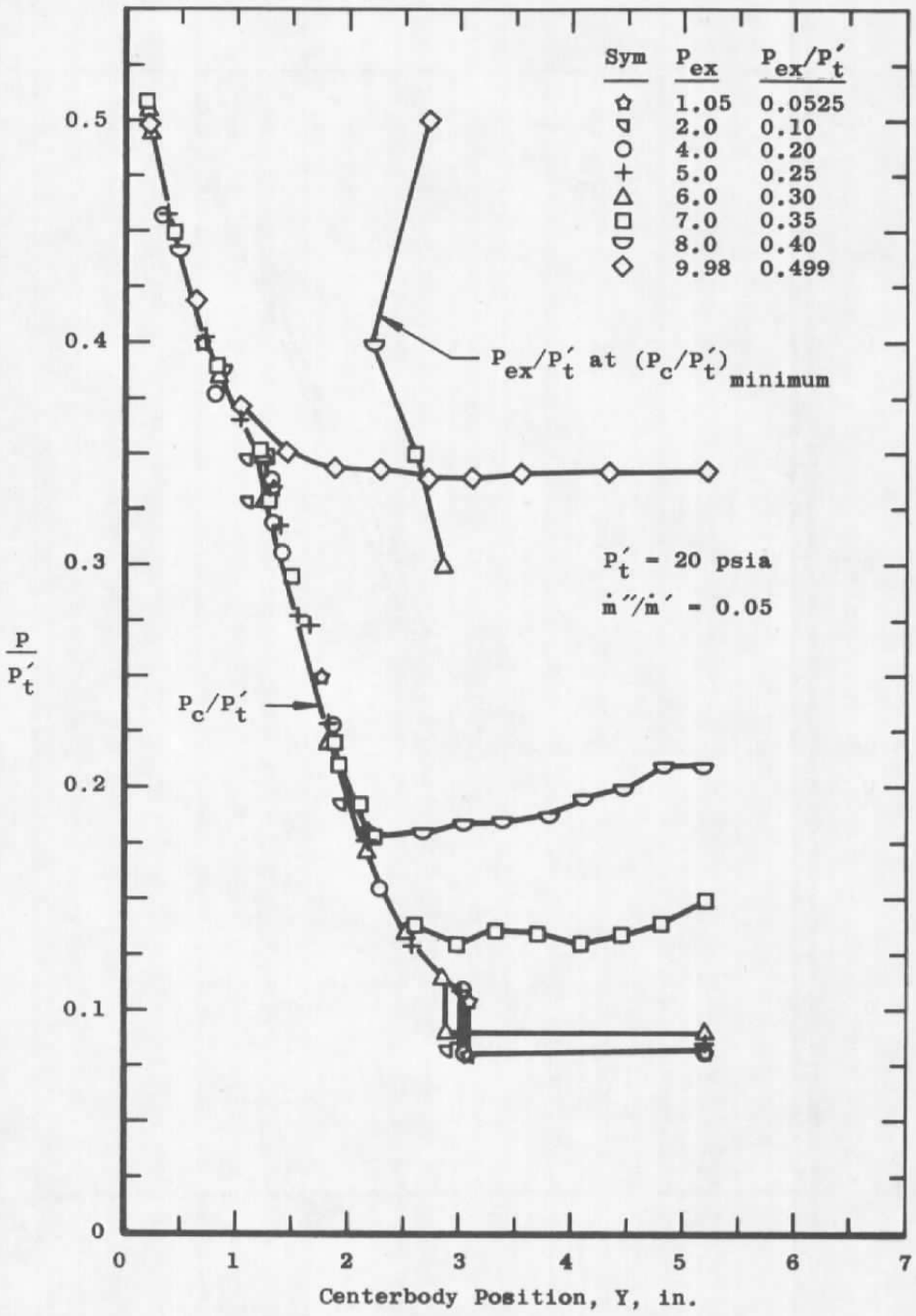

a. $A_d/A^* = 3.987$ (nozzle plug retracted)

Figure 26. Effect of centerbody position on P_c/P_t' at constant values of P_{ex}, with ejector with constant-area inlet.

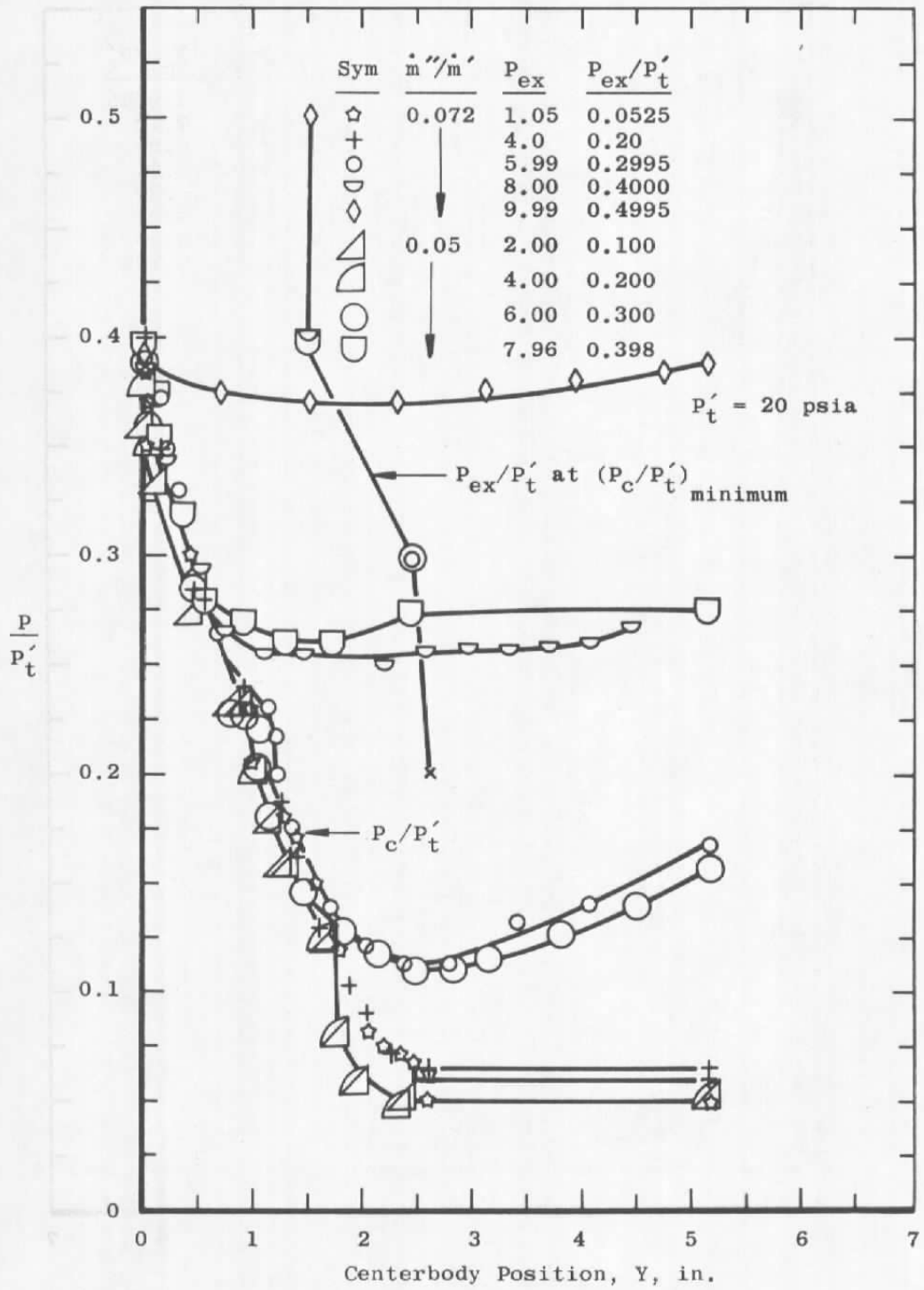

b. A_d/A^* = 5.756 (nozzle plug inserted)

Figure 26. Continued.

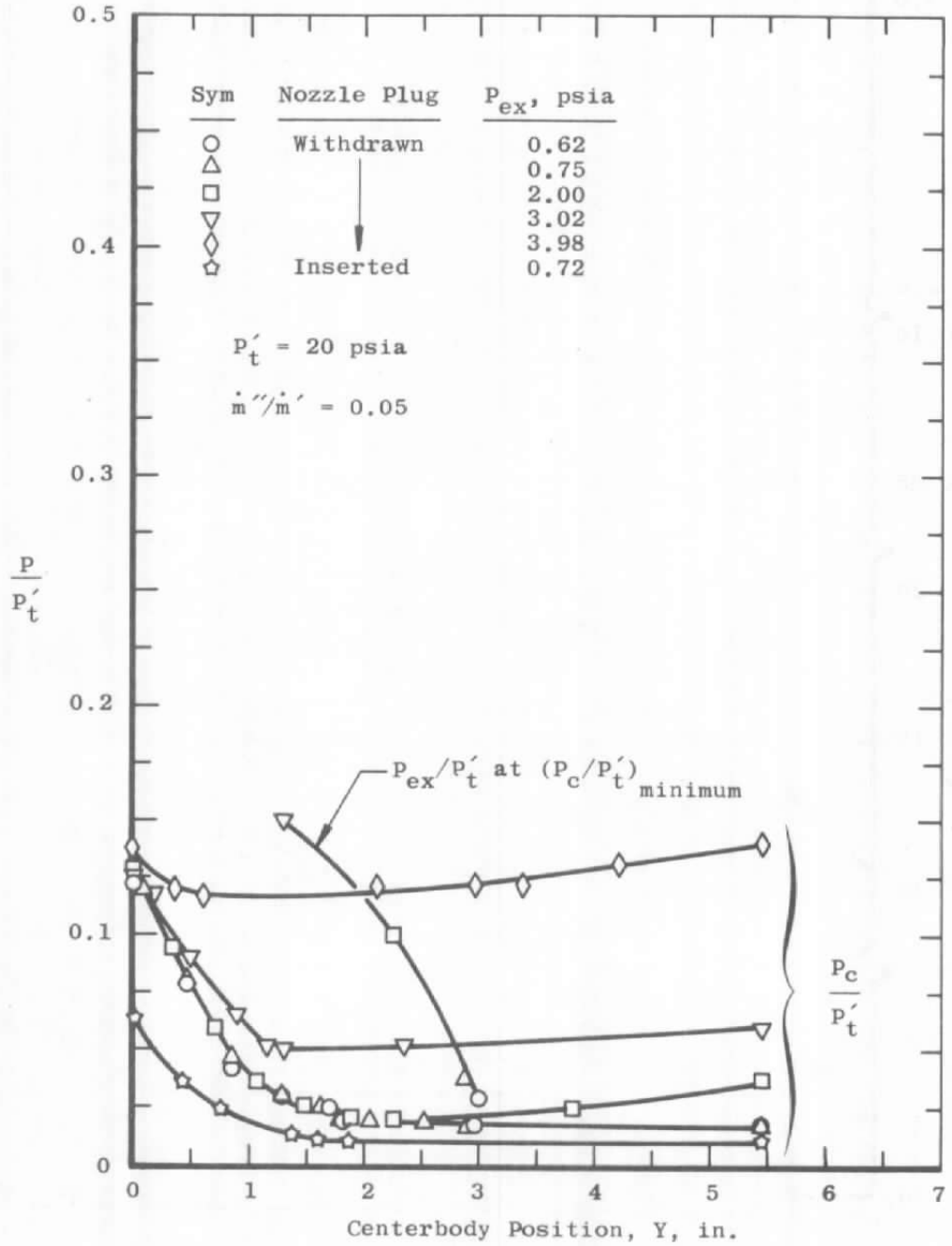

c. A_d/A^* = 17.283 and 28.351 (nozzle plug inserted)

Figure 26. Concluded.

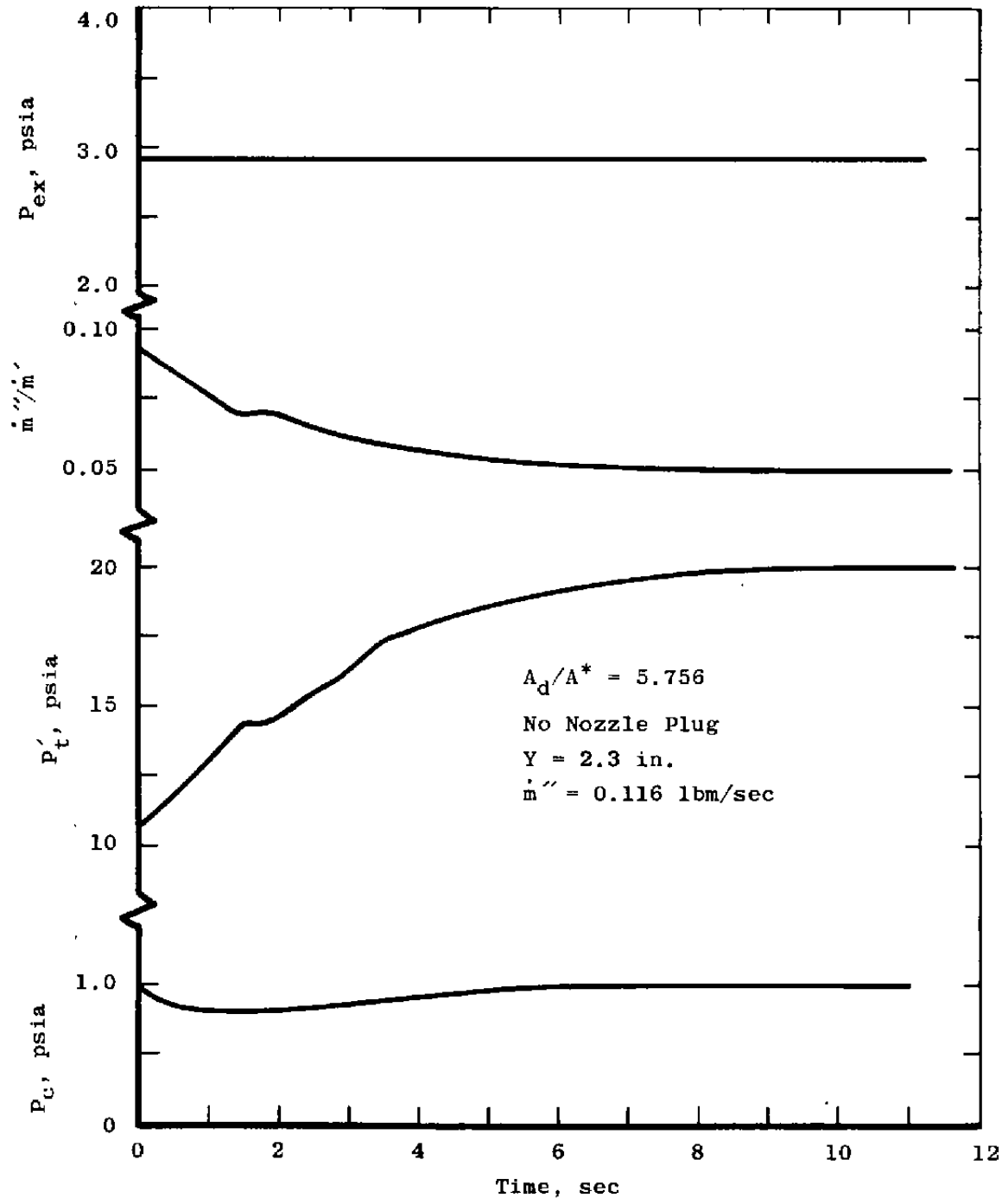

Figure 27. Response of variable-area ejector performance parameters to a ramp change in P_t'.

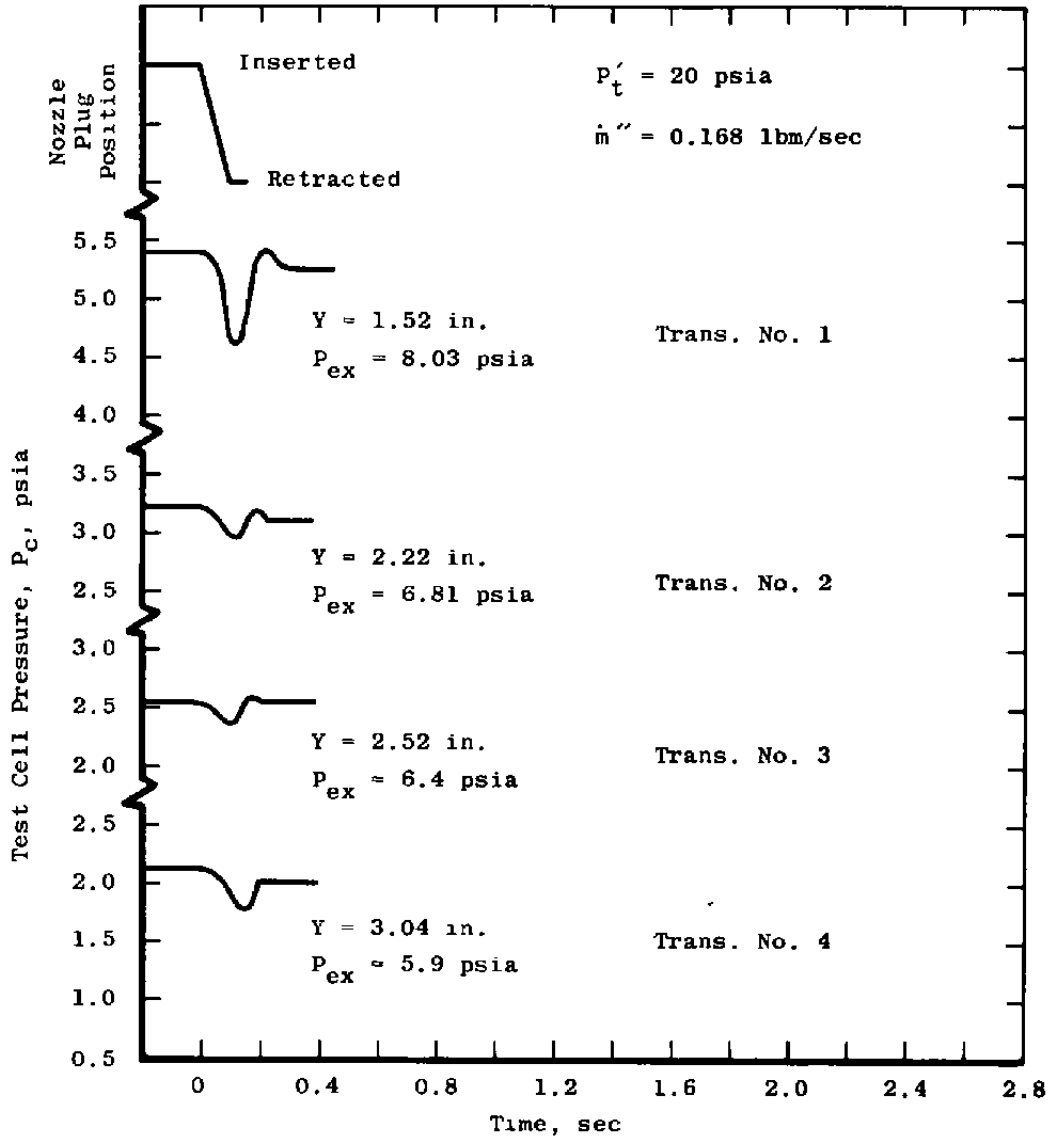

a. A_d/A^* = 5.756 (nozzle plug withdrawn rapidly)

Figure 28. Effect of withdrawing the primary nozzle plug on P_c (variable-area ejector).

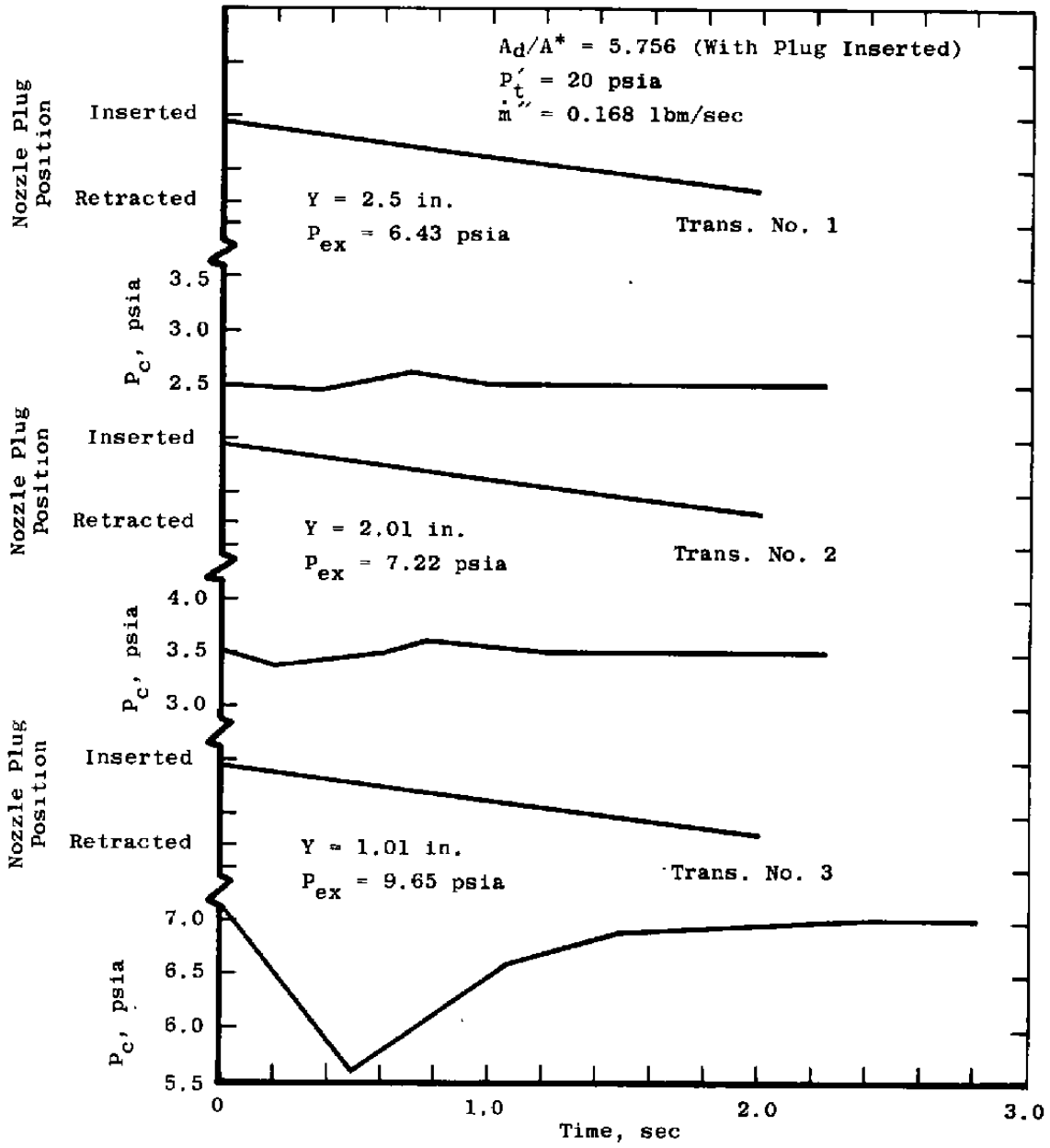

b. A_d/A^* = 5.756 (nozzle plug withdrawn slowly)

Figure 28. Continued.

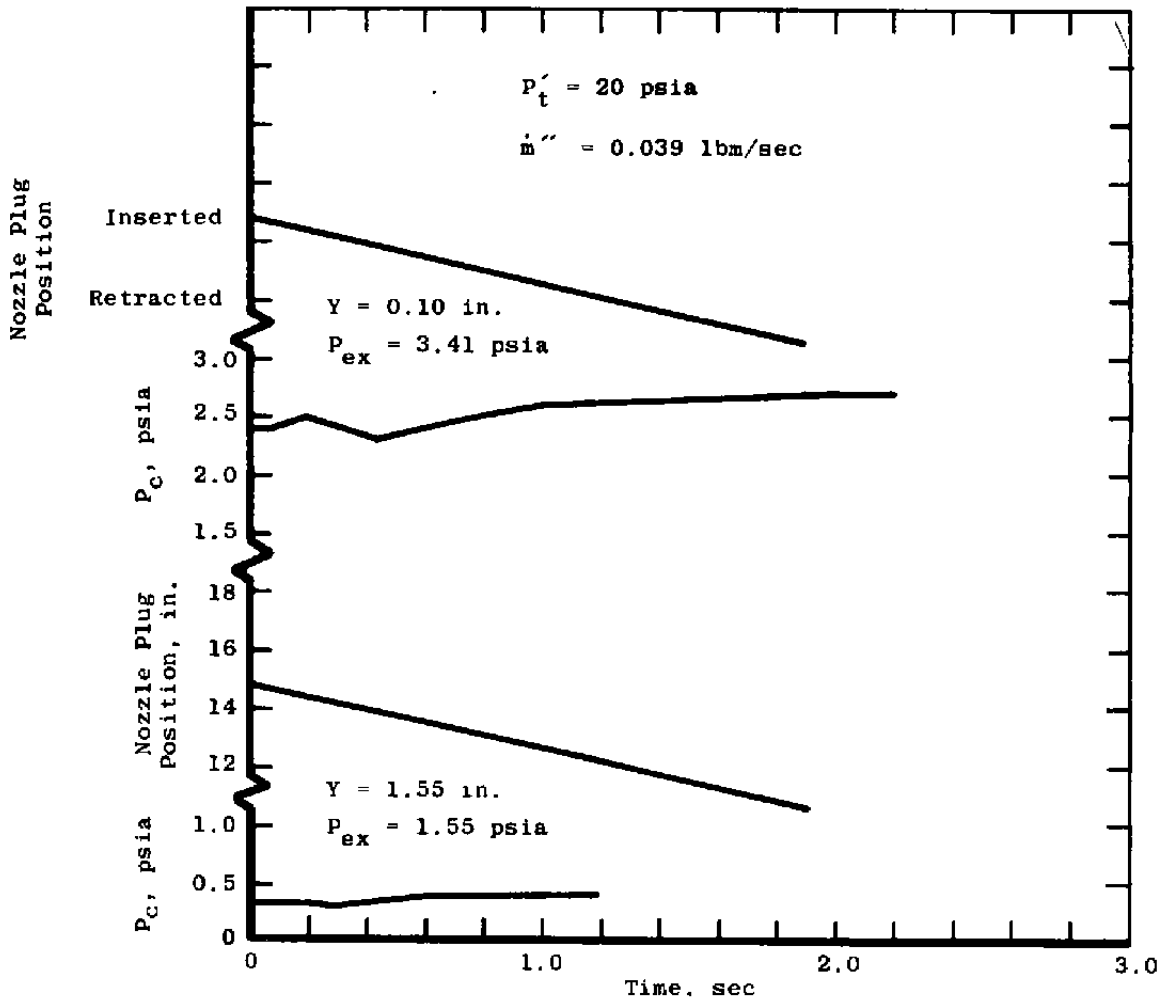

c. A_d/A^* = 28.351 (nozzle plug withdrawn slowly)

Figure 28. Concluded.

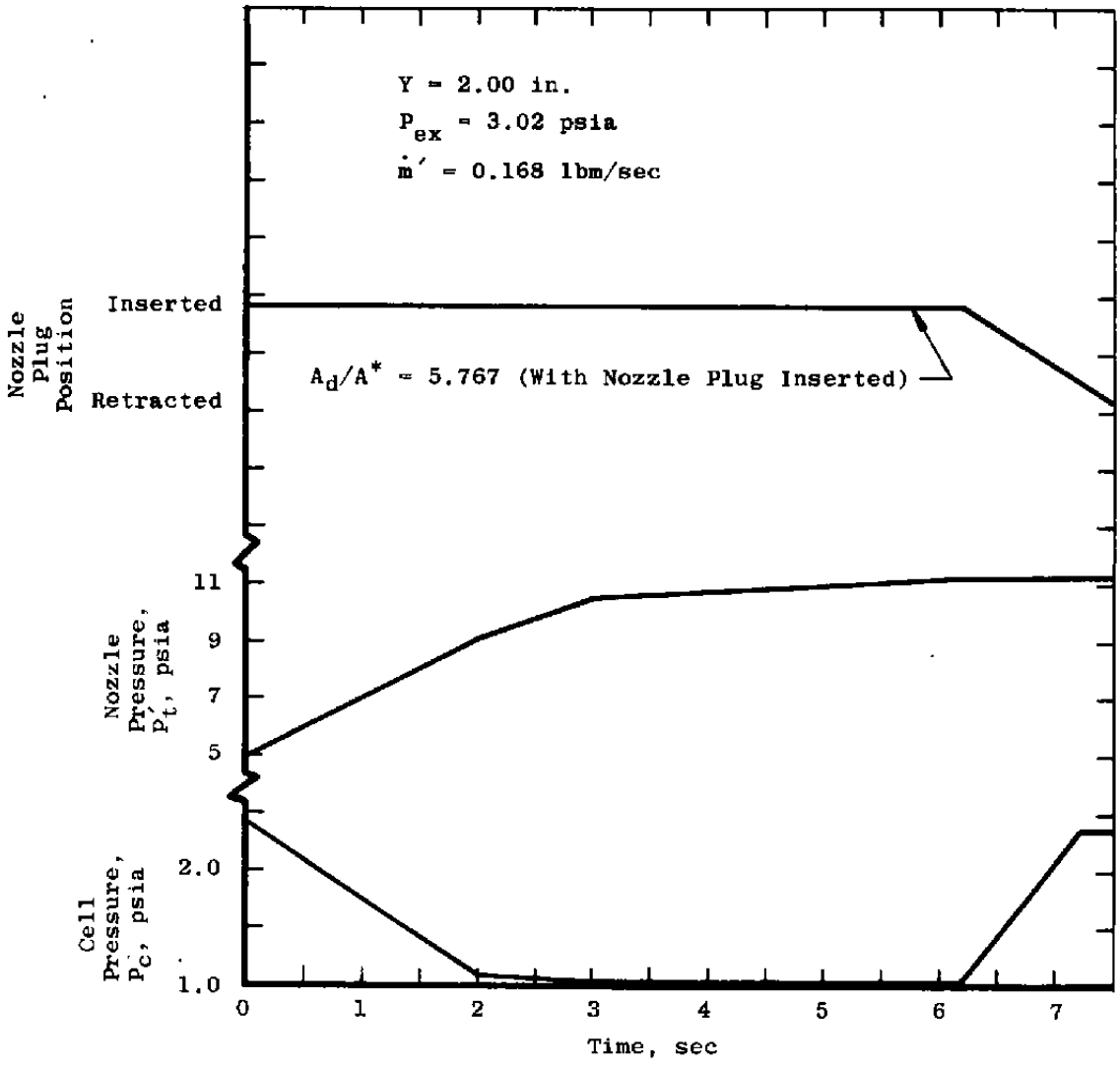

Figure 29. Response of test cell pressure to ramp changes in P_t' and primary nozzle plug retraction.

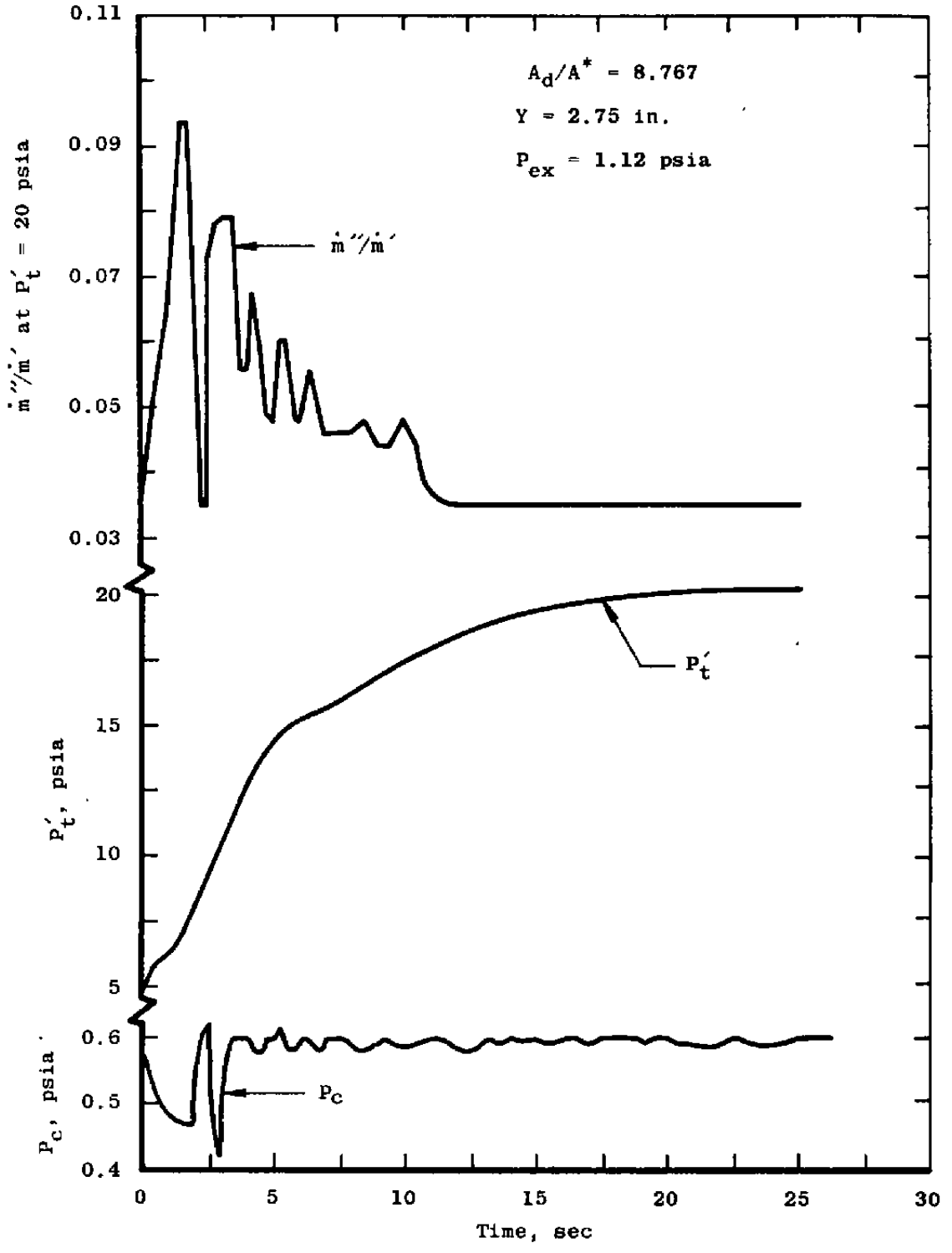

a. Run No. 1

Figure 30. Effect of $\dot{m}''/\dot{m}'$ on transient response of P_c to ramp-type increase in P_t'.

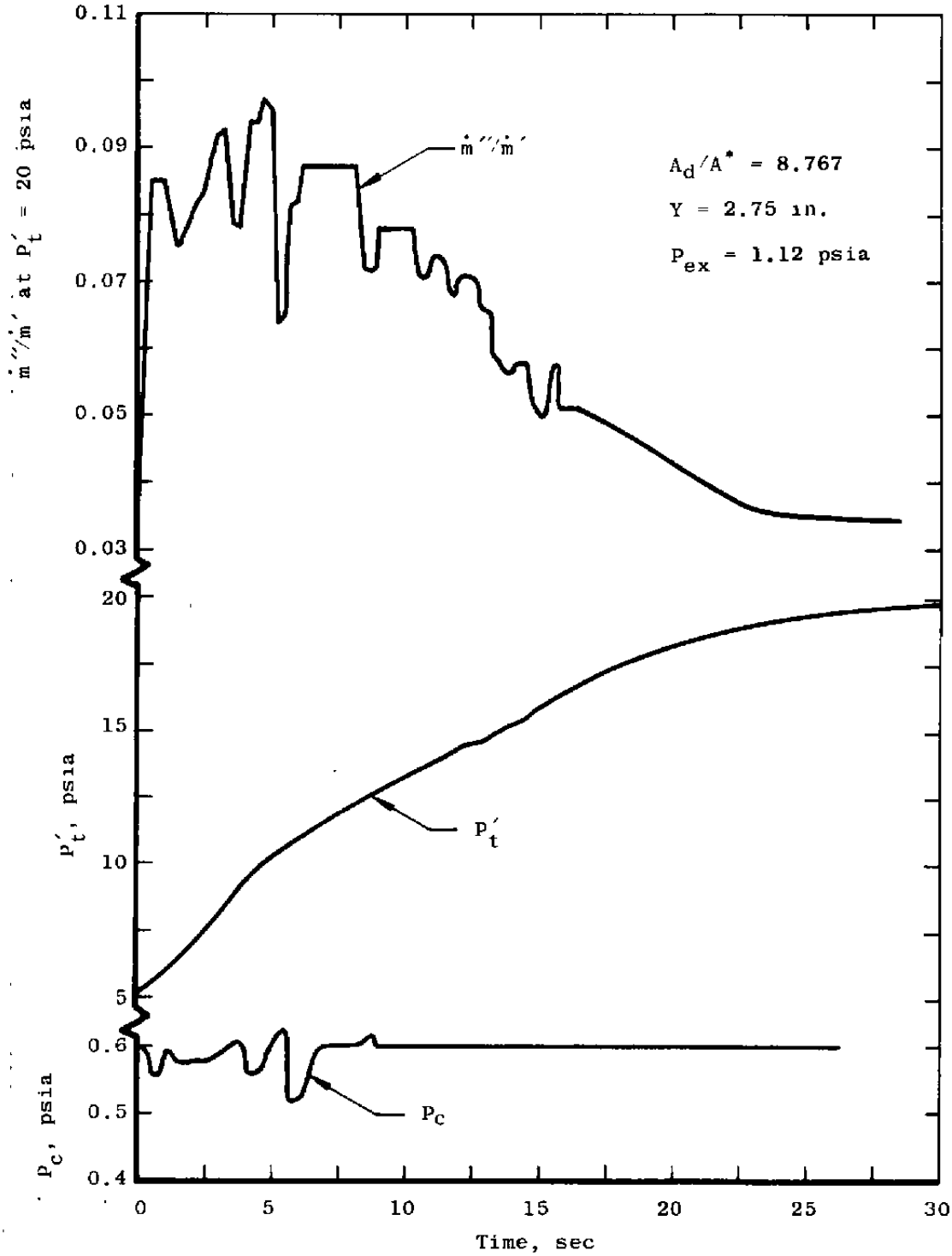

b. Run No. 2

Figure 30. Concluded.

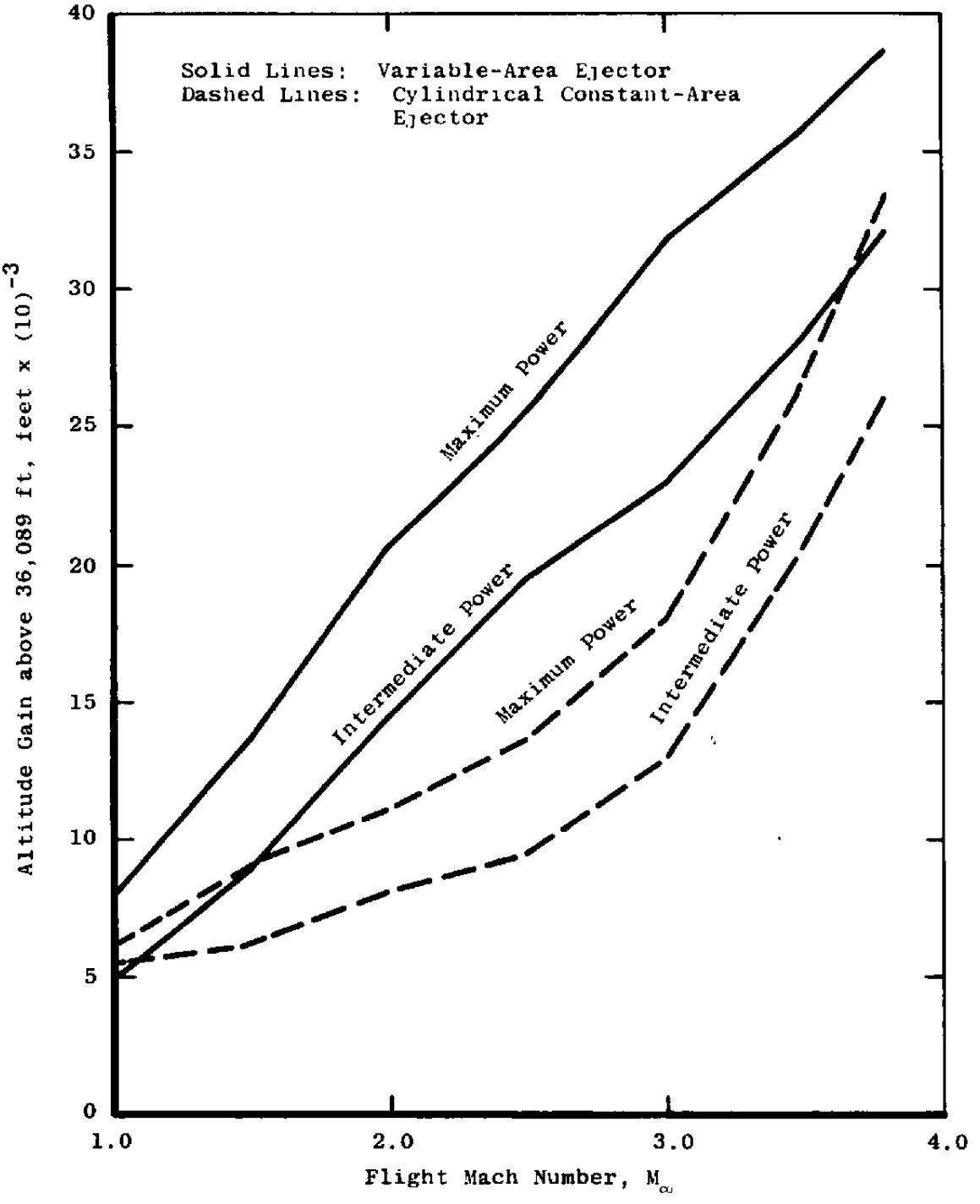

Figure 31. Ejector comparisons showing altitude gains with turbojet engine (design Mach number 3.8).

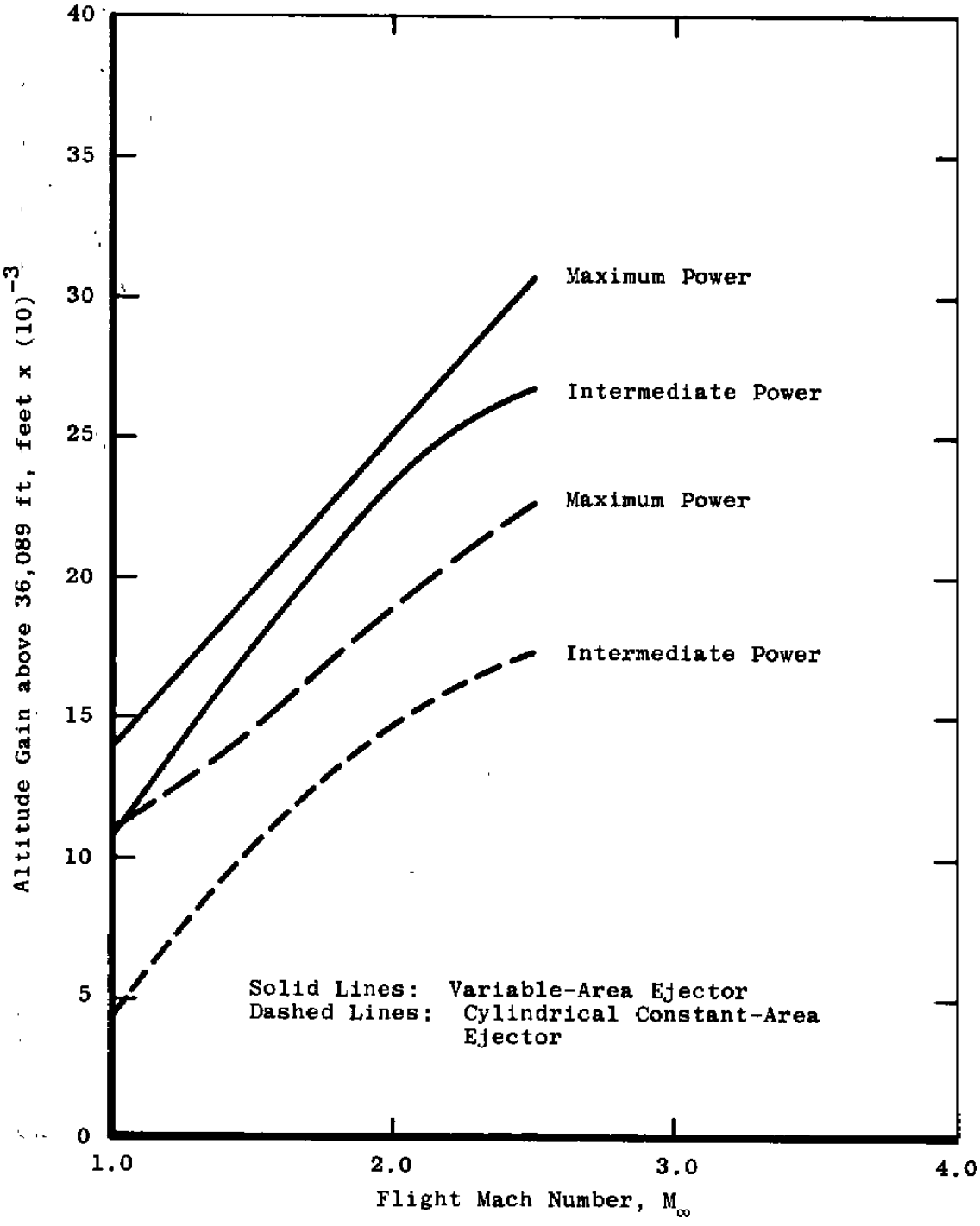

Figure 32. Ejector comparisons showing altitude gains with turbofan engine (design Mach number 2.5).

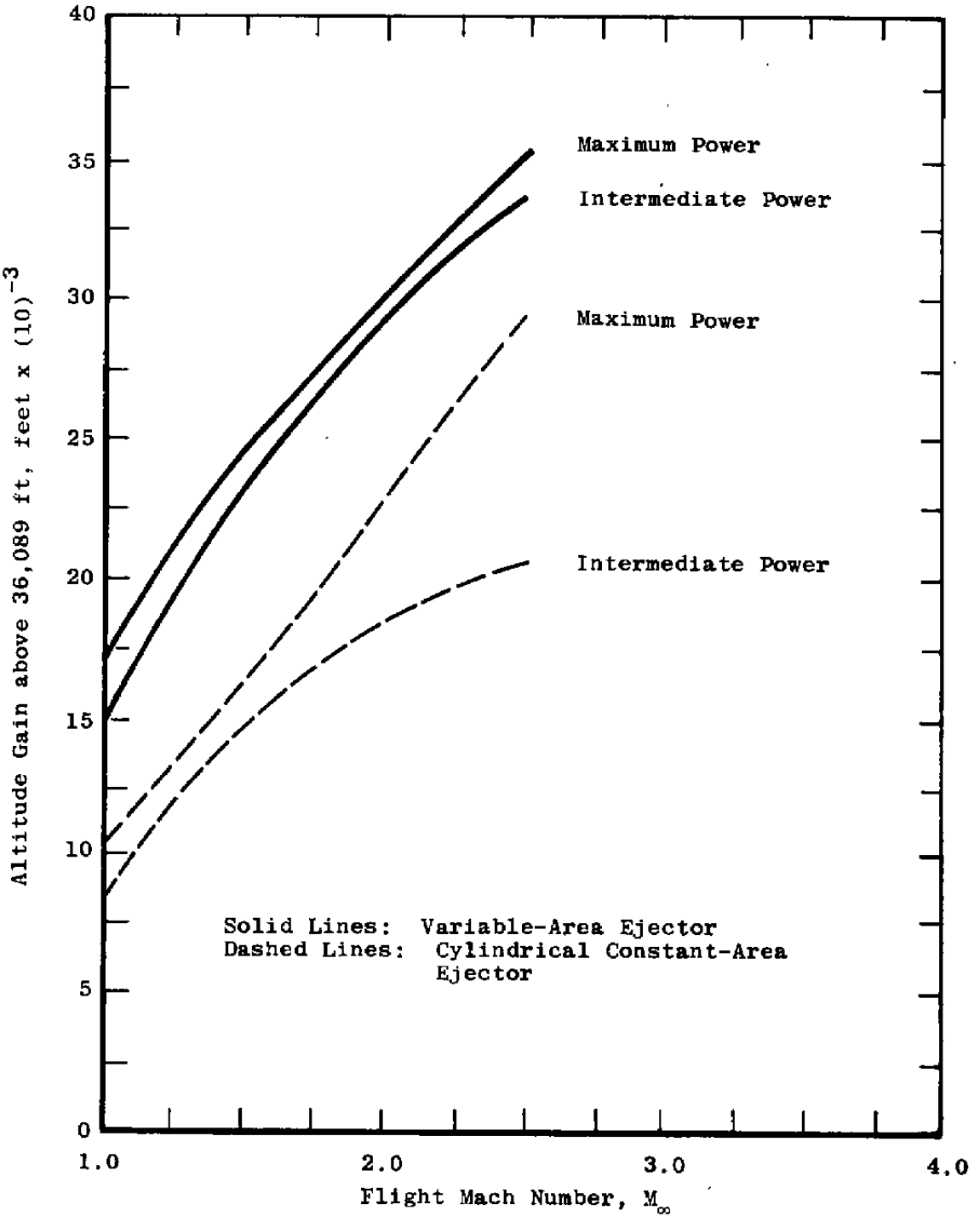

Figure 33. Ejector comparisons showing altitude gains with turbojet engine (design Mach number 2.5).

NOMENCLATURE

A	Area
C_p	Specific heat, Btu/lbm °R
D	Capture duct diameter (6.07 in.)
L	Ejector length (27.57 in.)
M	Mach number (dimensionless)
$\dot{m}$	Mass flow, lbm/sec
P	Pressure, psia
R	Gas constant, ft-lbf/lbm °R
Y	Centerbody position, in.
γ	Ratio of specific heat (dimensionless)

SUBSCRIPTS

air	air
amb	Ambient altitude conditions
c	Test cell
d	Ejector inlet mixing duct (see Figs. 3, 4, 5, and 6)
dw	Duct wall
ex	Exhaust Plenum
g	Gas
int	Intermediate power
max	Maximum power
ne	Nozzle exit

st	Second throat
t	Stagnation
∞	Flight Mach number

SUPERSCRIPTS

*	Nozzle throat
'	Primary flow
''	Secondary flow